

THE APPLICATION OF A RAINFALL-RUNOFF  
MODEL TO THE MAURY RIVER BASIN  
IN VIRGINIA

by

Thomas Mayfield Slaydon

Thesis submitted to the Graduate Faculty of the  
Virginia Polytechnic Institute and State University  
in partial fulfillment of the requirements of the degree of

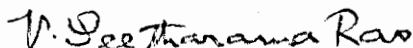
MASTER OF SCIENCE

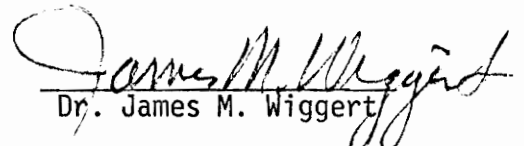
in

Civil Engineering

APPROVED:

  
Dinshaw N. Contractor  
Dr. Dinshaw N. Contractor, Chairman

  
V. Seetharama Rao  
Dr. V. Seetharama Rao

  
James M. Wiggert  
Dr. James M. Wiggert

LD  
5655  
V855  
1976  
SS93  
c. 2

## ACKNOWLEDGEMENTS

This research was supported by the former Virginia Department of Conservation and Economic Development, Division of Water Resources. The author expresses his appreciation for this support.

The author expresses his gratitude and appreciation to his committee chairman, Dr. Dinshaw N. Contractor for his guidance, constructive criticism, patience and continual encouragement during the research and preparation of this text.

The author also expresses his gratitude to committee members Dr. V. Seetharama Rao and Dr. James M. Wiggert for their advice and encouragement.

The author expresses his gratitude to his wife, Deborah, for her patience and encouragement during the course of his graduate study.

For typing the text, he expresses appreciation to Mrs. Charlotte Childrey.

For encouragement, support, and guidance throughout the author's academic career, he expresses profound gratitude and appreciation to his parents, Mrs. Thelma C. Slaydon and the late Harold Thomas Slaydon.

## TABLE OF CONTENTS

	<u>Page</u>
ACKNOWLEDGEMENTS .....	ii
LIST OF TABLES .....	vi
LIST OF FIGURES .....	vii
LIST OF APPENDICES TABLES .....	ix
LIST OF APPENDICES FIGURES .....	x
I. INTRODUCTION .....	1
The Hydrologic Cycle .....	1
Watershed Models .....	8
Objective .....	9
The Study Area .....	9
II. LITERATURE REVIEW .....	13
The Coaxial Model .....	14
Development of a Coaxial Model .....	16
Soil Conservation Service Curve Number Method ...	21
Development of the Curve Number Method .....	23
Retention Parameters .....	25
Introduction of Curve Number .....	27
Procedure to Produce Flood Hydrographs .....	29
Model Applications and Constraints .....	31

	<u>Page</u>
Corps of Engineers' Hydrologic Engineering Center	
Method .....	32
Loss Rate Function .....	32
Procedure for Hydrograph Reconstruction ....	34
Model Application and Constraints .....	37
Stanford Watershed Model IV .....	38
Model Concepts .....	39
Model Components .....	40
Watershed Parameters .....	41
Model Operation .....	49
Model Application and Constraints .....	49
III. THE MODEL .....	52
Justification of Selection .....	52
Model Description .....	53
Model Development .....	53
Data Requirements .....	62
Selected Study Area .....	64
IV. MODEL APPLICATION .....	66
Data Preparation for Calibration .....	66
Model Calibration .....	67
Calibration Results .....	76
Data Preparation for Storm Simulation .....	83
Model Application to Single Storm Events .....	91

	<u>Page</u>
Storm Simulation Model Results .....	94
Discussion of Simulation Results .....	97
V. CONCLUSIONS AND RECOMMENDATIONS .....	101
VI. BIBLIOGRAPHY .....	103
APPENDIX A .....	108
APPENDIX B .....	113
APPENDIX C .....	126
APPENDIX D .....	129
APPENDIX E .....	140
VII. VITA .....	154

## LIST OF TABLES

<u>Table</u>		<u>Page</u>
I	SCS Hydrologic Soil Groups .....	30
II	Land Surface Response as a Function of Mean Moisture Supply .....	47
III	TVA Model - Summary of Results .....	63
IV	Sample Error Analysis .....	75
V	Calibration Results for Maury River Near Buena Vista..	77
VI	Summary of Error Analysis .....	82

## LIST OF FIGURES

<u>Figure</u>		<u>Page</u>
1	Schematic of Hydrologic Cycle .....	2
2	Disposition of Storm Rainfall .....	4
3	Infiltration Rate Curve .....	6
4	Maury River Basin .....	10
5	A Typical Graphical Coaxial Rainfall-Runoff Relation...	15
6	Development of a Graphical Coaxial Model .....	17
7	Incremental Coaxial Relation Using Retention Index ....	22
8	Double Mass Curve of Rainfall and Runoff .....	24
9	Retention Parameters in SCS Curve Number Method .....	28
10	Hydrologic Engineering Center Method .....	33
11	General Loss Rate Function .....	35
12	Flowchart of the Stanford Watershed Model IV .....	41
13	Model Disposition of Moisture Subject to Infiltration..	44
14	Season Quadrant .....	54
15	Interpolation Function .....	56
16	Surface Runoff Relation .....	58
17	Revised Interpolation Function .....	61
18	Separation of Complex Hydrographs .....	68
19	General Organization of Calibration Program .....	70
20	Flowchart of Optimization Procedure .....	71
21	Actual Versus Computed Runoff for Maury River Solution	
	Set 3 .....	80

<u>Figure</u>	<u>Page</u>
22	Distribution of Errors for Solution Set 3 ..... 81
23	Week Number Versus Percentage Error for Solution Set 3.. 84
24	API Versus Percentage Error for Solution Set 3 ..... 85
25	Rain Versus Percentage Error for Solution Set 3 ..... 86
26	Runoff Versus Percentage Error for Solution Set 3 ..... 87
27	API Versus Error for Solution Set 3 ..... 88
28	General Flowchart of Storm Simulation Program ..... 93
29	Synthesis of Streamflow Hydrograph from Unit Hydrographs and Precipitation Excesses ..... 95
30	Results of Storm Simulation Program ..... 96

LIST OF APPENDICES TABLES

<u>Table</u>	<u>Page</u>
BI	Stream Gazetteer of the Maury River Basin ..... 114
BII	Description of Stream Gaging Stations ..... 117
BIII	Description of Precipitation Gaging Stations in the Vicinity of the Maury River Basin ..... 119
BIV	Description of Soil Associations ..... 125
CI	Curve Numbers of Hydrologic Soil-Cover Complexes .... 127
CII	Curve Number Conversion Table for Antecedent Moisture Conditions ..... 128
EI	Daily Precipitation for August 1969 Storm ..... 148
EII	Hourly Precipitation for Montebello Fish Nursery for August 1969 Storm ..... 149
EIII	Discharge for Maury River Near Buena Vista for August 1969 Storm ..... 153

## LIST OF APPENDICES FIGURES

<u>Figure</u>	<u>Page</u>
B1	Streamflow Gaging Stations in the Vicinity of the Maury River Basin ..... 116
B2	Precipitation Gages in the Maury River Basin ..... 118
B3	Profile of the Maury River ..... 120
B4	Flood Frequency Curve ..... 121
B5	Six Hour Unit Hydrograph for the Maury River Near Buena Vista ..... 122
B6	Geological Map of the Maury River Basin ..... 123
B7	Soil Associations in the Maury River Basin ..... 124
E1	Maury River Near Buena Vista, Virginia, August 1969 Flood ..... 151
E2	Double Mass Curve for Storm of August 1969 at Maury River Near Buena Vista, Virginia ..... 152

## I. INTRODUCTION

The value of hydrologic knowledge and data is especially evident in the design of any project that involves the use of natural watercourses or of the adjacent flood plains. In order to reduce flood damages and to prevent the loss of lives, hydrologists seek to develop accurate and rapid methods of predicting the timing and magnitude of peak flood discharges. Predicting watershed response via a watershed simulation system is also useful for land use planning, in designing hydraulic structures, and in analyzing pollutant propagation.

### The Hydrologic Cycle

The discharge hydrograph represents the manner by which the contributing watershed responds to the rainfall process of the hydrologic cycle. Figure 1 shows schematically the hydrologic cycle. Streamflow ultimately finds its source as precipitation in the form of rain, snow, or hail. Moisture from rain and snow melt is subject to runoff, evaporation, and infiltration. Precipitation falling directly on water surfaces and adjoining impervious areas contributes immediately to streamflow.

Part of the rain that falls in the initial stages of a storm is stored on the vegetal cover as interception. Usually, interception storage capacity is filled early during a storm; thus, during a small storm a large percentage of the rain is stored as interception. In a large storm the amount of water in

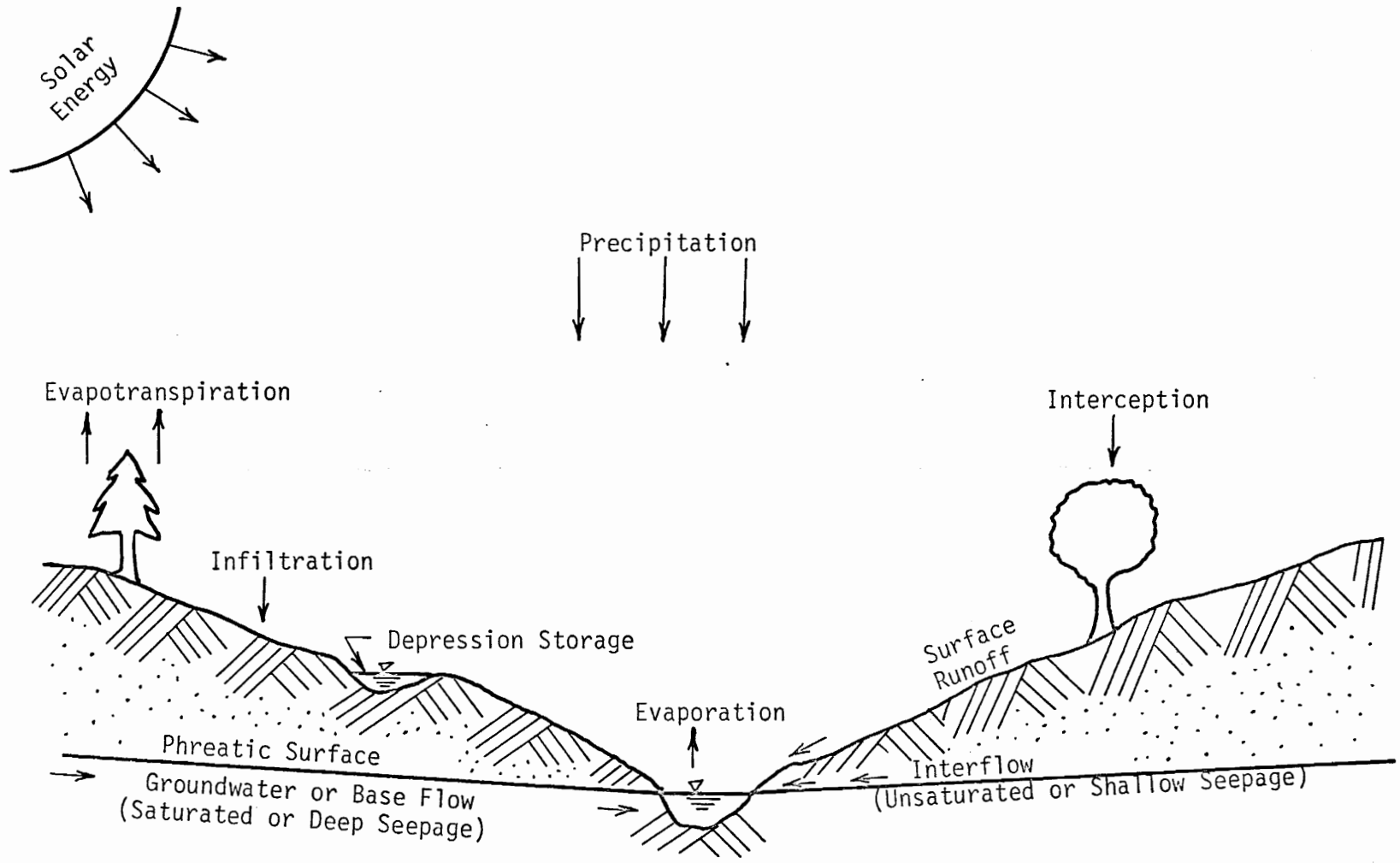


Figure 1 Schematic of Hydrologic Cycle

interception storage is insignificant. The volume of water that reaches the land surface is the rainfall less the interception storage. Figure 2 shows the disposition of storm rainfall.

Rain that reaches the land surface is stored in surface depressions as depression storage and as a film on the surface as surface retention. Water in depression storage and surface detention is subject to infiltration and evaporation. Surface depressions become filled when the rainfall rate exceeds the infiltration and evaporation rates combined. Overland flow results from surface detention and from overflowing depression storages. Infiltration and evaporation can also reduce the volume of overland flow. Portions of the overland flow drain into channels and portions drain to larger depression storages.

Infiltration is the predominant process on the land surface. Water in all phases of the runoff cycle on the land surface is subject to infiltration. Water that passes into the soil surface as infiltration becomes interflow, groundwater flow, or goes into subsurface storage. Interflow is that portion of infiltrated moisture that flows within the unsaturated soil profile and eventually contributes to streamflow. Interflow occurs above the water table or phreatic surface and is somewhat subject to evapotranspiration. Infiltration below the water table becomes groundwater flow. Groundwater flow is flow through a saturated

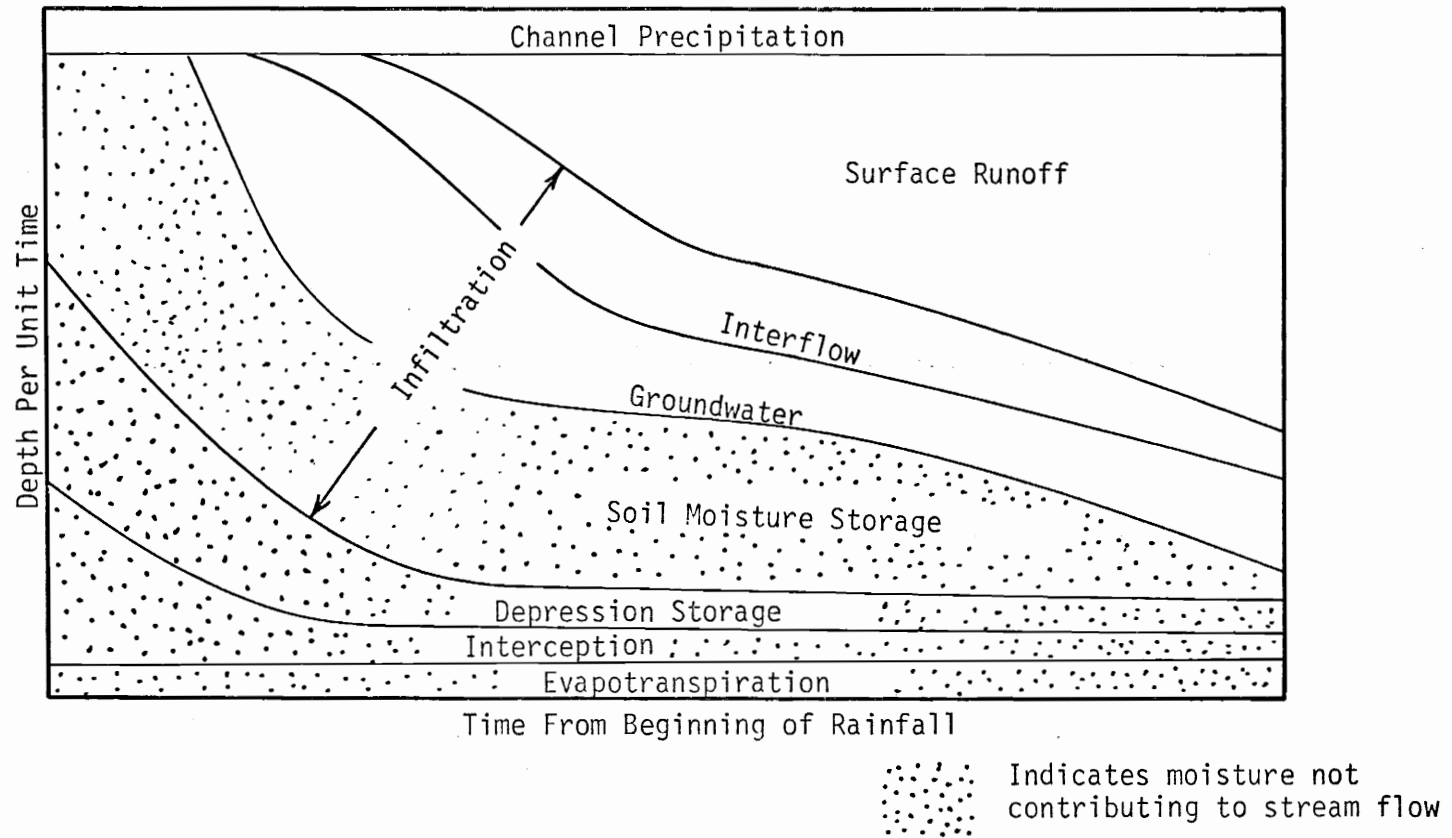


Figure 2 Disposition of Storm Rainfall (39)

soil, and eventually groundwater flow drains to a stream channel. Quantitative disposition of infiltrated water depends upon relative capacities of interflow, groundwater flow, and subsurface storage volumes.

The rate of infiltration is the depth per unit time that water will infiltrate into a unit area of soil. Infiltration rates are significant in determining watershed response. Figure 3 shows a typical infiltration rate curve. Horton (23, 24) found that infiltration rates decrease logarithmically with time. Factors such as soil types, vegetal cover, moisture content, and season of year affect the infiltration rate.

Evaporation is one part of the hydrologic cycle that returns water vapor to the atmosphere. Water stored in interception eventually evaporates as does some fraction of the water in depression storage, surface detention, overland flow, and channel flow. Rates of evaporation are not only dependent upon solar radiation, but are also affected by air temperature, vapor pressure, and wind speed. Evaporation from soil moisture occurs at a rate dependent upon the availability of water in the soil, that is, the evaporation opportunity. A saturated soil yields water to evaporation at a rate equal to the evaporation rate from water surface of the same temperature. Snow surfaces are also subject to a small amount of evaporation.

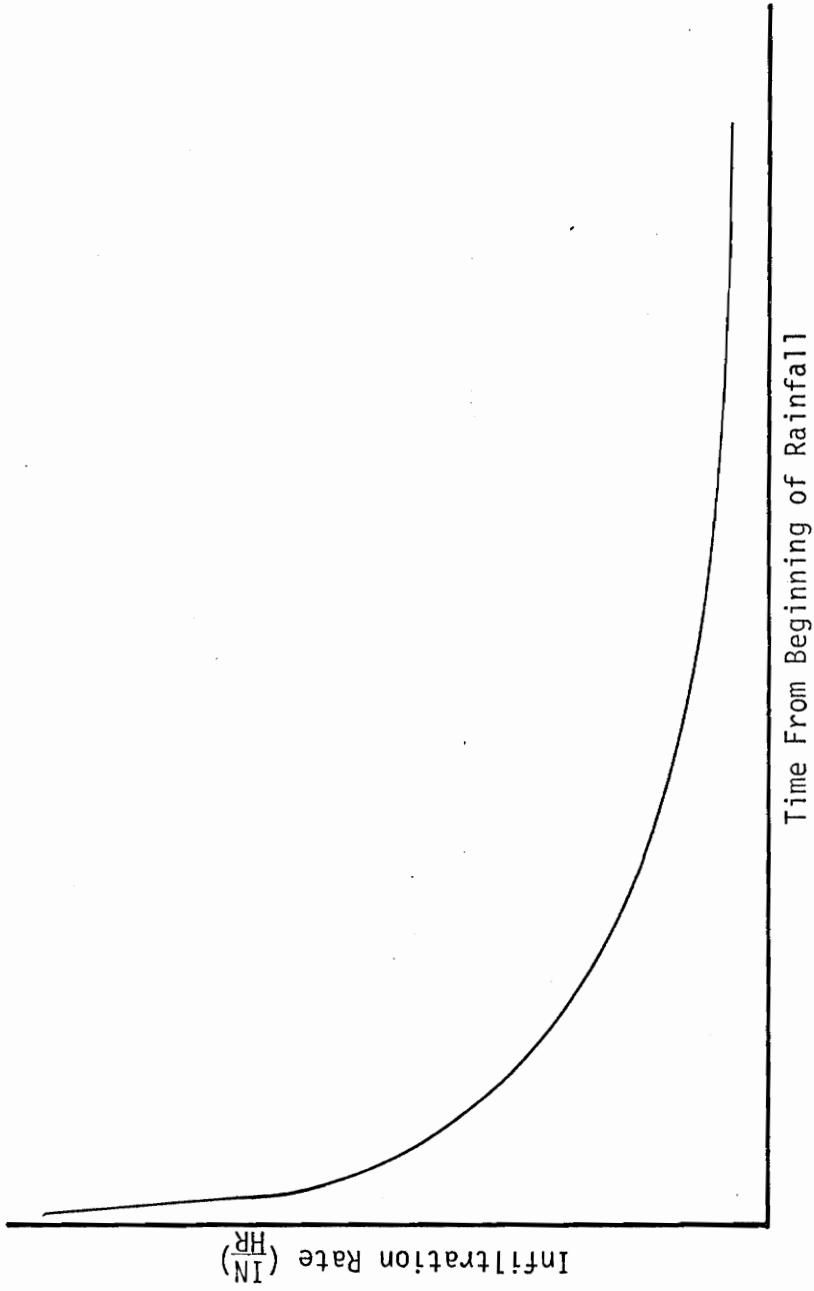


Figure 3 Infiltration Rate Curve (29)

Of the water absorbed by plant roots, virtually all is returned to the atmosphere as vapor by transpiration. Rates of transpiration are controlled by water available to the plants, solar radiation, temperature, and minimally by the type of plants. For most hydrologic applications, evaporation and transpiration are considered together as evapotranspiration. The rate of evapotranspiration is quantified by potential evapotranspiration which is a parameter that defines the amount of evapotranspiration that would occur if sufficient moisture were available.

A watershed's response to the hydrologic cycle is a function of basin characteristics. The location of the watershed is related to the climate which controls the water and energy available to the processes in the hydrologic cycle. Elevation, for instance, can be correlated with temperature, vapor pressure, and amount of precipitation.

Geomorphology also plays a significant role in determining basin response. The types of soils and mantle characteristics affect infiltration and groundwater processes. Slope, shape of the basin, stream channel network, and the size of the basin are all significant to watershed response to precipitation. Ground cover and man's intervention by land use relate to streamflow, groundwater, and evaporation. Thus in summary, the hydrologic cycle is a complex process that is dependent upon many variables.

### Watershed Models

"The ability to accurately predict behavior is a severe test of the adequacy of knowledge in any subject" (35). Since the historical data of precipitation, streamflow, and evaporation are the only parameters generally available for hydrologic analysis, and because the hydrologic cycle is difficult to quantify, the rainfall-runoff process is not easily simulated mathematically even though the process is readily described. Relationships such as the rational formula, in which discharge is a function of a runoff coefficient, rainfall intensity, and watershed area have proved useful for small design problems but are inadequate when used to model watershed behavior.

Much work has been done with electronic analogies to watershed behavior with analog computers (33). However analog models must be programmed and calibrated for each watershed simulated.

Graphical solutions, such as the Index type models, to the rainfall-runoff problem were developed (18,21,28,36,37), and subsequently adapted to digital computers. However the Antecedent Precipitation Index (API) type model is composed of empirical relationships that model the streamflow but do not model the processes involved.

State of the art, watershed simulation is now accomplished with conceptual type digital computer models (32,35,38). Conceptual models mathematically simulate the various processes in the hydrologic cycle. By numerical optimization techniques, the equations describing the components of watershed response are calibrated to fit the historical data for the simulated watershed. Such models are complex and require excessive computer time and storage.

#### Objective

The objective of this research is to apply an API type of rainfall-runoff relationship to the Maury River basin in order to develop discharge hydrographs for use in an implicit flood routing model developed for the James River by Contractor and Wiggert (5,6,7).

#### The Study Area

The Maury River rises in the Appalachian Mountains of West Central Virginia. The Maury drains most of Rockbridge County and parts of Augusta and Bath Counties. On its journey to the James River, the Maury flows through Buena Vista, and Lexington is one mile to the west of the Maury. Figure 4 shows the Maury River basin.

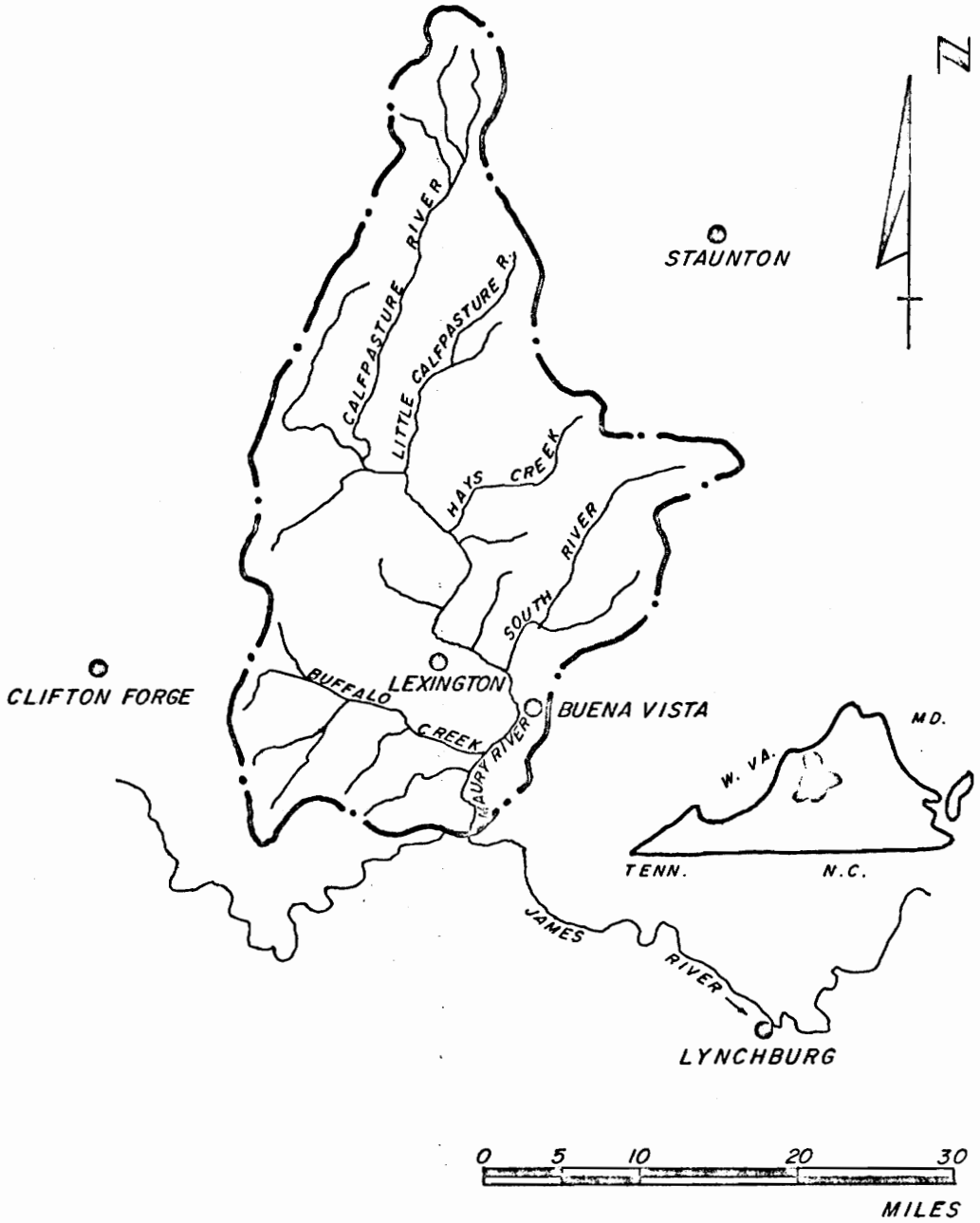


Figure 4 Maury River Basin

An area of 839.3 square miles is drained by the Maury River and its tributaries. From the most distant point on the drainage divide, near the headwaters of the Cowpasture River at elevation 3802 feet above mean sea level, the Maury River drops 3101 feet over an 80 mile course to its confluence with the James River at elevation 701. The Maury River joins the James River some 281 miles upstream of the mouth of the James River. The Maury River and its tributaries flow generally in a southerly direction. The greatest north-south dimension of the basin is 52 miles and the greatest east-west dimension is 30 miles.

The climate of the Maury River basin is classified as humid temperate. Average annual precipitation ranges from 38 to 40 inches. A record 6 hour rainfall of 27 inches fell on August 19 and 20, 1969, near the adjacent Montebello precipitation gage. Temperatures range from  $-20^{\circ}$  F to  $98^{\circ}$  F with an average temperature of  $36^{\circ}$  F. Annual evaporation is 43 to 56 inches with 80% occurring from April to October. For 36 years of record the average annual runoff is 13.58 inches. The Maury River basin contains no large urban areas but is approximately 70% forested. Additional geohydrologic information is given in Appendix B.

The geology of the basin is characteristic of West Central Virginia. Sedimentary rocks generally underlie the Maury basin. Most of the basin is underlain by quartzites, sandstones, shales, and limestones of Mississippian, Silurian, and Devonian age. The

remainder is underlain by Ordovician and Cambrian shales, limestones, and dolomites. Two major faults run through the basin, the Pulaski-Staunton fault and the Blue Ridge fault. Both faults trend northeast-southwest with the Pulaski-Staunton fault located near the center of the basin and the Blue Ridge fault located on the eastern edge of the basin. Also the Blue Ridge fault divides the basin into two physiographic provinces which are the Valley and Ridge physiographic province to the southeast, and the Blue Ridge physiographic province to the northwest.

Soil association distributions are also found in northeast-southwest bands. Dekalb-Wiekert-Hayter-Jefferson is the soil association in the western region of the basin; Frederick-Hagerstown-Berks soil association comprises the central band; and the eastern edge is the Porters-Chester-Clifton-Ramsey soil association (43).

Basin topography consists of linear, northeast trending ridges and valleys. The Valley and Ridge physiographic province is a mountainous region of folded and thrust-faulted sedimentary rocks. The Blue Ridge physiographic province is similar in surface topography to the Valley and Ridge province.

## II. LITERATURE REVIEW

Hydrologists and engineers have collected hydrologic data in order to develop methods to simulate watershed response. The rational formula, while being adequate for simple storm drainage problems, has not proved worthwhile for general application. Since the hydrologic cycle, when expressed mathematically, is very complicated, a manual procedure developed by Sugawara was the first comprehensive model developed (35). Graphical methods were developed (8, 21, 39) to predict runoff from rainfall. With the advent of digital computers, graphical coaxial methods were expressed mathematically and adapted to digital computers. Eventually more refined conceptual models (32,33,34,38) were developed and the present state of the art is a conceptual digital computer model. Several agencies use computer adapted conceptual rainfall-runoff models to predict flood stages (38,46,47). Other agencies use computer models to generate flood hydrographs from precipitation data for general hydrologic analysis (36,37,45).

The following schemes will be discussed: the graphical coaxial model, the Soil Conservation Service curve number method, the Corps of Engineers Hydrologic Engineering Center method, and the Stanford watershed model.

### The Coaxial Model

Kohler and Linsley (21) analyzed a large number of storms and developed a graphical correlation to predict the total storm runoff from various storm parameters. Generally antecedent precipitation index or API, time of year, storm duration, and storm rainfall were correlated graphically to predict either storm runoff or basin recharge. Figure 5 presents a typical graphical coaxial relation.

API was used as an index to upper level soil moisture. It is a decay function of precipitation. When precipitation does not occur API is given as

$$API_t = API_0 K^t \quad (1)$$

where  $API_t$  = the antecedent precipitation index at time,  $t$ , in inches;

$API_0$  = the initial antecedent precipitation index at  $t=0$ , in inches;

$K$  = a recession constant ranging from 0.85 and 0.98; and

$t$  = time in days.

Letting  $t$  equal unity,

$$API_1 = API_0 K \quad (2)$$

When precipitation occurs, then the day's precipitation is added to the API, or

$$API_t = API_{t-1} K + PRECIP_{t-1} \quad (3)$$

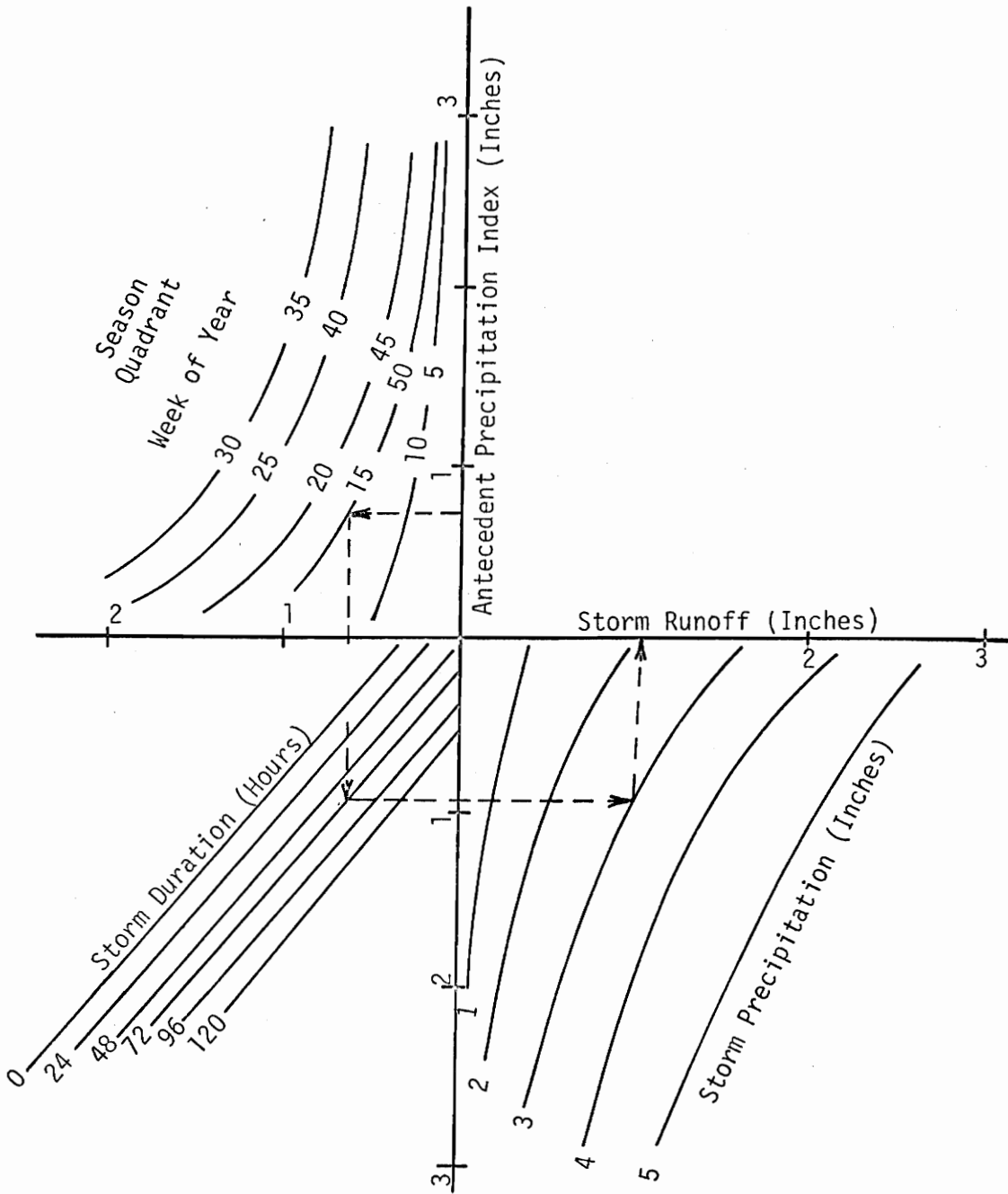


Figure 5 A Typical Graphical Coaxial Rainfall-Runoff Relation (39)

where  $PRECIP_t$  = the precipitation falling on day  $t$ .

Since surface runoff does not contribute to the residual soil moisture then a more accurate measure of antecedent soil moisture would be the  $API_t$  plus the basin recharge for day  $t$ , but the additional accuracy does not justify the computation.

Time of year also affects runoff, and week number relative to the calendar year is also correlated. Thus a season quadrant is used. From Figure 5 it can be seen that the seasonal affects are cyclic.

Storm duration also affects runoff. Thus a storm duration quadrant is used. Again from Figure 5 it is seen that runoff decreases with increased storm duration.

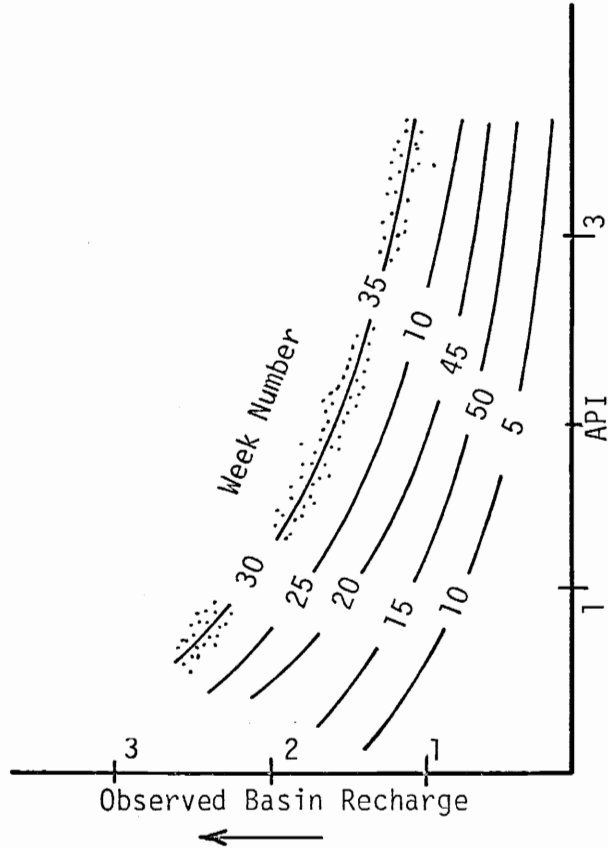
Precipitation is the total volume of water that is available to the runoff process and a precipitation quadrant is provided. Depending on the desired results precipitation can be either total storm precipitation or incremental precipitation.

The results can be total storm runoff, incremental runoff, or basin recharge.

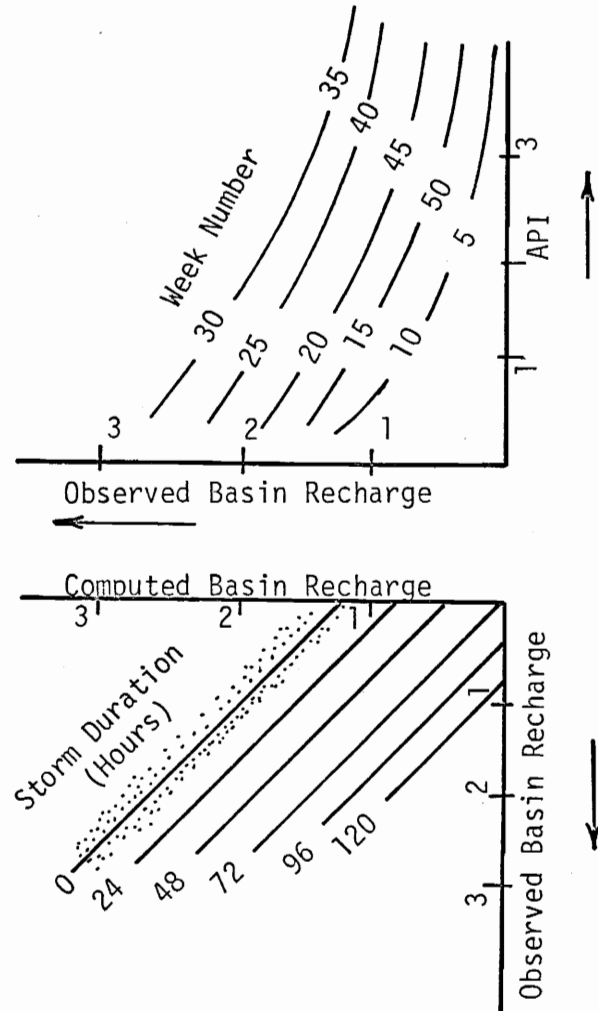
#### Development of a coaxial model

Assuming basin recharge is the desired result, then  $API$  is plotted against observed basin recharge for a large number of storms, say fifty or greater. Each point is then labeled with its respective week number. Then a family of curves is fitted through common week numbers. The aforementioned steps produce a first approximation of the season quadrant. Figure 6a depicts the procedure.

API and Basin Recharge  
in Inches

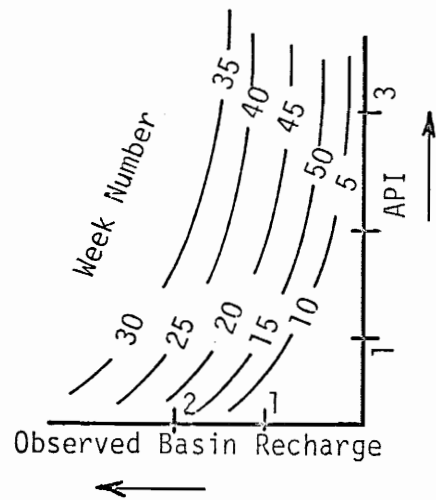


(a)  
Season Quadrant

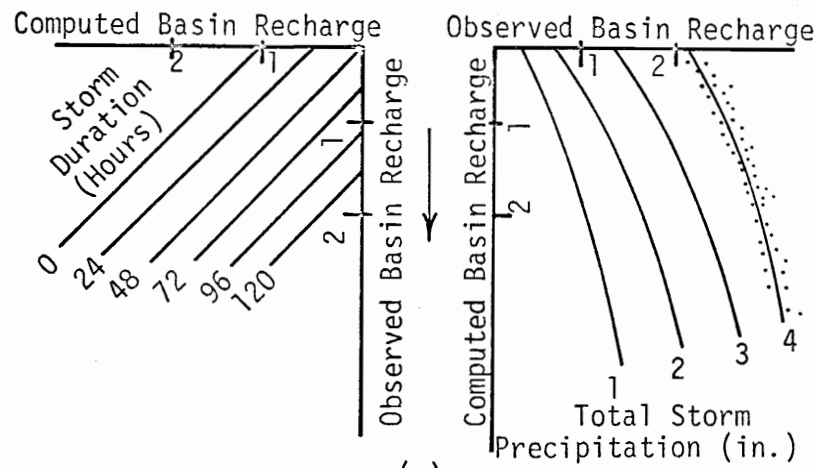
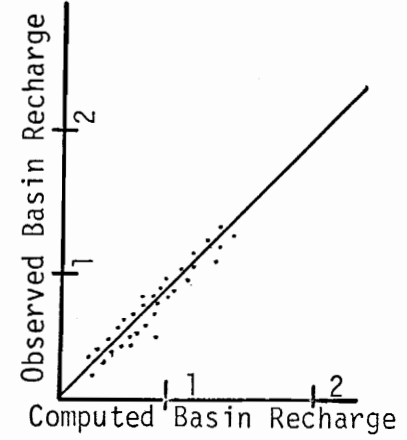
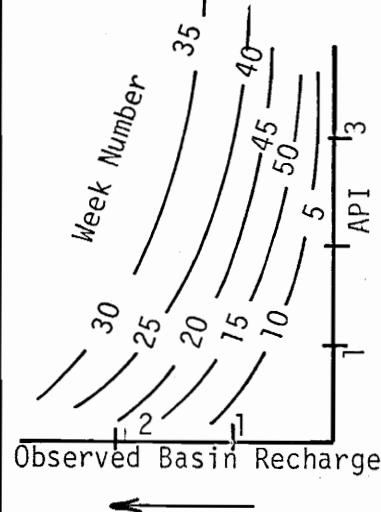


(b)  
Storm Duration Quadrant

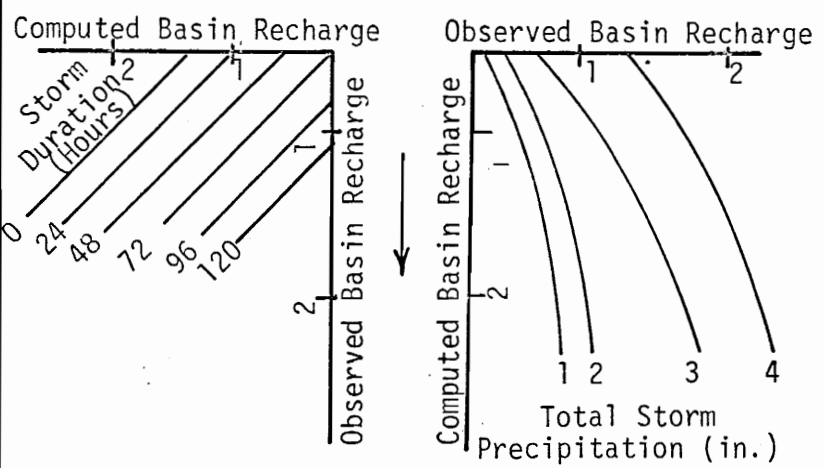
Figure 6(a) and 6(b) Development of a Graphical Coaxial Model (39)



API and Basin Recharge in Inches



(c) Precipitation Quadrant



(d) Accuracy Quadrant

Figure 6(c) and 6(d) Development of a Graphical Coaxial Model (39)

Next a storm duration quadrant is developed. The basin recharge computed from API and week number is plotted against observed basin recharge and storm duration labeled for each point. A set of curves is fitted through common storm durations. Figure 6b depicts this procedure.

The relationship is next refined by considering total storm precipitation. In a similar fashion basin recharge computed from the season quadrant and the storm duration quadrant is plotted versus observed basin recharge. Points are labeled as to storm precipitation and a set of curves are fitted through points of equal precipitation. Development of the precipitation quadrant is shown in Figure 6c.

Finally computed basin recharge is plotted against observed basin recharge to allow for determination of the accuracy of the relation as shown in Figure 6d. Accuracy is improved by refining sets of curves by entering the plots in reverse order and adjusted by entering the charts with observed basin recharge in the accuracy quadrant, proceeding to the line of storm precipitation, hence to the storm duration curve, then to the week curve and finally API is read from the axis. If the API found in the above manner is not sufficiently close to the observed API for that storm, then the week curve is adjusted accordingly. The remaining quadrants are likewise refined.

Instead of basin recharge total storm runoff can be the final result. Total storm runoff is the total volume of runoff associated with a storm event; however for river forecasting purposes, runoff from incremental time periods is preferable.

An incremental runoff coaxial relationship is derived from an existing coaxial chart for total storm runoff. For a large number of storms accumulated runoff is calculated time increment by increment. Incremental runoff is the difference between successive accumulations. Using a unit hydrograph of one increment duration the storm hydrograph is calculated by multiplying the ordinates of the unit hydrograph by the incremental runoff, lagging the resulting incremental hydrographs, and summing. The calculated storm hydrograph is then compared to the observed storm hydrograph and adjustments made to the calculated incremental runoff until the computed hydrograph and the observed hydrograph are sufficiently similar. API is recalculated for each interval with incremental precipitation. Then using the adjusted API, incremental runoff, week number, and incremental precipitation, a new coaxial chart is developed as previously described, but since the relation is incremental a duration quadrant is not required.

The United States Weather Bureau (18) introduced a retention index to facilitate incremental coaxial relations. Retention index reflects the water in interception and depression storage

and as such is a short term moisture index. Retention index is also a decaying function but the recession factor is less than that for API. Retention index is assumed to be zero at the start of the storm event and is increased with precipitation. Figure 7 shows an incremental coaxial relationship using retention index.

The United States Weather Bureau (18) has adapted the coaxial type of rainfall-runoff relation to the digital computer. The curves involved in a coaxial relation can be expressed as higher order polynomial equations. Using historical climatological and hydrologic data, constants in the polynomials can be derived with numerical optimization techniques. Comparisons of computed and observed runoff are good for mean daily flow.

Although the graphical and the computer coaxial relation can successfully approximate the rainfall-runoff data with which the relations were calibrated, the coaxial relation does not describe the rainfall runoff phenomenon in terms that can be related to basin or storm characteristics.

#### Soil Conservation Service Curve Number Method

The Soil Conservation Service of the United States Department of Agriculture designs and builds hydraulic structures. For these purposes, SCS developed a method to predict storm runoff from rainfall (45). Generally the SCS method has been developed from

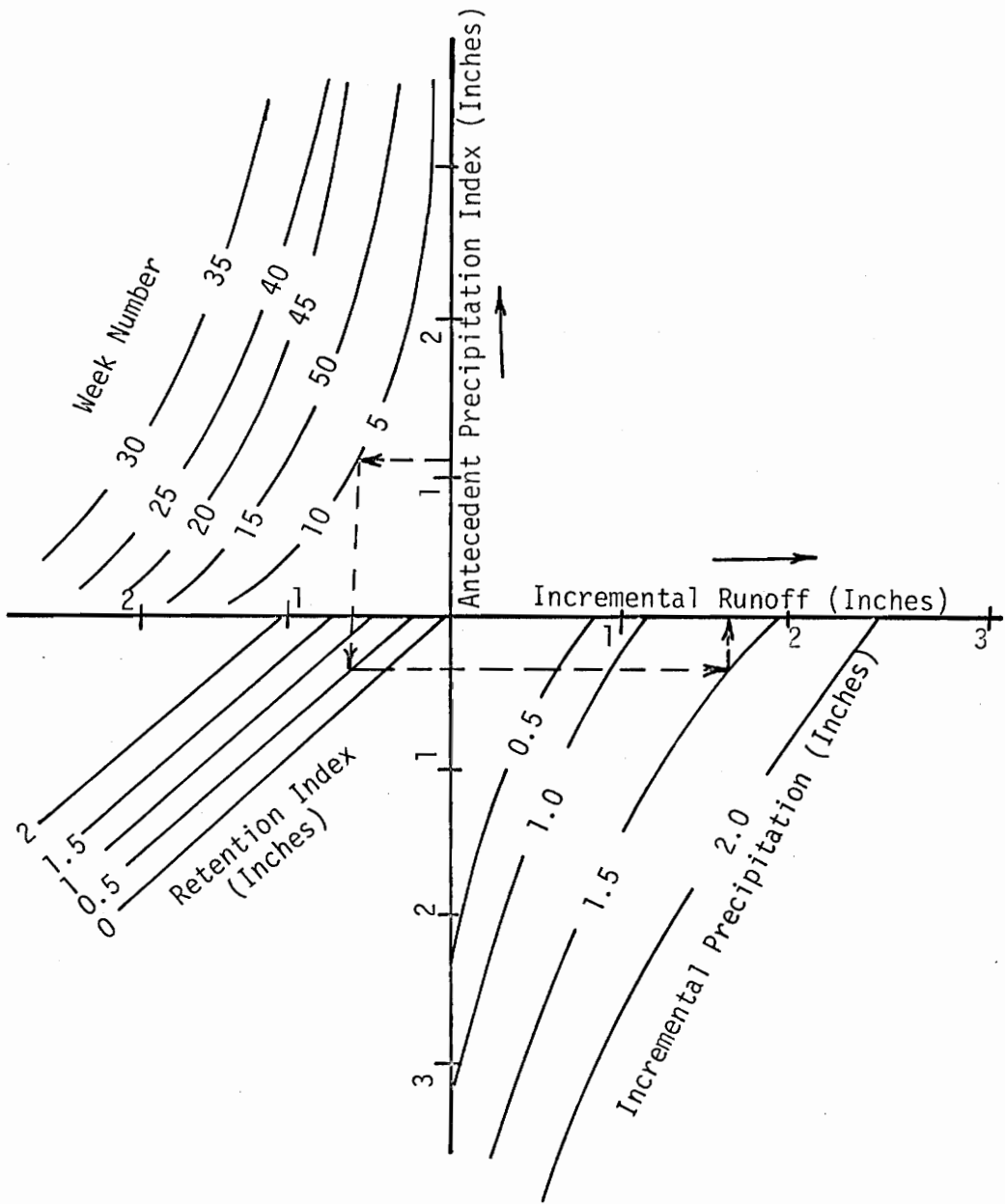


Figure 7 Incremental Coaxial Relation Using Retention Index (18)

data from small nonurban watersheds. The SCS curve number method estimates direct runoff which consists of channel runoff, surface runoff, and subsurface flow in unknown proportions.

#### Development of the curve number method

From a double mass analysis as shown on Figure 8, and neglecting initial abstraction it can be shown that:

$$\frac{F}{S'} = \frac{Q}{P} \quad (4)$$

when  $I_a = 0$ , where

$F$  = the actual retention;

$S'$  = the potential maximum retention ( $F \leq S'$ );

$Q$  = the actual runoff;

$P$  = the potential maximum runoff; and

$I_a$  = the initial abstraction.

Also from Figure 8,

$$F = P - Q \quad (5)$$

Substituting (5) into (4) and solving for  $Q$  yields

$$Q = \frac{P^2}{P + S'} \quad (6)$$

The initial abstraction is taken into account by replacing  $P$  with  $(P - I_a)$  and  $S'$  with  $S$ , where  $S = S' + I_a$ , and  $S$  = the total possible retention. Rewriting (4) and (5) gives,

$$\frac{F}{S} = \frac{Q}{P - I_a} \quad \text{and} \quad (7)$$

$$F = (P - I_a) - Q \quad (8)$$

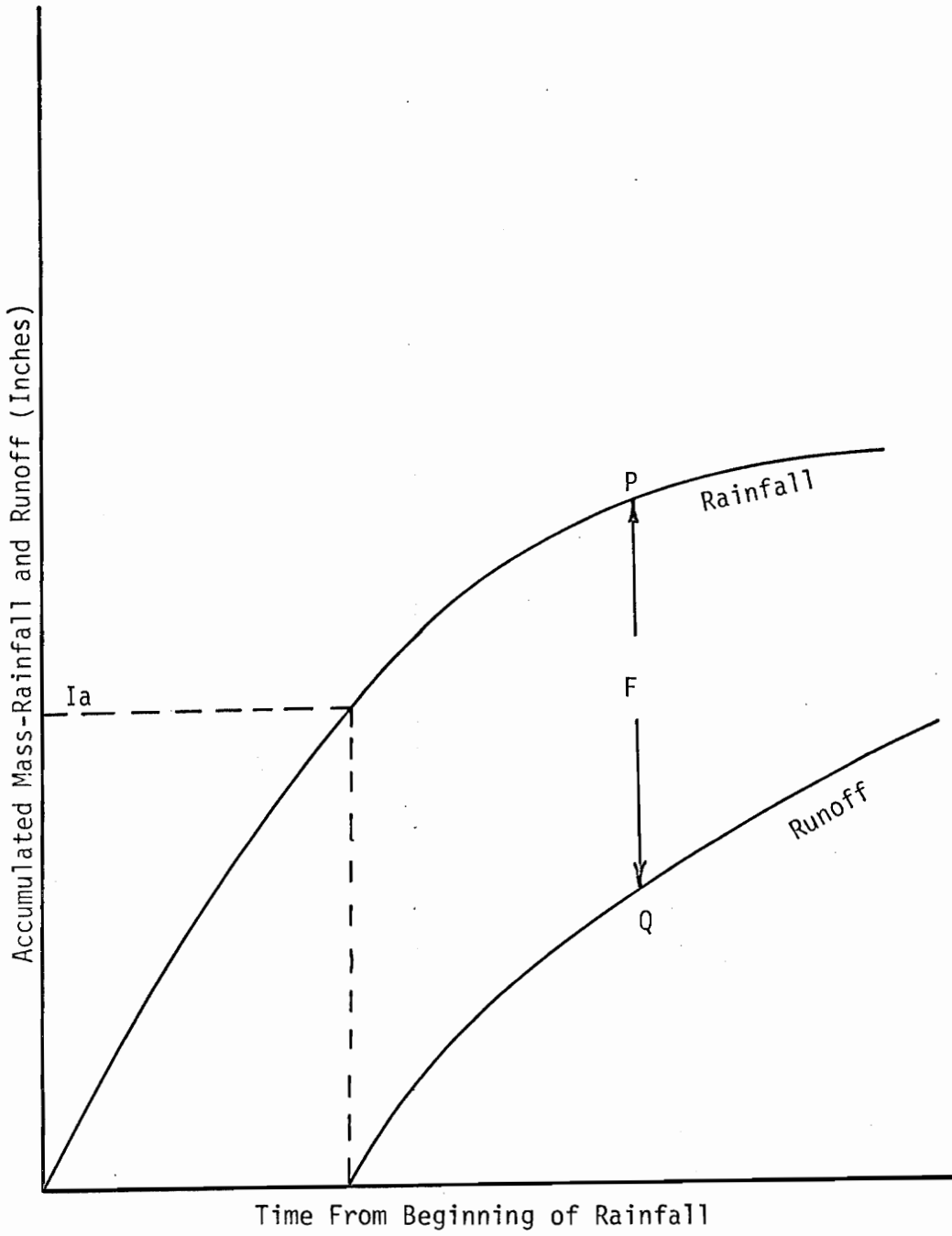


Figure 8 Double Mass Curve of Rainfall and Runoff (45)

where  $S = S' + I_a$ ;

$Q \leq (P - I_a)$ ; and

$F \leq S$ .

Combining (7) and (8) and solving for  $Q$  yields

$$Q = \frac{(P - I_a)^2}{(P - I_a) + S} \quad (9)$$

Equation (9) is the rainfall-runoff relationship including the initial abstraction.  $(P - I_a)$  is the total possible runoff, that is, the precipitation less the initial abstraction and  $S$  is the total possible retention.

#### Retention parameters

A succession of storms, say one per day for a week, will reduce the magnitude of  $S$  each day because the infiltration rate, transmission rate, or soil storage capacity will have been reduced. The controlling factor will not have had the opportunity to recover its rate or capacity through weathering, evapotranspiration, or drainage. There is a lower limit to  $S$ . Even after several large storms over two to three days  $S$  will remain virtually constant. Also an upper limit exists for  $S$  beyond which  $S$  will not recover unless the watershed complex is altered.

The change in  $S$  is a function of antecedent moisture conditions or AMC. AMC is a moisture relating parameter that reflects the total rainfall for a five day period preceding the time being

studied. Three levels of AMC are used: AMC I is the lower limit of moisture or the upper limit of  $S$ , AMC II is the average condition, and AMC III is the upper limit of moisture or the lower limit of  $S$ .

$S$  was estimated by plotting total storm runoff against rainfall. Errors in  $S$  result from errors in average watershed rainfall, but these errors are small.

The total basin retention consists of all the losses that occur from precipitation. Evapotranspiration, surface and subsurface storage, and interception all are a part of  $S$ .  $F$  are those losses that occur after runoff begins, and  $I_a$  are those losses that occur before runoff commences.

$I_a$ , the initial abstraction, consists mainly of water lost to interception, infiltration, and the filling of surface storages all of which occur before runoff begins.  $I_a$  was calculated from many storms on several small watersheds as being the accumulated rainfall to the time that runoff begins. Figure 8 shows  $I_a$ . Errors in  $I_a$  are due to difficulty of determining time when rainfall commenced because of storm travel and lack of instrumentation, difficulty in determining when runoff began, and the inability to determine how much interception prior to runoff later contributes to runoff. Standard errors of estimates for  $I_a$  are large.

Using the values of  $S$  and  $I_a$  as developed above,  $S$  was correlated with  $I_a$  and it was found that

$$I_a = 0.2S \quad (10)$$

Equation (10) shows that 20% of the potential, maximum retention is  $I_a$ . The remaining 80% is mainly the infiltration that occurs after runoff begins. This is controlled by the rate of infiltration at the soil surface, by the rate of transmission in the soil profile, or by water storage capacity of the soil profile. Figure 9 shows the retention parameters. Combining (10) and (9) yields

$$Q = \frac{(P - 0.2S)^2}{P + 0.8S} \quad (11)$$

Equation (11) is the rainfall-runoff relationship used in the SCS method of estimating direct runoff from storm rainfall.

#### Introduction of curve number

Equation (11) shows that direct runoff is a function of precipitation and a basin retention parameter  $S$ . To aid in interpolating, averaging, and weighting operations, a transformation of  $S$  is introduced as the curve number. The transformation is

$$CN = \frac{1000}{S + 10} \quad (12)$$

where  $CN$  = the curve number.

Curve number is a function of soil types, vegetative cover, land use, hydrologic conditions, and antecedent moisture conditions. Soil types are divided into four groups used to determine hydrologic soil cover complexes. When runoff from an isolated storm is of

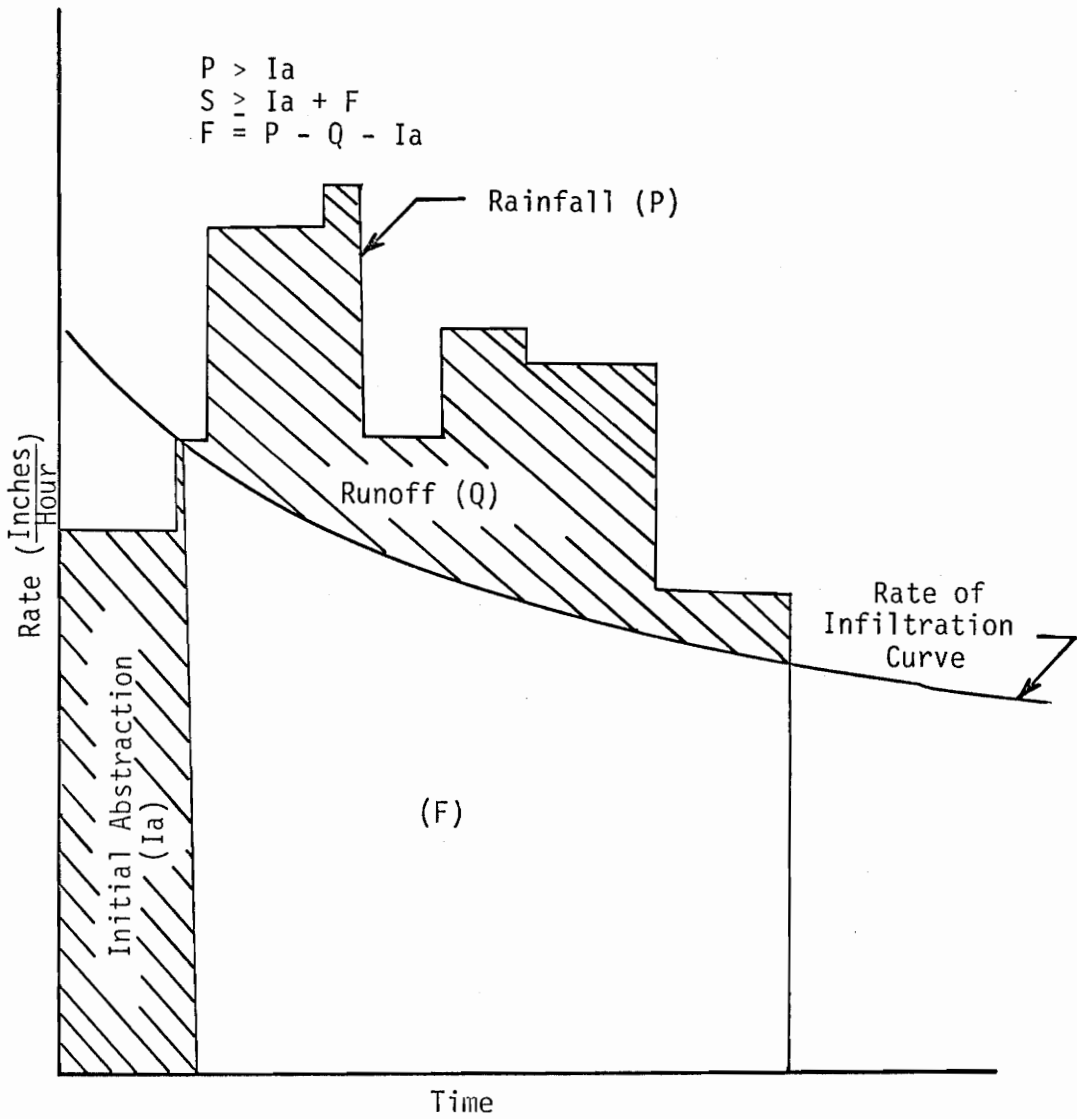


Figure 9 Retention Parameters in SCS Curve Number Method (45)

interest as in flood hydrology, the soil properties can be represented by a hydrologic parameter, i. e. the minimum rate of infiltration obtained for a bare soil after prolonged wetting. This infiltration potential is the qualitative basis for the four group classification. Table I gives the four soil groups. Land use includes watershed cover including vegetation, litter-mulch, fallow soil, water surfaces, and impervious surfaces. Land treatment applies mainly to agricultural practices including terracing, grazing control and rotation of crops.

Hydrologic condition relates the surface retention capability of the soil cover complex. The hydrologic conditions qualitatively range from poor to good as the soil cover complex retains less to more moisture. Antecedent moisture conditions are considered as wet, average, and dry. Appendix C presents tables that show curve numbers for various hydrologic soil cover complexes and antecedent moisture conditions.

#### Procedure to produce flood hydrographs

The above method can be used to compute a flood hydrograph. First the watershed is surveyed to determine hydrologic soil cover complex. Antecedent moisture conditions and curve numbers are next determined. Using the aids given in Appendix C, the curve number is refined more for each hydrologic soil cover complex.

TABLE I SCS HYDROLOGIC SOIL GROUPS (45)

- A. (Low runoff potential) Soils have high infiltration rates even when thoroughly wetted and consist chiefly of deep, well to excessively drained sands or gravels. These soils have a high rate of water transmission.
- B. Soils have moderate infiltration rates when thoroughly wetted and consist chiefly of moderately deep to deep, moderately well to well drained soils with moderately fine to moderately coarse textures. These soils have a moderate rate of water transmission.
- C. Soils have slow infiltration rates when thoroughly wetted and consist chiefly of soils with a layer that impedes downward movement of waters, or soils with moderately fine to fine texture. These soils have a slow rate of water transmission.
- D. (High runoff potential) Soils have very slow infiltration rates when thoroughly wetted and consist chiefly of clay soils with a high swelling potential, soils with a permanent high water table, soils with a claypan or clay layer at or near the surface, and shallow soils over nearly impervious material. These soils have a very slow rate of water transmission.

The curve number is averaged for the watershed. Accumulated precipitation for time increments during the storm event are next determined. Using Equations (11) and (12) the accumulated runoff is calculated. The incremental runoff is the difference between successive accumulated runoff values. Applying unit hydrograph methods to the calculated precipitation excess or runoff produces the flood hydrograph.

#### Model applications and constraints

Assuming accurate precipitation values, the accuracy is dependent upon the proper selection of curve number. Experience and sound judgement are essential for successful application of the curve number method. Since the curve number method was formulated for small rural watersheds, larger watersheds must be broken down into smaller subbasins to accurately apply the method. Urban areas have presented some problems for SCS due to the impervious surfaces in urban watersheds. Presently SCS is considering an urban revision to the method. Errors can result if curve number is not reinvestigated for each season. For example, a field could be in corn, a row crop, one season with a curve number of say 75 and in ground cover the next season with a curve number of 64. The SCS curve number method of estimated direct runoff from precipitation was developed as an aid in designing small flood retention structures. A design frequency storm is developed for

the watershed under study and the runoff predicted using the rainfall-runoff relation. River forecasting can be accomplished with the curve number method and the method is readily adapted to the digital computer. Although simple to use, the SCS rainfall-runoff relation does not quantify the various processes that compose the hydrologic cycle, but considers the watershed characteristics in terms of the lumped parameter, namely the curve number.

#### Corps of Engineers' Hydrologic Engineering Center Method

The Corps of Engineers' Hydrologic Engineering Center formulated a predictive rainfall-runoff relationship to aid the Corps' efforts in flood control (36,37,40). Figure 10 shows the method of modeling river behavior.

Precipitation excess is calculated by reducing the precipitation available for runoff by a loss rate function. A unit hydrograph is next applied to the precipitation excess to produce a streamflow hydrograph, which is then hydraulically routed.

#### Loss rate function

The loss rate function is given by

$$L = K_1 P_1^E \quad (13)$$

where  $L$  = the loss rate in ( $\frac{\text{inches}}{\text{hour}}$ ),

$K_1$  = a coefficient decreasing with ground wetness,

$P_1$  = the precipitation rate in ( $\frac{\text{inches}}{\text{hour}}$ ), and

$E$  = an exponent depending on the variations of factors

within the basin,  $0 \leq E \leq 1.0$

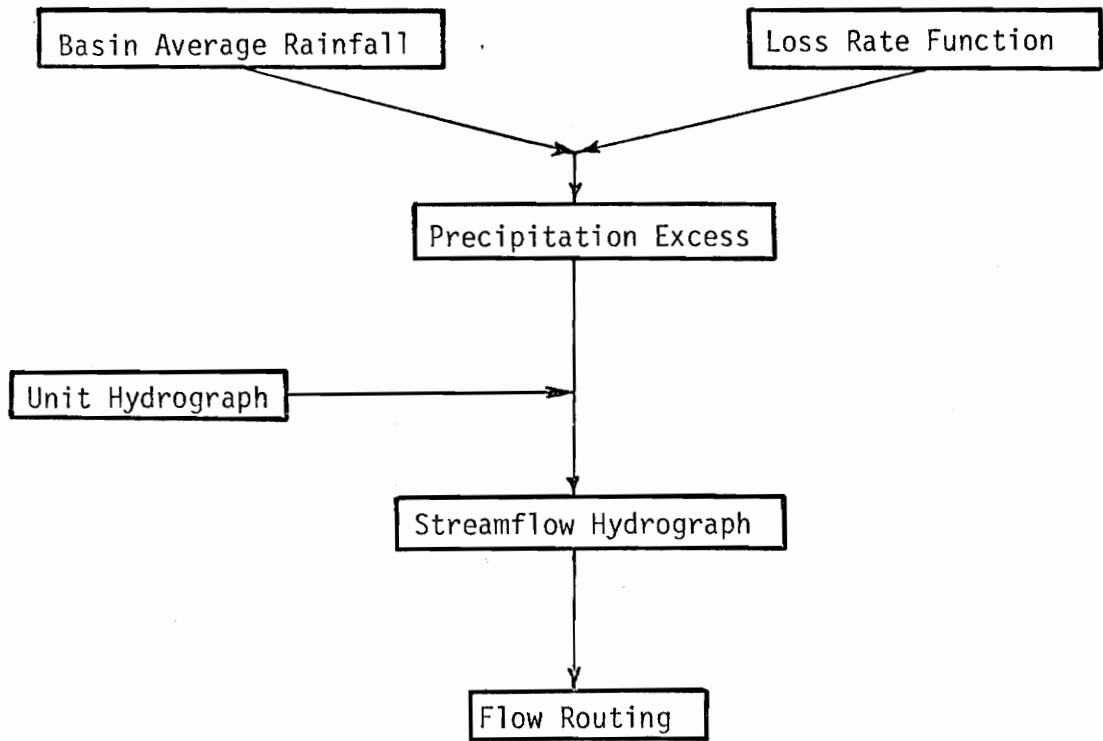


Figure 10 Hydrologic Engineering Center Method (40)

When  $E = 0$  the loss rate is independent of the rainfall intensity but when  $0 < E < 1$ , the loss rate is a function of rainfall intensity. Hydrograph reconstruction indicates that  $E$  ranges from 0.3 to 0.9. Frequently  $E$  is used as 0.7 for uniformity.

The loss rate coefficient  $K$  in Equation (13) decreases with ground wetness and is given by

$$K_1 = K_0 C^{\left(\frac{-L_1}{T_0}\right)} \quad (14)$$

where  $K_0$  = the loss rate coefficient at the start of the storm,

$C$  = the coefficient controlling the rate of decrease of  $K_1$ , and

$L_1$  = the accumulated loss during the storm.

To account for initial soil moisture deficiency, Equation (13) is usually modified to

$$L_1 = (K_1 + K') P_1^E \quad (15)$$

where  $K'$  = a modified coefficient given by

$$K' = 0.2D \left(1 - \frac{L}{D}\right)^2 \quad (16)$$

where  $\frac{L}{D} \leq 1.0$ , and

$D$  = the initial soil moisture deficiency in inches.

The general loss rate function is shown in Figure 11.

#### Procedure for hydrograph reconstruction

Streamflow and precipitation gages are first selected for the study region. The tributary areas should be within a size range comparable to the tributary watershed sizes.

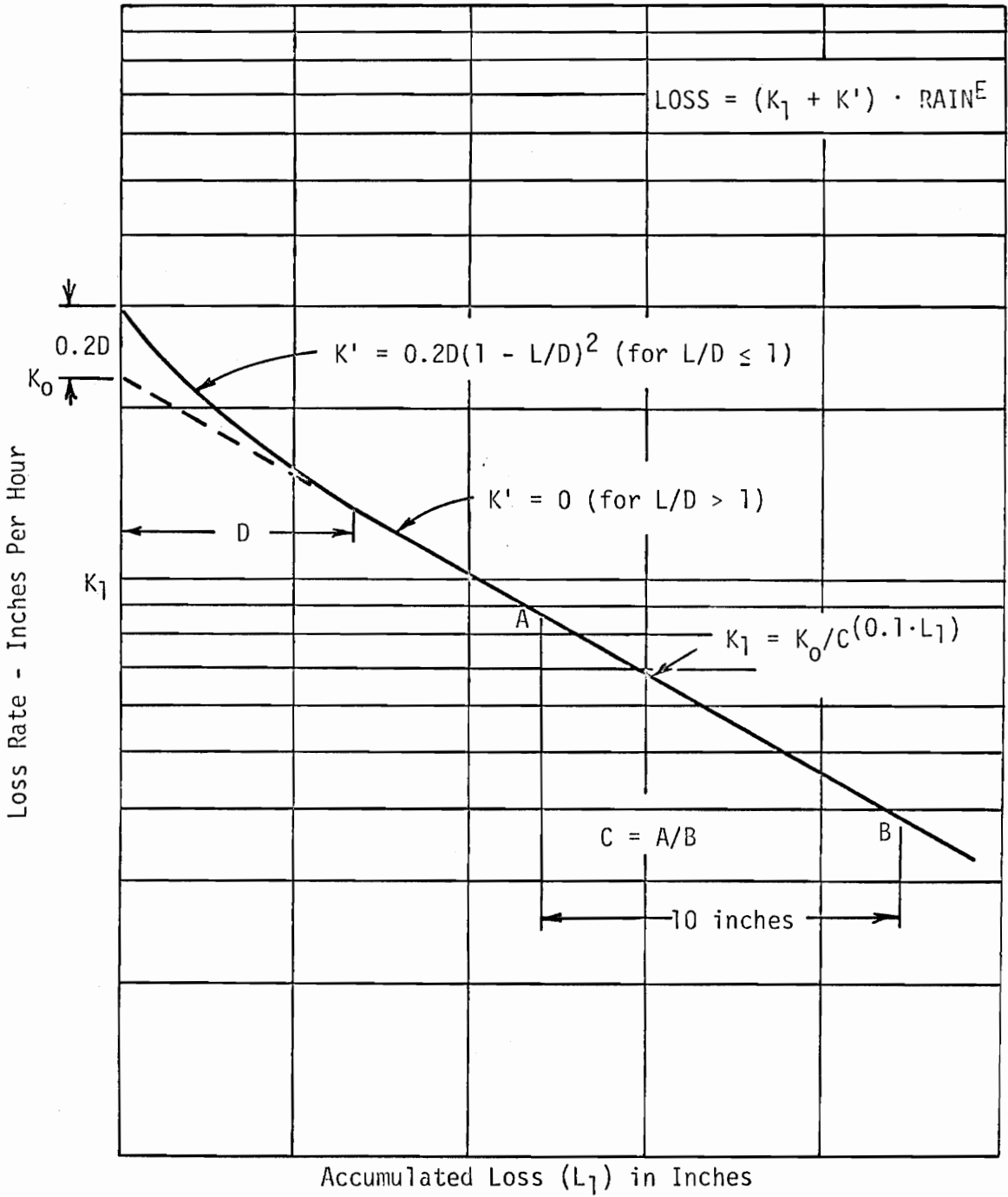


Figure 11 General Loss Rate Function (40)

The gaged areas also should have roughly the same soil types, land use, and vegetal cover. Precipitation and flow data are collected at each gage so that basin average precipitation, applicable to each subbasin being studied, can be computed during reconstruction.

For each streamflow gage and storm, the recession flow for antecedent runoff is determined. The recession coefficient for each storm and gage is then calculated from a semi-logarithmic plot of recession flow versus time. Using computer optimization techniques the starting value of the loss coefficient,  $K_0$ , on an exponential recession curve for rain losses is computed.  $K_0$  is a function of infiltration capacity and thus depends upon soil types, land uses, and vegetal cover. Next the amount of initial accumulated rain loss during which the loss rate coefficient increases is calculated. This initial loss is dependent upon antecedent soil moisture deficiency and is also calculated by an optimum gradient search method.  $C$  in Equation (14) is computed as the ratio of rain loss coefficient on an exponential loss curve to that  $K$  corresponding to 10 inches more of accumulated loss.  $C$  can be considered as a function of the ability of the basin surface to absorb precipitation. The value of  $C$  for each storm and gage is also optimized by computer.  $E$  the precipitation

exponent in Equation (13) is calculated for each storm and gage by computer optimization. The initial soil moisture deficiency is similarly calculated for each storm and gage. Using the values calculated above, regional values of E and C are selected.

After an initial set of coefficients is selected, the calculated rainfall loss is deducted from the basin average precipitation to yield an incremental precipitation excess. The time increment corresponds to the duration of a previously derived unit hydrograph. Applying the unit hydrograph to the calculated precipitation excess, lagging, and summing the resultant incremental hydrographs yields a reconstructed storm hydrograph. The observed and reconstructed hydrographs are compared and the various constants adjusted if necessary.

#### Model application and constraints

All the parameters are lumped temporally and spatially. If area averages are not appropriate, then a smaller subarea should be used. Also the time interval used should be small enough so that averages over the interval computations are applicable.

An important limitation is that the HEC model is not a continuous model. The HEC model can be applied to single storm events or for multi-storm events sufficiently close in time. No provision is made for loss rate recovery during periods of no precipitation. This limitation restricts the use of the HEC model as a forecast tool.

In order to use the HEC model as a predictive model, the initial loss rate  $K_0$  and the initial soil moisture deficiency  $D$  would have to be determined.  $K_0$  and  $D$  could be calculated by considering  $K_0$  and  $D$  as a function of season and antecedent moisture conditions for a given watershed.

Like the SCS method the HEC model does not quantify the rainfall-runoff cycle by actually modeling the process. The phenomenon is accurately simulated but the simulation does not follow the correct physical process.

#### Stanford Watershed Model

Crawford and Linsley (39) developed a rational detailed quantitative model of the hydrologic cycle. The Stanford watershed model was one of the first attempts to simulate on a digital computer the individual components comprising the hydrologic cycle. Incoming moisture is allocated to each of the several hydrologic components which are each modeled by a separate routine. Just as the hydrologic cycle on the land surface can be considered as moisture into the system - moisture out of the system, the Stanford model is basically moisture into the stream, i.e. precipitation - moisture out of the system, i.e. streamflow, evapotranspiration.

### Model concepts

The water budget of an area is mathematically simulated by a soil water accounting process that is expressed as

$$SM_t = SM_{t-1} + P_{1t} + (ML_g) - Q_t - PC_t - ET_t - (ML_l)_t \quad (17)$$

where  $SM$  = the soil moisture status;

$P_1$  = all natural or applied water, i.e. precipitation;

$(ML_g)$  = the minor gains;

$(ML_l)$  = the minor losses;

$Q$  = the stream flow;

$PC$  = the deep percolation;

$ET$  = the evapotranspiration; and

$t$  = a subscript denoting time.

From continuity Equation (17) becomes

$$\frac{\partial SM}{\partial t} = \frac{\partial (P_1 + ML_g)}{\partial t} - \frac{\partial (Q + PC + ET + ML_l)}{\partial t} \quad (18)$$

Equation (18) is solved by calculating each of the individual components over the time interval  $\Delta t$ .

Precipitation and potential evapotranspiration are the major data inputs. Temperature and radiation data are used if snowmelt is to be considered. Moisture conditions are either known or assumed, from which computation commences and is continued until the input data is exhausted. Three soil moisture storages and any existing snowpack receive the incoming precipitation.

Variable soil moisture profiles and groundwater conditions are represented by upper zone, lower zone, and groundwater storages. Overland flow, infiltration, interflow, and inflow to groundwater storage are controlled by upper and lower zone storages. Initial watershed response to rainfall is simulated by the upper zone which is of primary importance for smaller storms and for the first few hours of larger storms. The lower zone controls watershed response to major storms by controlling longer infiltration rates. Base flow into stream channels and deep seepage is supplied from the groundwater storage. The model considers all of the storages susceptible to evapotranspiration. Finally total inflow to the channel is simulated and the hydrograph routed. Mean daily flows, hourly flows, and monthly flows can be simulated by the Stanford watershed model IV. Figure 12 shows the structure of the model by means of a flow chart.

#### Model components

Volume of precipitation, snowmelt, plus the surface detention carryover which is available to infiltration is the moisture supply.

Interception is governed by watershed cover and the current volume of water in interception storage. All precipitation enters the interception storage until some preassigned value is reached. Evapotranspiration occurs for interception storage at a rate equal to the input potential evapotranspiration rate.

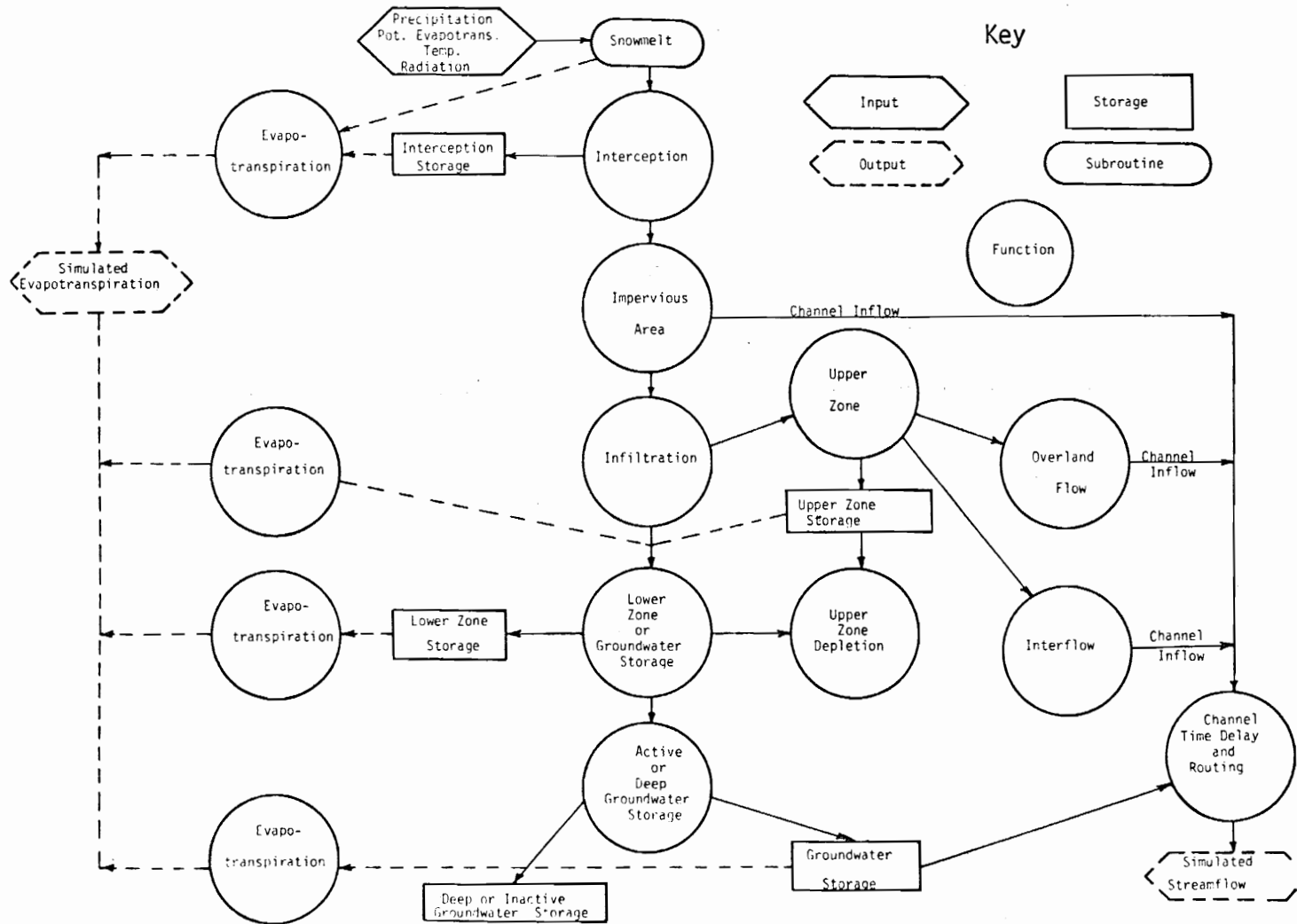


Figure 12 Flowchart of the Stanford Watershed Model IV (39)

Precipitation onto the water surface and impervious areas contiguous to the stream channel contributes to direct surface runoff. This impervious fraction of the watershed is represented by a preset parameter. Other impervious areas not directly connected to a stream channel are represented by direct infiltration functions of the model as water falling on these surfaces is eventually subject to flow over pervious surfaces.

Direct infiltration is continuously simulated by two interlocking calculations. The two calculations describe the direct infiltration into the soil profile and the increases in temporary storages that result in delayed infiltration. Available moisture is first subject to the cumulative watershed infiltration capacity functions that model overall watershed reaction, and control direct flows into the long term lower zone and groundwater storage. Water that remains in surface detention after direct infiltration to the lower zone is calculated and is subject to operations of the upper zone storages. Diversion of overland flows into depression storages, soil fissures, and dry or disturbed surface soil is modeled by the upper zone. Both the upper and lower zone are assigned nominal storage capacities.

Upper zone storage controls delayed infiltration simulation in the model. Moisture not directly infiltrated to the lower zone will augment water in surface detention storage which either becomes interflow, overland flow or goes into upper zone storage.

Upper zone inflow rates are independent of rainfall intensity, but upper zone storage capacity is low. The volume of water stored in the upper zone and the nominal upper zone storage controls overland flow surface detention. Evapotranspiration removes water from the upper zone storage at the potential rate.

Delayed infiltration or percolation occurs from the upper zone to groundwater and to the lower zone when

$$\frac{U Z S}{U Z SN} > \frac{L Z S}{L Z SN} \quad (19)$$

where  $U Z S$  and  $L Z S$  = the current water in the upper and lower storages respectively, and

$U Z SN$  and  $L Z SN$  = the nominal storages for the upper and lower zones respectively.

Percolation is a function of  $U Z S$ ,  $U Z SN$ ,  $L Z S$ ,  $L Z SN$ , and a preassigned value  $CB$ . Interflow occurs from the upper zone as a function of interflow detention storage,  $IDS$ ; and a preassigned daily recession constant,  $DRC$ ; or

$$\text{Interflow} = IDS \left(1 - DRC^{\frac{1}{96}}\right) \quad (20)$$

Figure 13 shows the model's concept of the disposition of moisture subject to the action of the upper and lower zones, and Table II presents the disposition as land surface response.

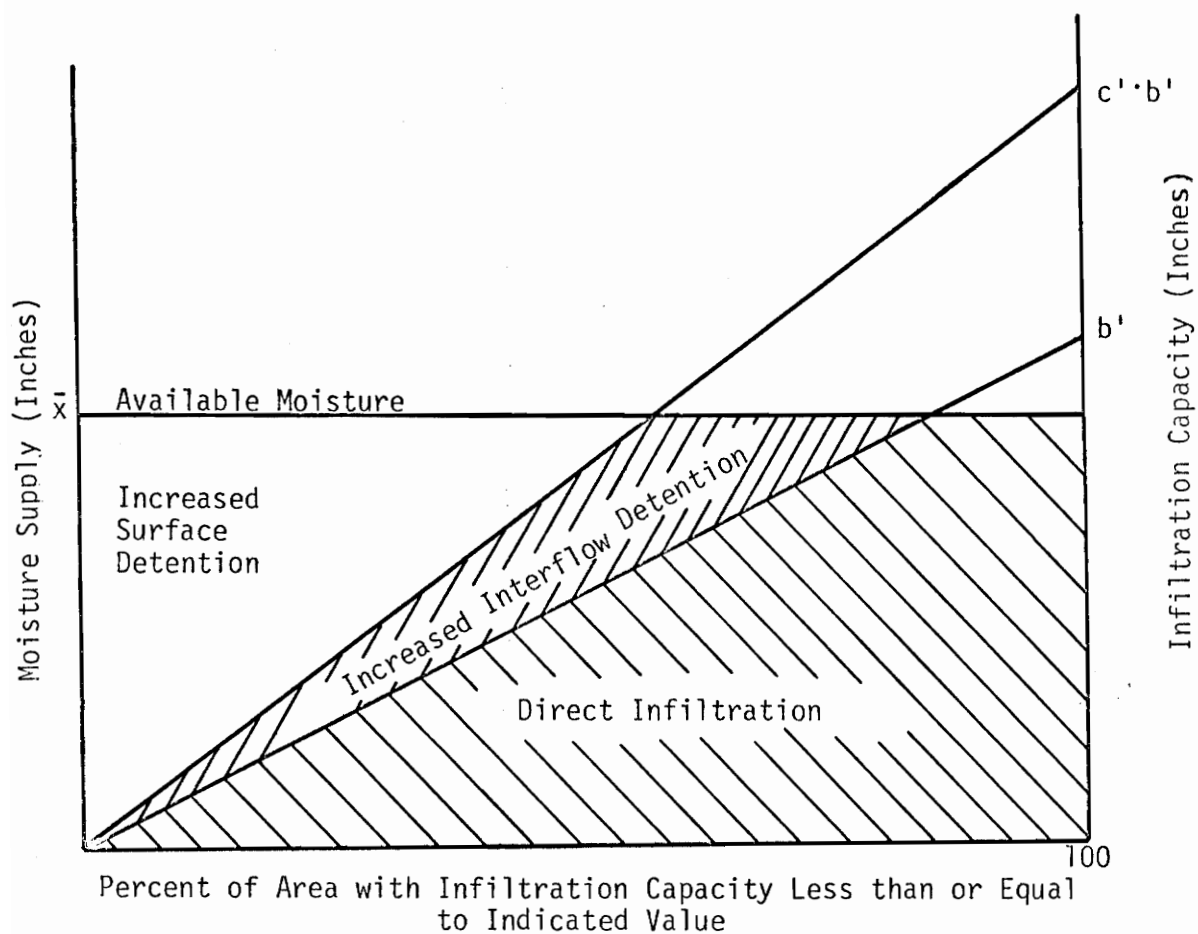


Figure 13 Model Disposition of Moisture Subject to Infiltration (39)

The lower zone controls groundwater flow, groundwater storages, and deep seepage. The quantity of groundwater infiltration to storage is dependent upon  $b$  and  $c$  which are functions of preassigned constants,  $L Z S$ , and  $L Z SN$ . Groundwater flow is a function of groundwater storages, a preassigned recession constant, and the groundwater slope. Percolation to deep or inactive groundwater storage is modeled as a function of a preassigned value and the inflow to groundwater storage. Lower zone storage is also subject to evapotranspiration and is simulated as a function of the potential evapotranspiration,  $L Z S$ ,  $L Z SN$ , and a preassigned constant.

Evapotranspiration removes moisture from water on the land surface and from within the soil profile. From the upper zone, moisture is subject to evapotranspiration at the potential rate, while evapotranspiration opportunity controls evapotranspiration from the lower zone. The area of surface water, which is an input parameter, is subject to evapotranspiration also at the potential rate. Potential evapotranspiration will result in actual evapotranspiration, a water loss, only if water is available. The model first attempts to satisfy potential evapotranspiration from interception storage and the upper zone in that order and then from the lower zone.

Overland flow is simulated by the continuity equation:

$$D_2 = D_1 + \Delta D - \bar{q} \Delta t \quad (21)$$

where  $D_2$  = the surface detention at the end of the time interval  $\Delta t$ ;

$D_1$  = the surface detention at the beginning of the time interval  $\Delta t$ ;

$\Delta D$  = the increment of water added to surface detention during the time increment  $\Delta t$ ; and

$\bar{q}$  = the rate at which overland flow drains into the stream channel.

The routing of overland flows is modeled using preassigned values of slope, length, and roughness.

If snowmelt is considered, the model utilizes temperature, short wave radiation, and precipitation data to calculate snowmelt and the amount of precipitation stored in the snowpack. Energy relationships are used to determine water released from snowpack.

Once water available to stream flow is calculated channel routing is done by using an empirical storage routing method. The model assumes the overflow hydrograph is based upon a time-area histogram and an instantaneous rainfall.

#### Watershed parameters

Some twenty-eight parameters are used in the model to describe the watershed and thus quantify hydrologic response. There are four groups of parameters.

TABLE II LAND SURFACE RESPONSE AS A FUNCTION OF  
MEAN MOISTURE SUPPLY,  $\bar{x}$  (39)

Component	$\bar{x} < b$	$b < x < c, b$	$\bar{x} > c, b$
Net Infiltration	$x - \frac{\bar{x}^2}{2b}$	$\frac{b}{2}$	$\frac{b}{2}$
Increase in Interflow Detention	$\frac{\bar{x}^2}{2b} (1 - \frac{1}{c})$	$\bar{x} - \frac{b}{2} - \frac{\bar{x}}{2 \frac{c}{b}}$	$\frac{b}{2}(c - 1)$
Increase in Surface Detention	$\frac{\bar{x}^2}{2 c, b}$	$\frac{\bar{x}^2}{2 c, b}$	$\bar{x} = \frac{c, b}{2}$
Percentage of Increased Detention Assigned to Interflow	$100(1 - \frac{1}{c})$	$100(1 - \frac{\bar{x}^2}{2 c, b(\bar{x} - \frac{b}{2})})$	$100(\frac{c - 1}{(\frac{2\bar{x}}{b} - 1)})$

Initial moisture status is quantified by five parameters. These parameters describe the water content on the land surface, within the soil profile, and in the groundwater. Each parameter is estimated for a first simulation run of the model, and then adjusted as required.

Parameters obtained from watershed characteristics comprise the second group. Such parameters are measurable from topographic maps and field surveys. Included are drainage area, slope, area of water surface, impervious fraction of watershed adjacent to stream channels; Manning's roughness values, length of overland flow, and the fraction of watershed area from which moisture is lost from groundwater through phreatophytes.

A third group consists of parameters estimated from historical records. Parameters for interception, evaporation, and variables relating to the stream channel system are included.

The last group contains parameters which are estimated from trial adjustments. In the model these parameters direct the allocation of incoming moisture to the various storages, control flow regimes, and control seasonal variation and water yields. Since the model is sensitive to this group and parameters in the group do interact, several computer optimization runs may be needed to determine an optimum set.

### Model operation

The model utilizes input data from any number of recording precipitation gages and a hydrograph is generated for a series of stations along the stream channel. A large watershed is divided into subbasins which are individually modeled. Each subbasin should contain at least one daily or storage rain gage, but one or more subbasins may utilize the same recording gage. Flow to the downstream end of the stream channel in a subbasin, or flow point, is calculated. Inflow from each subbasin is simulated independently so that areal variations in precipitation and watershed characteristics can be represented. The model calculates the flow hydrograph at each flowpoint from the discharge calculated for the adjacent upstream subbasin and the inflow from the contributing subbasin. There is no limit to the number of flow points that can be simulated.

### Model application and constraints

The model is capable of simulating mean daily flows, hourly flows, and monthly flows. Both small and large watersheds are within the range of capability of the model. Linsley and Crawford (30) applied the model to watersheds ranging from 0.38 square miles to 1300 square miles of drainage area with good results. For mean daily flows, the correlation coefficient for observed and simulated flows ranged from 0.9907 to 0.9928 and the standard errors were low.

Shanholtz (32) applied the model to two rural watersheds of 786 and 893 acres. Estimates of annual runoff were within measurement accuracy while monthly estimates were within 5% of the observed monthly discharges. However estimates of maximum mean daily peak discharges were erratic, and although the absolute error was small, the percentage error was large due to the small water yield.

Shanholtz (32) made the following conclusions regarding the Stanford watershed model:

1. Considerable familiarity with the model is necessary to arrive at an optimal set of values for those parameters requiring trial and adjustment.
2. Care must be exercised when using the model to generate streamflow for an area in which no historical streamflow records are available for comparative purposes.
3. The model, like all current deterministic watershed models, is not an exact formulation of the process occurring within the hydrologic cycle and therefore must be used accordingly.
4. The model can provide approximations for the practicing engineer which would be difficult to obtain otherwise.

5. By judicious use of the model, insight can be obtained on the effect of specific changes within the system being synthesized.
6. For the most part, the model appears to simulate the hydrologic process within the accuracy of basin input data.
7. Modification of the upper zone storage allocation procedure appears to be necessary to better simulate the response from small storm events.

Of the four schemes discussed, the Stanford watershed model is the most versatile, the most accurate, and by far the most complicated. A great understanding of the model is necessary to utilize the model to its fullest extent. More computer capability is required for the Stanford model than for the other three yet the core storage required is not excessive as it is of the order of 180,000 bytes for simulation runs. The Stanford model is well suited for flood peak predictive purposes once proper calibration is attained. No mention is made in the literature as to the accuracy of the flow routing procedures.

Since the development of the Stanford model, other conceptual models of the rainfall-runoff process have been introduced (38,46,47).

### III. THE MODEL

#### Justification of Selection

Selection of a method to predict runoff from precipitation depends upon the anticipated use and the ease of application of the method. The desired use of the method presented herein was to provide a precipitation excess generator to calculate runoff values to be used in an implicit flood routing scheme. It was desired to transform precipitation into surface runoff which by applying unit hydrograph methods would yield a stream-flow hydrograph.

Criteria for selection of a method also included the ease of application both to the existing flood routing program and to the river basins being modeled. Therefore the selected method was desired to be simple and readily programmable. It was essential that model calibration be made utilizing readily obtainable hydrologic and meteorologic data for the modeled river basin.

Both the SCS curve number method and the Corps HEC model were best suited to design type applications and not actually formulated for river forecasting. The Stanford watershed model was suited for use as a river forecasting tool, but the Stanford model was an extensive complicated program. Considerable modification would have been required to utilize the Corps' or SCS' methods and some changes would have been required to use the

Stanford model. Because too much computer storage would have been needed to store the various curves of a coaxial API type model, it too was not considered further. However a mathematical model similar in concept to the graphical API model was selected.

#### Model Description

The model used in the present study is an API type rainfall-runoff model developed by the Tennessee Valley Authority (28). The model predicted surface runoff from rainfall, API, and calendar week number. Two equations with five coefficients and three parameters expressed the relation.

#### Model Development

TVA began by considering a mathematical API model as developed by the U. S. Weather Bureau. Successive restrictions were imposed on the U. S. W. B. version until the model was as concise as possible.

The season quadrant of the coaxial model was retained conceptually by the Weather Bureau. A winter condition, or high flow curve, and a summer condition, or low flow curve, were the extremes that defined the operating region as shown in Figure 14. TVA defined the winter and summer extremes as exponential expressions which were:

$$RI_w = wc + wa (e^{-wb.API}) \quad (22)$$

and

$$RI_s = sc + sa (e^{-sb.API}) \quad (23)$$

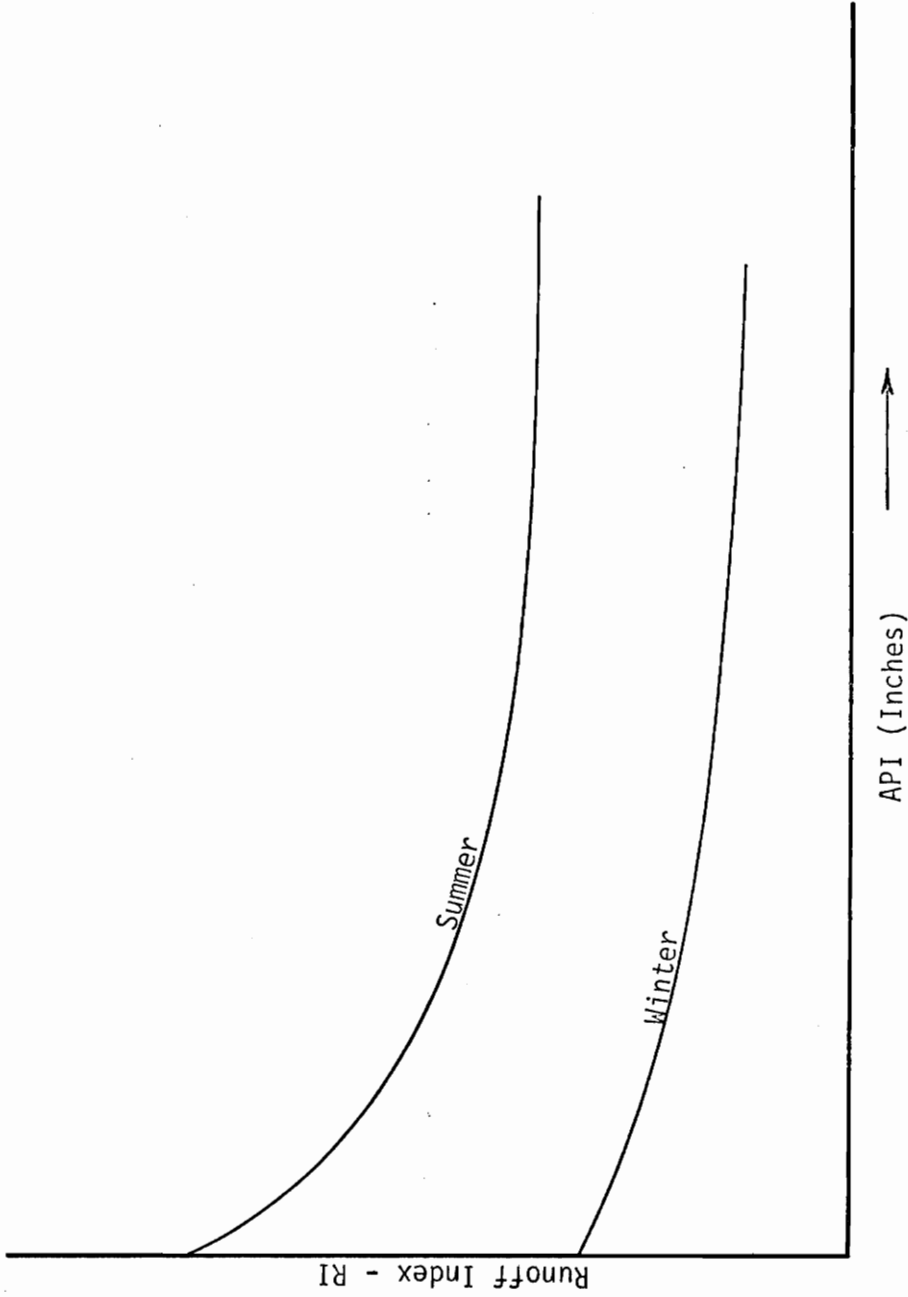


Figure 14 Season Quadrant (28)

where  $w_a, w_b,$  and  $w_c$  = model coefficients for the winter curve;  
 $s_a, s_b,$  and  $s_c$  = model coefficients for the summer curve; and  
 $s$  and  $w$  = subscripts denoting summer and winter,  
 respectively.

To interpolate between the winter and summer extremes the Weather Bureau devised an interpolation function as shown on Figure 15. A Fourier approximation, which has the effect of defining a continuous smooth function, was applied to the straight-line segments of Figure 15 so that the breakpoints between the seasons could be determined analytically. Using the interpolation function the interpolation relationship for RI became:

$$RI = RI_w + (RI_s - RI_w) SI \quad (24)$$

where  $SI$  = the season index as given in Figure 15.

The season quadrant required nine parameters at this stage of development.

A duration quadrant as used in the coaxial model was not included.

A mathematical relation for the surface runoff quadrant of the coaxial method as developed by the Weather Bureau was utilized by TVA. Surface runoff was given by:

$$SRO = (RF^N + D^N)^{\frac{1}{N}} - D \quad (25)$$

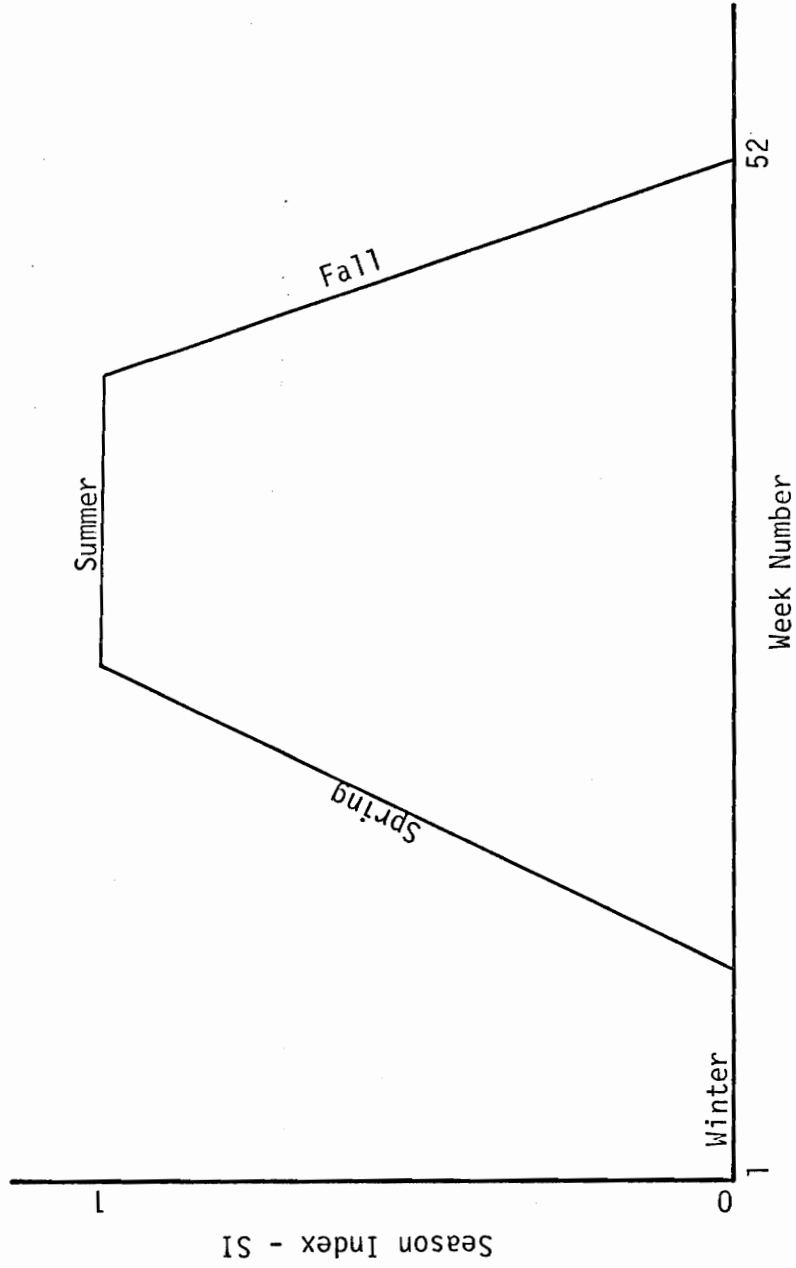


Figure 15 Interpolation Function (28)

where SRO = the storm surface runoff in inches;

RF = the storm rainfall in inches;

D = the deficiency parameter; and

N = the degree of curvature parameter.

The expression for the surface runoff relation was Equation (25) which was asymptotic to a 45 degree line, i.e., incremental rainfall equaled incremental runoff, which had an intercept equal to D. Figure 16 shows the surface runoff relation. D and N were related to the seasonal relation by:

$$D = d_a + d_b RI^{d_c} \quad (26)$$

and

$$N = n_a + n_b RI^{n_c} \quad (27)$$

where  $d_a$ ,  $d_b$ , and  $d_c$  = model coefficients that define D; and

$n_a$ ,  $n_b$ , and  $n_c$  = model coefficients that define N.

At this stage of development, the model contained fourteen coefficients. TVA determined the values of the fourteen coefficients by a method of steepest descent optimization technique that minimized the sum of the square of the errors. As expected, the accuracy of the results of this mathematical relation was comparable to those obtained with the original coaxial model. However, the solution was oscillatory and did not converge. The lack of convergence was attributed to an over-determined model or too many interrelated coefficients.

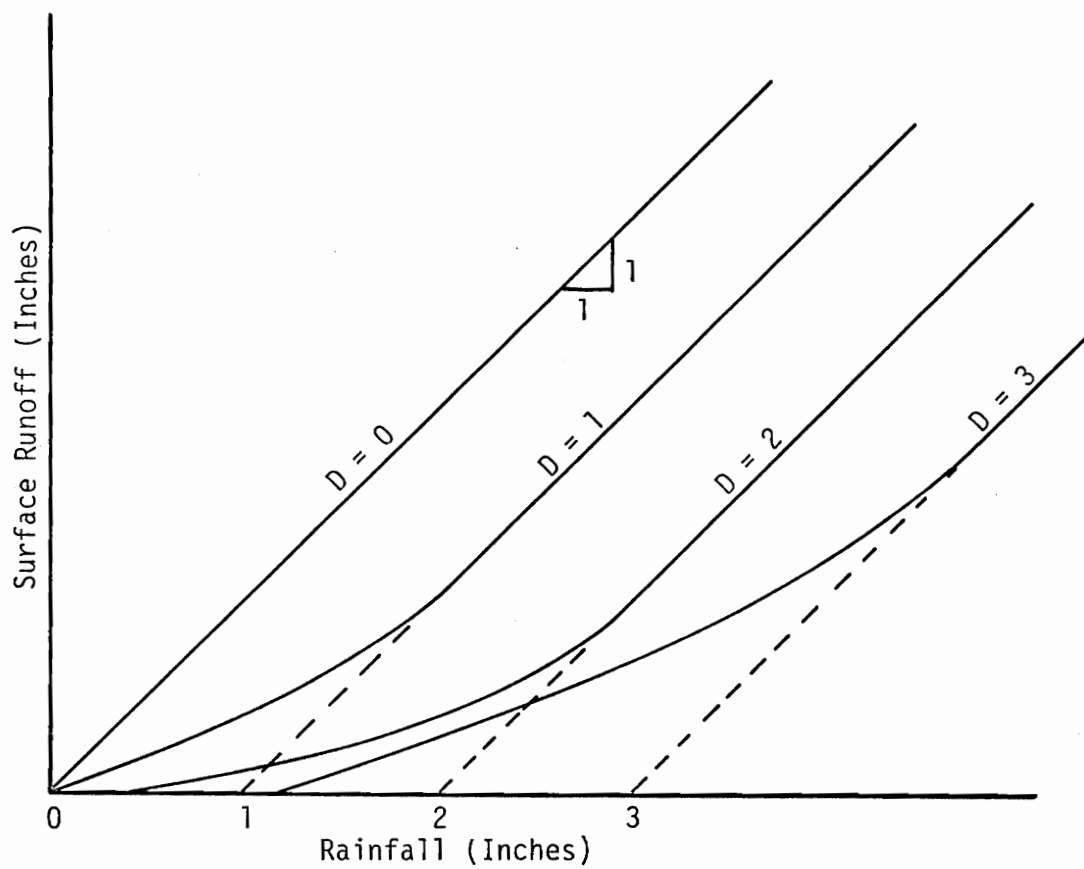


Figure 16 Surface Runoff Relation (28)

In order to reduce the number of coefficients, the model coefficients were analyzed to determine model sensitivity to each coefficient. Those that least affected the results were deleted or fixed. Each improvement was based upon an error analysis and a study of the interactions of coefficients.

First the N relationship was simplified. Equation (27) was eliminated and N in Equation (25) was replaced by n. Thus n was not a function of RI. Simultaneously  $w_c$  and  $s_c$  in Equations (22) and (23), the seasonal extreme equations, were replaced by a single coefficient c which assured that season curves would not cross. c limited the value of  $RI_S$  and  $RI_W$  as API grows large. Next,  $d_c$  in Equation (26) was set to unity thus D became linearly equivalent to RI, and Equation (26) was eliminated. At this stage of refinement Equation (24) remained unchanged; Equations (26) and (27) were eliminated; and Equation (25) was revised to:

$$SRO = (RF^n + RI^n)^{\frac{1}{n}} - RI \quad (28)$$

Equation (22) became:

$$RI_W = c + wa (e^{-wb \cdot API}) \quad (29)$$

and Equation (23) was rewritten as:

$$RI_S = c + sa (e^{-sb \cdot API}) \quad (30)$$

The model then was defined by four equations with nine coefficients.

This model produced better results than preceding versions yet only two coefficients,  $n$  and  $c$ , were converging. A study of the convergency patterns yielded the fact that an interaction existed between the interpolation function and the season curves. Therefore, the interpolation function was restricted and the Fourier approximation coefficients were eliminated. The remaining coefficients were forced to adjust to compensate for errors arising from the restriction of the interpolation functions. Figure 17 presents the restricted interpolation function. The restriction of the interpolation function resulted in the elimination of three coefficients and fixed the seasonal breakpoints at 11, 27 and 42 weeks.

With the six coefficient model, rapid convergency was usually obtained. However since most of the storm data was for winter storms, the coefficients,  $s_a$  and  $s_b$  in Equation (30) sometimes became unreasonable because the data was not sufficient to define  $RI_S$ . Therefore TVA forced each storm to influence both season curves by replacing Equations(24), (29) and (30) with a single equation:

$$RI = c + (a + d.SI) e^{-b.API} \quad (31)$$

where  $a$ ,  $b$ ,  $c$ , and  $d$  = model coefficients.

Also  $SI$  was limited to  $-1.0$  for the winter extreme and to  $1.0$  for the summer extreme. The final model was defined by two equations with five coefficients and a seasonal interpolation function, i.e. Equations (28) and (31) and Figure 17.

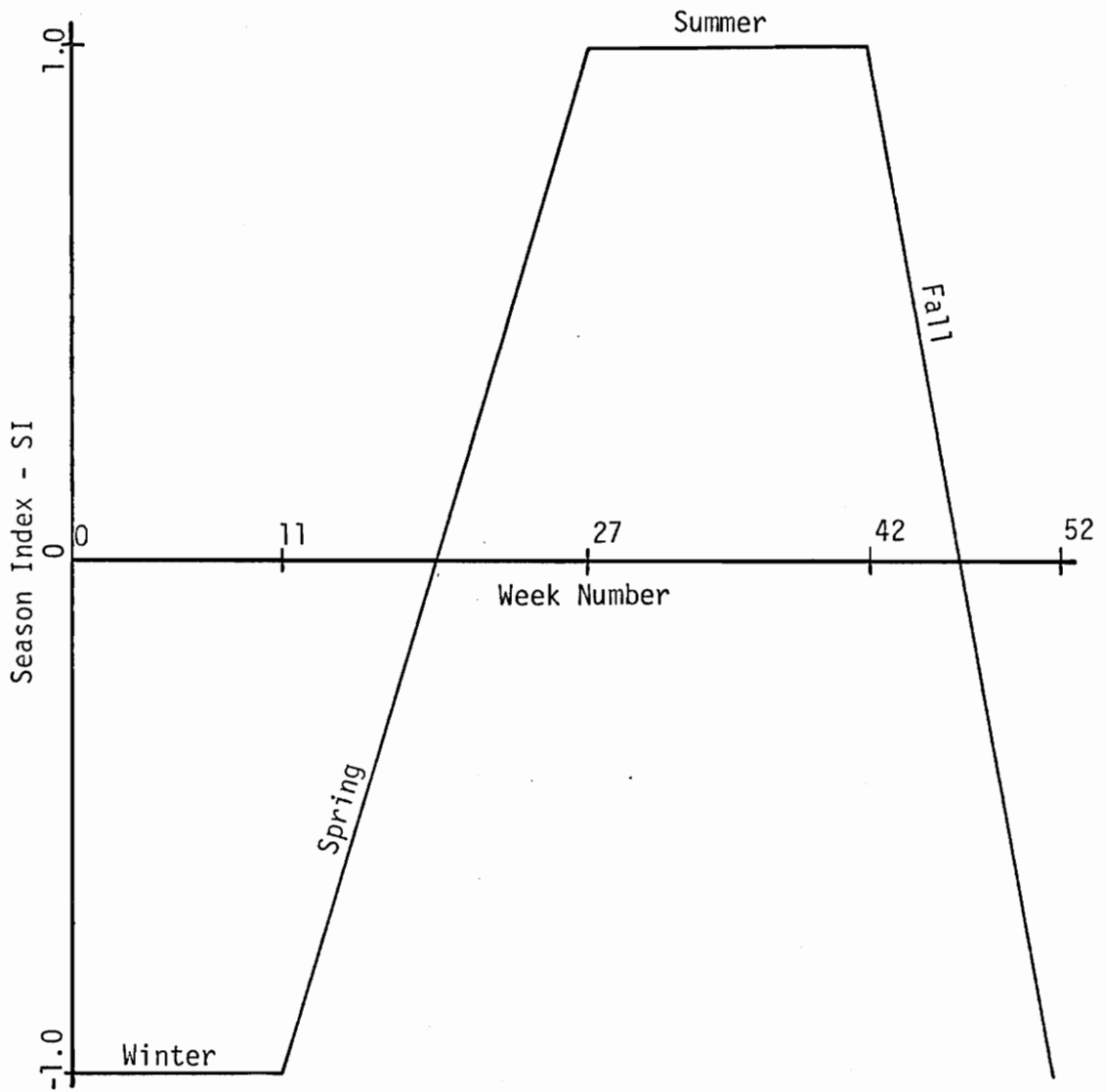


Figure 17 Revised Interpolation Function (28)

TVA tested the model for a variety of watersheds in Tennessee ranging from 37.8 square miles to 1784 square miles of drainage area. Table III shows that the results from the TVA model were slightly better than from the coaxial model.

TVA found that the coefficients given in Table III were in general consistent which implied that the coefficients were reasonably stable and were not uniquely associated with a particular data set. In order to project a solution set of coefficients to other watersheds or to future events, the coefficients were required to be consistent. TVA demonstrated that a solution could be projected in time with reasonable accuracy. Also it was determined that the model coefficients were sensitive to watershed characteristics, but unfortunately the transfer of a solution set to another watershed was found to be very subjective. The model did not project well into other watersheds.

#### Data Requirements

The data required to calibrate the TVA model to a particular watershed could be found in the historical records. Discharge hydrographs for stream gaging stations were required to calculate the surface runoff. Mean daily flow hydrographs were used to determine the total volume of storm runoff. API and rainfall were calculated from data obtained from recording and nonrecording precipitation gages. Week number for each storm was taken from the abscissa of the mean daily flow hydrograph.

TABLE III TVA MODEL - SUMMARY OF RESULTS (28)

Watershed	Drainage Area (Mi <sup>2</sup> )	TVA Model Coefficients					No. Storms	Prediction Statistics			
		a	d	b	c	n		TVA Model		Coaxial	
								SSE (in. <sup>2</sup> )	R	SSE (in. <sup>2</sup> )	R
Obey River	220	8.1	4.7	0.64	1.3	1.89	133	3.74 (0.028)	0.98	3.52	0.98
Wolf River	105	8.8	5.7	1.64	1.3	2.39	28	1.66 (0.059)	0.97	2.41	0.95
Chestuee Creek Nr. Dentville	117	14.0	9.2	0.44	2.1	1.73	138	2.81 (0.020)	0.97	6.13	0.94
Chestuee Creek Nr. Zion City	37.8	15.6	9.3	0.41	0	1.70	114	1.88 (0.016)	0.98	3.60	0.97
Elk River	1784	14.2	10.8	0.43	1.4	1.77	100	2.20 (0.022)	0.94	2.89	0.92
S. Fork Holston River	813	12.8	9.4	0.47	1.6	1.66	113	2.90 (0.026)	0.92	3.98	0.89
Clinch River	528	13.7	11.0	0.69	1.0	1.71	136	2.66 (0.020)	0.89	4.76	0.80
Big Sandy River	205	12.5	10.4	0.98	1.9	1.90	129	3.00 (0.023)	0.96	2.79	0.96
Tuskasegee River	655	7.9	12.8	0.31	12.3	1.65	166	2.50 (0.015)	0.94	3.44	0.92

NOTE: Values in parenthesis are  $\frac{SSE}{No. Storms}$ .

SSE = sum of squares error

R = correlation coefficient

If the TVA model was to be used to calculate total storm runoff then API, rainfall and week number would have been required for each storm.

When utilizing the model to compute storm runoff hydrographs, hourly rainfall, beginning API, and week number were required. Also certain watershed describing parameters were required. Such parameters included API decay coefficient, watershed area, length, and slope. A unit hydrograph was also needed.

#### Selected Study Area

The Maury River basin was selected for application because the required data was readily available. Period of record for the streamflow gage Maury River near Buena Vista was 1938 through 1973. Precipitation data was generally available for the years 1948 through 1972 for the applicable precipitation stations. The Virginia Division of Water Resources provided a six hour unit hydrograph for the Maury River near Buena Vista. Appendix B contains information concerning gaging and precipitation stations in the Maury River basin.

Watershed characteristics also contributed to the selection of the Maury River. Having a drainage area of 646 square miles at the Buena Vista gage, the Maury River was within the range of watershed sizes determined by TVA. Similarity with other upper James River basin watersheds was a factor in the choosing of the Maury River since the model was to be incorporated in a flood

routing system for the James River. Calibrated also were the Jackson and Rivanna Rivers, but these were not considered further due to poor calibration results.

#### IV. MODEL APPLICATION

The TVA rainfall-runoff model consisting of two equations with five coefficients was adapted for use on an IBM 370 - model 155 computer. Calibration of the model was made for the Maury River, the Jackson River, and the Rivanna River. Rainfall and discharge data for the water years 1961 through 1970 was utilized for model calibration. With the solution set of coefficients that was determined for calibration, the model was then applied to an individual storm.

##### Data Preparation for Calibration

Data required to calibrate and apply the model included discharge hydrographs, daily precipitation, hourly precipitation, API, week number, and a unit hydrograph.

Discharge hydrographs were utilized to determine surface runoff. Hydrographs of mean daily discharge were plotted by a Calcomp plotter from values obtained from the United States Geological Survey's gage "Maury River near Buena Vista" (42). Base flow was separated from direct runoff for each storm event. The separation was done by hand after procedures developed by Linsley (39). The volume of storm runoff was then calculated by planimetering the area under the hydrograph and converting the area to inches of runoff. For complex hydrographs with more than one peak, each peak was separated by constructing a recession

curve between peaks as shown on Figure 18. Storm runoff was determined for 124 storms, but after combining smaller storms and eliminating some storms, only 87 storms were used for calibration. Storm runoff ranged from 0.02 inches to 1.34 inches, and the average runoff was 0.42 inches. This information was stored on eighty column computer cards.

Daily precipitation totals were obtained from climatological data which had been stored on magnetic computer tape by Mr. Curtis W. Crockett, former Climatologist for Virginia. Precipitation data were transferred to computer cards for the entire period of record. Four stations in the Maury River basin were selected for calibration purposes on the basis of concurrent periods of record. The four stations were Buena Vista, Deerfield, Goshen, and Lexington. In many instances daily totals were missing; and when a missing value occurred, the value was set to the average daily rainfall for that station. For all four stations the average daily rainfall was 0.10 inches. The period of record was January 1960 to December 1970, or 4100 days.

#### Model Calibration

The calibration program was written in Fortran IV. Containing 284 source statements, the program required approximately 150,000 bytes. For each set of initial values of coefficients, usually sixty to one hundred and twenty seconds of computer time were required to reach a solution. Originally the calibration program

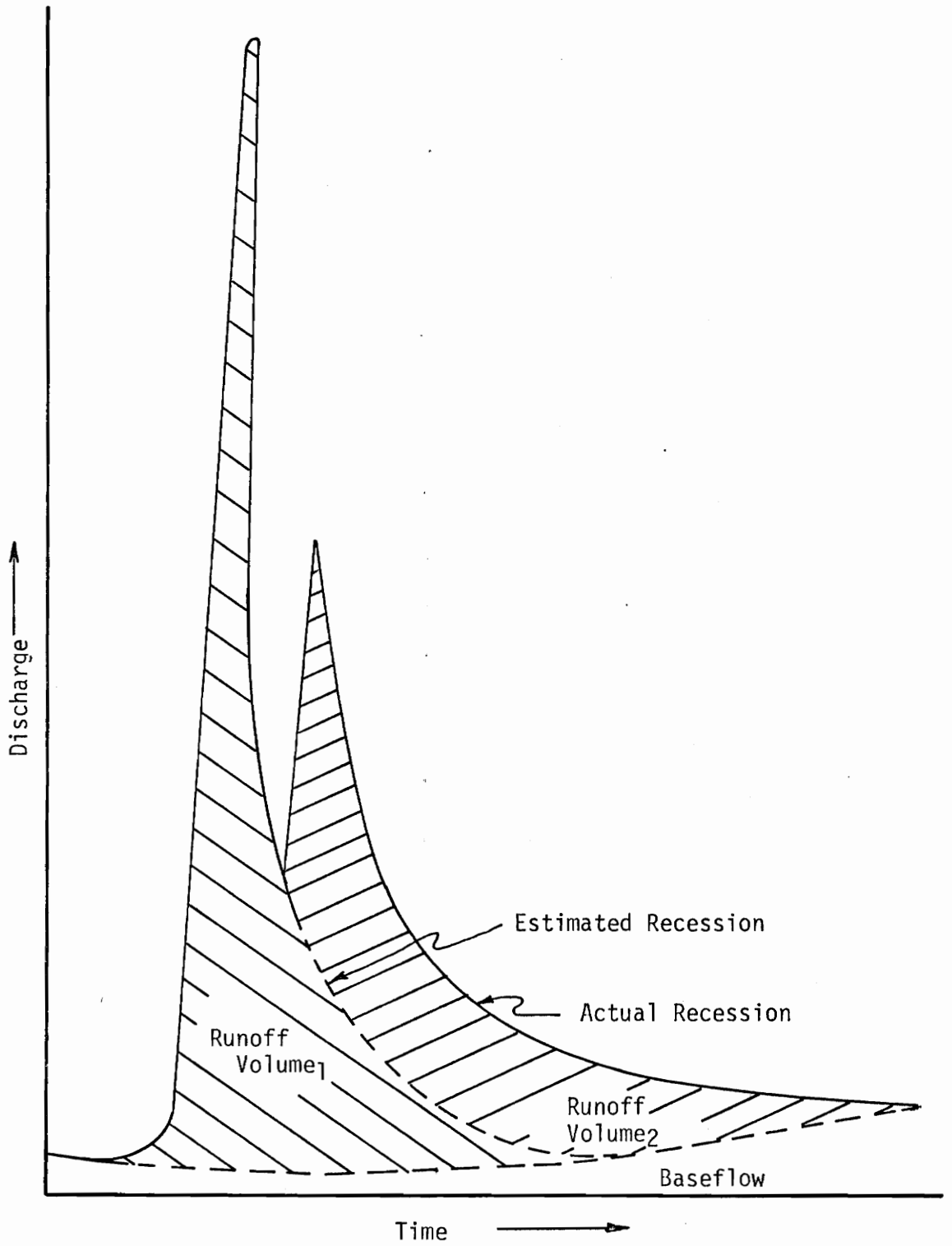


Figure 18 Separation of Complex Hydrographs (39)

was written for the Virginia Polytechnic Institute and State University's IBM 370/155 computer with real storage. However the majority of the calibration runs were made on Virginia Commonwealth University's IBM 370/145 virtual storage system. The program was compatible for both systems; however time and storage requirements did vary. Appendix D contains a calibration program listing. Organization of the program is given on Figure 19, and consists of an input block, an optimization of coefficients block, an error analysis block, and an output block.

Input to the calibration model was all contained on eighty column computer cards. Included as input were the initial values of the five coefficients,  $a$ ,  $b$ ,  $c$ ,  $d$ , and  $n$ , which were based upon those values used by TVA (28). Parameters relating to optimization and other program operations were also input data. Storm information including week number, storm runoff, API, and rainfall were the final input records.

The method of steepest descent was used to calculate an optimized set of coefficients. Figure 20 shows a flowchart of the optimization procedure.

The iterative procedure commenced from an initial set of coefficients as provided in the input data. Values of the coefficients as determined by TVA were used as guides in selecting

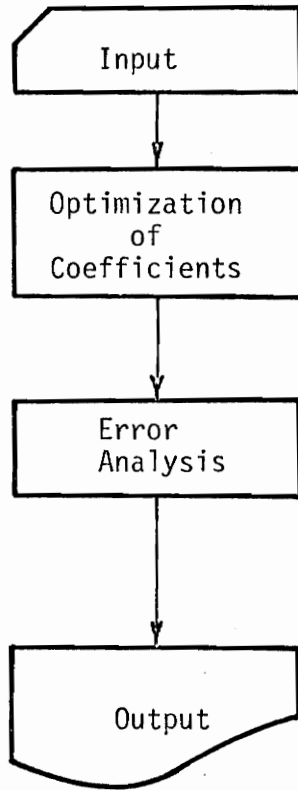


Figure 19 General Organization of Calibration Program

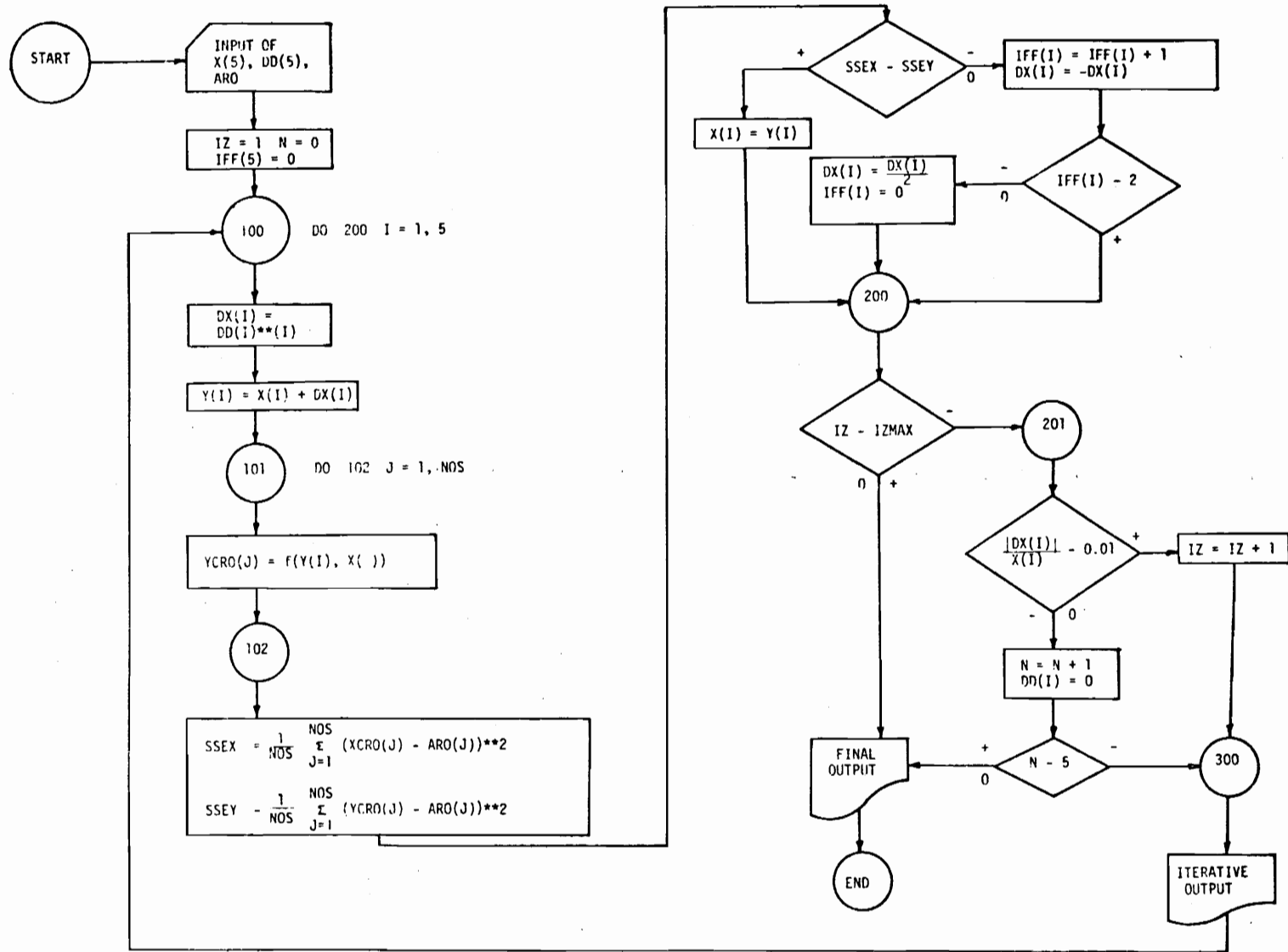


Figure 20 Flowchart of Optimization Procedure

the initial set of coefficients. Each initial coefficient  $X(I)$ , was incremented by some amount  $DX(I)$  to yield  $Y(I)$ , the trial coefficient.  $Y(I)$  was expressed as:

$$Y(I) = X(I) + DX(I) \quad (32)$$

where  $Y(I)$  = the trial coefficient value;

$X(I)$  = the initial coefficient value;

$DX(I)$  = the change increment; and

$I$  = a subscript indicating each coefficient, i.e. when  $I = 1, 2, 3, 4, 5$ ; the coefficient was  $a, b, c, d, n$  respectively.

$DX(I)$  was given by:

$$DX(I) = DD(I) * X(I) \quad (33)$$

where  $DD(I)$  = the fractional change in  $X(I)$ .

For each trial coefficient  $Y(I)$ , surface runoff for each storm  $J$  was computed as:

$$\begin{aligned} YCRO(1,J) &= f(Y(1), X(2), X(3), X(4), X(5)) \\ YCRO(2,J) &= f(X(1), Y(2), X(3), X(4), X(5)) \\ YCRO(3,J) &= f(X(1), X(2), Y(3), X(4), X(5)) \\ YCRO(4,J) &= f(X(1), X(2), X(3), Y(4), X(5)) \\ YCRO(5,J) &= f(X(1), X(2), X(3), X(4), Y(5)) \end{aligned} \quad (34)$$

where  $YCRO(1,J)$  = the calculated surface runoff for storm  $J$  that was a function of the trial coefficient  $Y(I)$  and the remaining initial coefficients.

Surface runoff for the initial set of coefficients was computed as:

$$XCRO(J) = f(X(1), X(2), X(3), X(4), X(5)) \quad (35)$$

where  $XCRO(J)$  = the surface runoff for storm  $J$  computed as a function of the initial coefficients.

A sum of squares error over the storm list was computed for each trial coefficient and for the initial set. For the trial set,

$$SSEY(I) = \frac{1}{NOS} \sum_{J=1}^{NOS} (YCRO(I,J) - ARO(J))^2 \quad (36)$$

where  $SSEY(I)$  = the sum of squares error for each  $Y(I)$ ;

$NOS$  = the number of storms; and

$ARO(J)$  = the observed surface runoff for storm  $J$ .

For the initial set:

$$SSEX = \frac{1}{NOS} \sum_{J=1}^{NOS} (XCRO(J) - ARO(J))^2 \quad (37)$$

where  $SSEX$  = the sum of squares error for the initial coefficient set  $X$ .

$SSEY(I)$  was then compared to  $SSEX$  to determine which was less, that is, whether  $X(I)$  was a better value than  $Y(I)$ . If  $SSEY(I)$  was less than  $SSEX$ , the  $X(I)$  for the next iteration became  $Y(I)$  and  $DD(I)$  did not change. If instead  $SSEX$  was less than or equal to  $SSEY(I)$ , then  $X(I)$  for the next iteration did not change, but  $DD(I)$  became  $-DD(I)$ . If for two consecutive iterations  $SSEX$

was less than or equal to  $SSEY(I)$ , the  $DD(I)$  became  $\frac{1}{2} DD(I)$ . The iterative procedure then repeated itself beginning with Equation (32), and utilized the new initial values of  $X(I)$  and  $DD(I)$  as calculated from the preceding iteration.

The iterative procedure was terminated when one of two conditions was met. A maximum number of iterations was specified. When this maximum number of iterations was exceeded, optimization was terminated. Iteration also ceased when for all five  $X(I)$  the absolute value of  $DX(I)$  was less than or equal to one percent of  $X(I)$ .

With each iteration, output containing current trial and initial values of coefficients was provided. This output aided in analysis of convergence patterns and in debugging.

An error analysis was then performed for the optimized coefficients. The error analysis was intended to provide a means to evaluate the accuracy of the optimized coefficients. Included in the error analyses were the errors in computed runoff for each storm and the runoff error for each storm expressed as a fraction of the storm rainfall. The remainder of the error analysis is presented as Table IV. Data items that yielded very poor results for all solution sets were replaced by items giving less error.

TABLE IV. SAMPLE ERROR ANALYSIS

Average Value of  $(ARO-CRO)/RAIN = 0.060$   
 Average Value of  $ABS((ARO-CRO)/RAIN) = 0.225$   
 Average Value of  $ABS(ARO-CRO) = 0.254$  in.  
 Sum of  $(ARO-CRO)**2/NOS = 0.1174$  sq. in.

No. of Times ARI was set to RISET = 0  
 Correlation Coefficient Relating ARO to CRO = 0.772  
 Standard Error of Estimate = 0.346 in.  
 Mean CRO = 0.412 in. Mean ARO = 0.452 in. STD DEV CRO = 0.452 in.  
 STD DEV ARO = 0.544 in.

Distribution of Errors....Error = $(ARO-CRO)/RAIN$			
Lower Limit	Upper Limit	No.	Percentage
0.90	1.00	0	0.0
0.80	0.90	0	0.0
0.70	0.80	1	1.0
0.60	0.70	3	2.9
0.50	0.60	2	2.0
0.40	0.50	6	5.9
0.30	0.40	6	5.9
0.20	0.30	16	15.7
0.10	0.20	8	7.8
0.00	0.10	12	11.8
-0.10	0.00	14	13.7
-0.20	-0.10	19	18.6
-0.30	-0.20	5	4.9
-0.40	-0.30	6	5.9
-0.50	-0.40	3	2.9
-0.60	-0.50	1	1.0
-0.70	-0.60	0	0.0
-0.80	-0.70	0	0.0
-0.90	-0.80	0	0.0
-1.00	-0.90	0	0.0

### Calibration Results

The calibration procedure was performed for five sets of initial values of the coefficients. These initial sets were based upon values derived for watersheds in the Tennessee Valley by TVA (28). From the TVA derived coefficients, the high, low, and average values for each of the five coefficients, were calculated. Table V lists the initial values and the final optimized values.

Each initial set converged to a unique set of coefficients. The range of values of the final coefficients can be seen in Table V. It was obvious that the final range was somewhat related to the initial range, however with c this was not the case. The coefficients b, c, and n, ranged within  $\pm$  36, 67, and 19 percent of the average value respectively, while a and d had ranges of 111 and 122 percent. Generally the greater the initial value was, the greater the final value. From Table V it can also be seen that the final values were usually greater than the initial values. The order in which the coefficients converged is also presented in Table V. For all initial sets, n converged first while c converged last. This convergence pattern indicated that n was least sensitive to changes in the other four coefficients while c was most sensitive to the four other coefficients.

TABLE V. CALIBRATION RESULTS FOR MAURY RIVER NEAR BUENA VISTA

Set		Initial and Final Values of Coefficients					Statistics for Final Values			No. of Iterations
		a	b	c	d	n	Correlation Coefficient	Standard Error of Estimate (in.)	SSE <sub>2</sub> (in. <sup>2</sup> )	
1	Initial	7.90	0.31	1.00	4.70	1.60	0.870	0.190	3.097	40
	Final	10.100	1.688	1.601	7.722	1.794				
2	Initial	11.75	0.98	6.65	8.75	2.00	0.863	0.191	3.115	41
	Final	18.118	1.651	2.466	14.281	1.559				
3	Initial	15.60	1.64	12.30	12.80	2.39	0.866	0.187	3.010	36
	Final	25.297	1.812	2.775	20.039	1.512				
4	Initial	7.90	0.31	12.30	5.00	1.65	0.838	0.208	3.784	67
	Final	10.794	1.239	2.896	9.059	1.557				
5	Initial	8.59	1.21	1.01	5.45	1.75	0.864	0.196	3.271	39
	Final	8.992	1.554	1.408	6.089	1.824				

Solution  
Set

Order of Convergence  
1 2 3 4 5

1	n	a	b	d	c
2	n	b	d	a	c
3	n	b	d	a	c
4	n	d	b	a	c
5	n	a	d	b	c

Coefficients a, b and d showed no marked pattern in the order in which each converged. A study of the percentage change that each coefficient underwent from initial to final values indicated that order of convergence was not dependent on how close the initial value was to the final value.

From the data presented in Table V, it can be seen that each initial coefficient set converged to a different final set. The five coefficients apparently were significantly interrelated. Based upon the data in Table V and the optimization method used, it could not be determined if the global optimum coefficient set was obtained or if only a local optimum set was reached. Since the final coefficients were comparable to those coefficients derived by TVA (28), the final values were considered reasonable.

Maury River solution sets were compared with TVA's solution sets. The correlation coefficients for Maury River solution sets were comparable to TVA's solution sets. TVA's correlation coefficients were generally closer to unity than those calculated for the Maury River. A sum of squares error comparison was also made; but to take into account the number of storms used, the sum of squares errors was divided by the number of storms. The modified sum of squares errors as calculated herein and the modified sum of squares errors as calculated by TVA were again comparable. Table III

and Table VI show that the errors for the Maury River solution sets were similar to the errors for the TVA solution sets, but the TVA sets generally provided somewhat greater accuracy.

An error analysis was performed for each final coefficient set. Table VI gives a summary of the error analysis. On the basis of Table VI, solution sets 1 and 3 were considered to give the best results, and solution set 3 was deemed to be the overall best set. Figure 21 shows actual runoff plotted against computed runoff for solution set 3. The standard error of estimate for sets 1 and 3 were slightly less than 50 percent of the mean actual runoff. The average values of  $ABS(ARO-CRO)$  were generally one third of the mean actual runoff. To compare the errors,  $ABS(ARO-CRO)$ , with the total water involved in each storm, RAIN, the average value of  $ABS(ARO-CRO)/RAIN$  was calculated. The average absolute error was 11.5 percent and 10.6 percent of the storm rainfall for solution sets 1 and 3 respectively. Thus the absolute error was large with respect to runoff and small with respect to rainfall. Figure 22 gives the distribution of errors as a percentage of rainfall. From Figure 22 it can be seen that the average percentage error was in the range of 2 percent, but the distribution was skewed to the positive side. A positive percentage error occurred when the actual runoff exceeded the computed runoff, thus using solution set 3 a lower calculated than actual runoff was anticipated. The positive skew was seen for all Maury River solution sets.

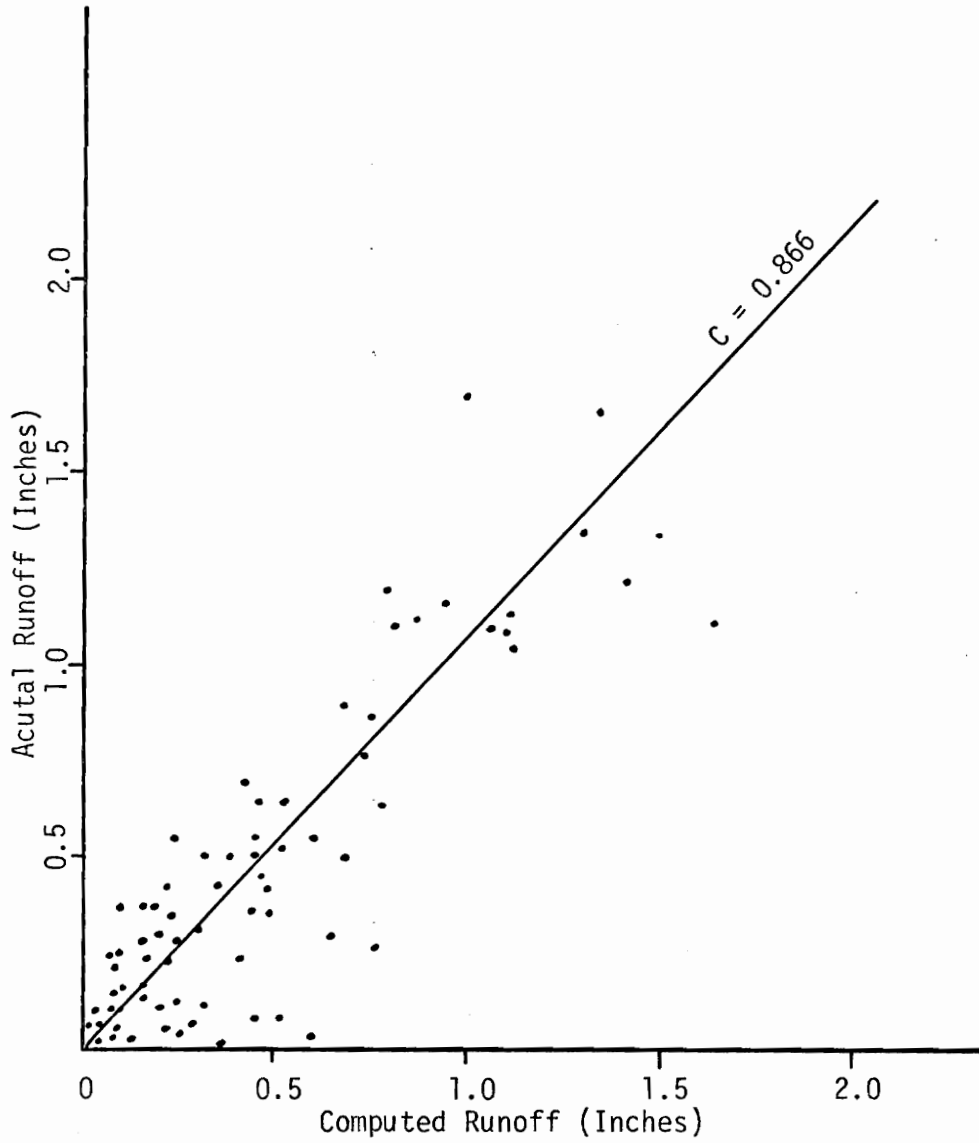


Figure 21 Actual Versus Computed Runoff for Maury River Solution Set 3

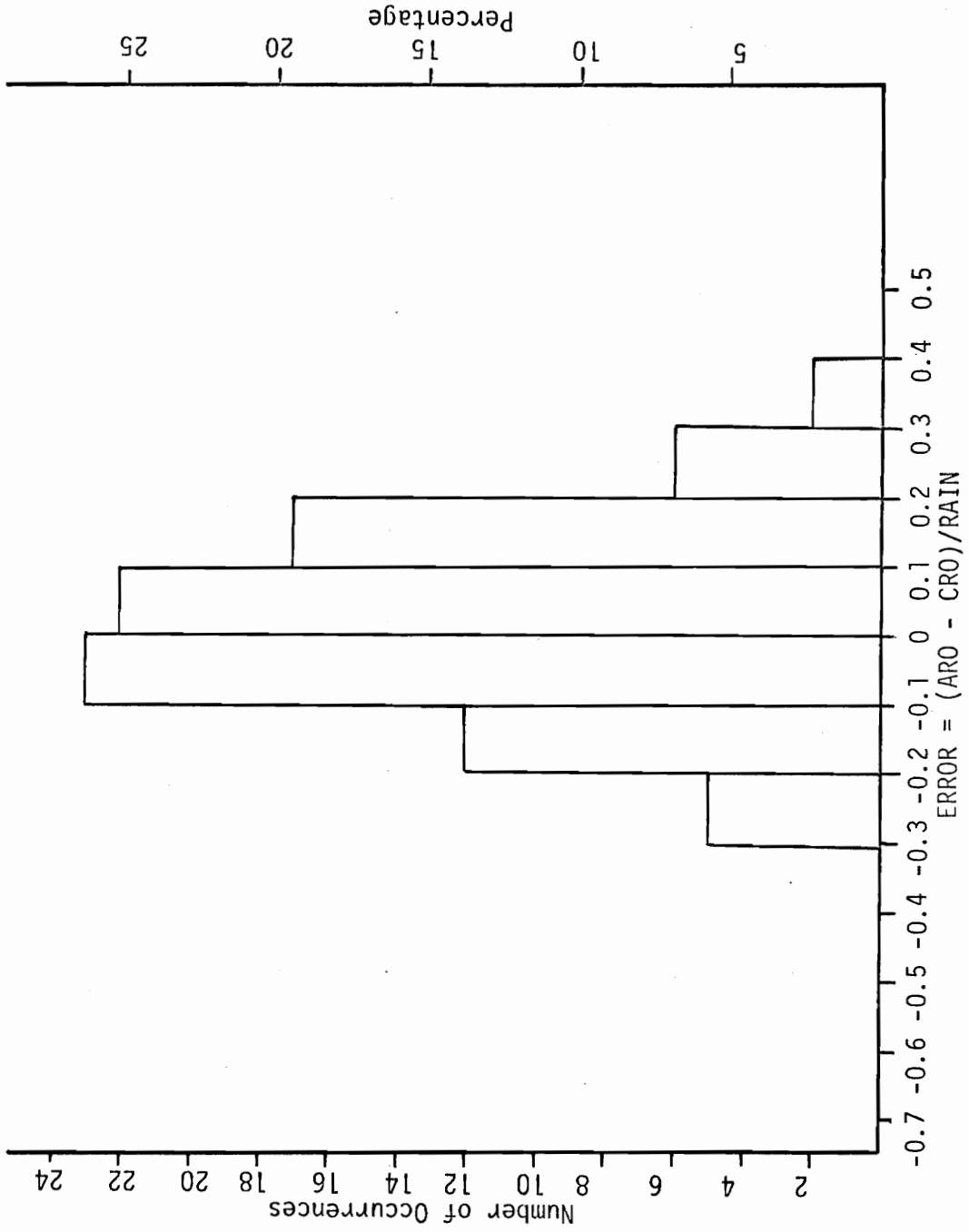


Figure 22 Distribution of Errors for Solution Set 3

TABLE VI. SUMMARY OF ERROR ANALYSIS

	Solution Set				
	1	2	3	4	5
Average value of (ARO-CRO)/RAIN	0.046	0.023	0.016	0.023	0.049
Average value of ABS((ARO-CRO)/RAIN)	0.115	0.107	0.106	0.105	0.118
Average Value of ABS(ARO-CRO), in.	0.142	0.137	0.136	0.139	0.145
Sum of (ARO-CRO)**2/NOS <sup>†</sup>	0.0356	0.0358	0.0346	0.0435	0.0376
Correlation Coefficient	0.870	0.863	0.866	0.838	0.864
Standard Error of Estimate, in.	0.190	0.191	0.187	0.208	0.196
Mean CRO, in.	0.398	0.418	0.423	0.421	0.395
STD DEV CRO, in.	0.384	0.369	0.362	0.376	0.385
Mean ARO, in.	0.422	0.422	0.422	0.422	0.422
STD DEV ARO, in.	0.384	0.384	0.384	0.384	0.384

ARO = the actual runoff,  
 CRO = the computed runoff, and  
 RAIN = the storm rainfall, in.

<sup>†</sup> sq. in.

Figures 23 through 27 show percentage errors and the magnitude of errors plotted against various input data. From these figures it was concluded that the calibration results errors were not correlated with API, rainfall, week number, or runoff.

The magnitude of errors equal to the differences in actual and calculated runoff seemed reasonable when considering the possible magnitude of error associated with data preparation. Only four precipitation stations were considered for the calibration, and some error resulted from the lack of rain gages in the 646 square mile basin. A standard error of approximately 17 percent could be expected for the precipitation average for a basin with four rain gages in 646 square miles (29). Error could also have resulted from inaccurate separation of direct runoff from baseflow. It was felt that separation errors were the greatest sources of error. In many instances, the association of a rainfall event with a runoff event proved difficult, and errors resulted from the association process. The errors in API could be attributed to the errors in basin average precipitation. Each type of data input introduced some error into the calibration.

#### Data Preparation for Storm Simulation

Hourly precipitation values were used to simulate individual storm response. The only recording precipitation station that was used was Montebello Fish Nursery which is located to the southeast

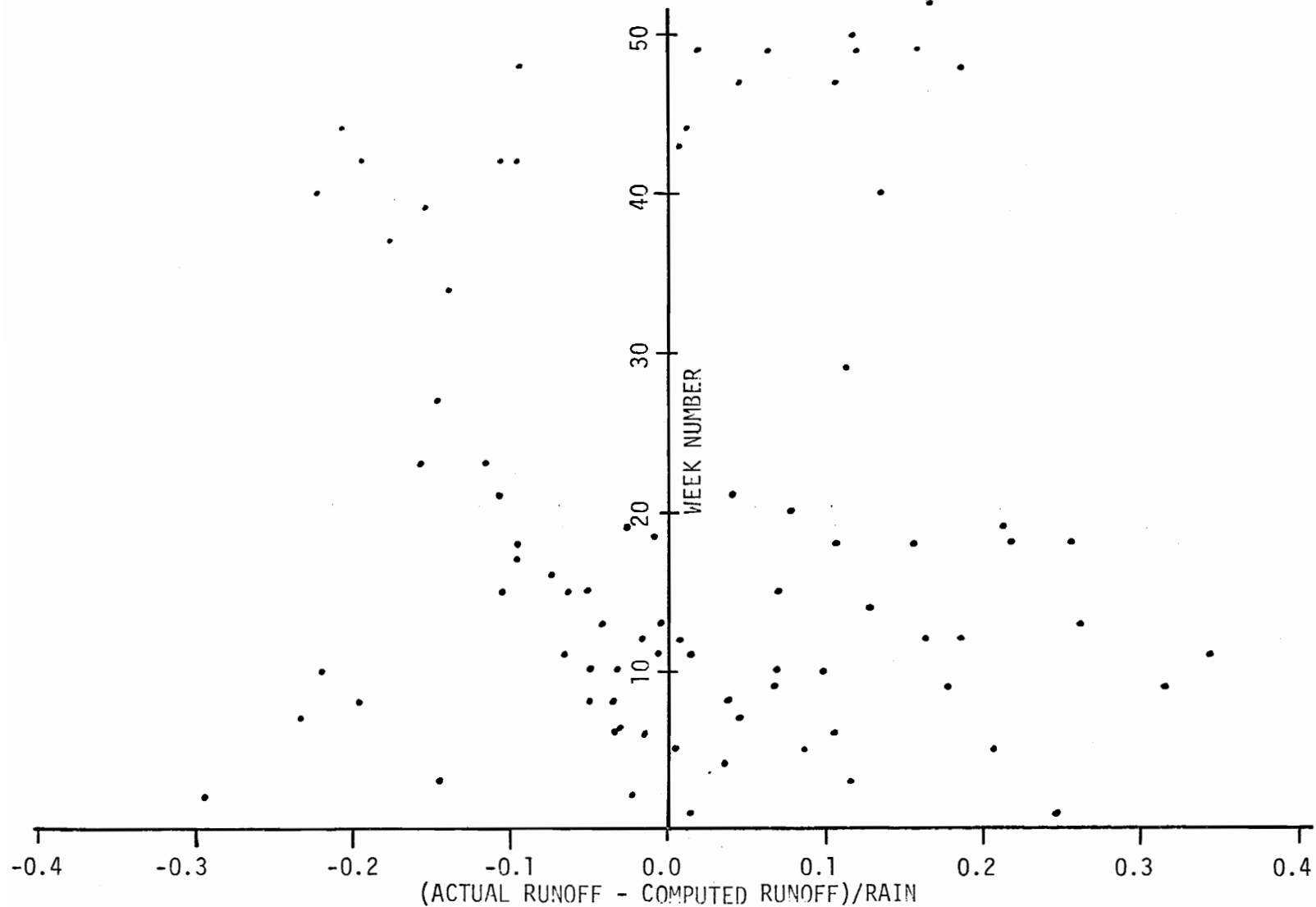


Figure 23 Week Number Versus Percentage Error for Solution Set 3

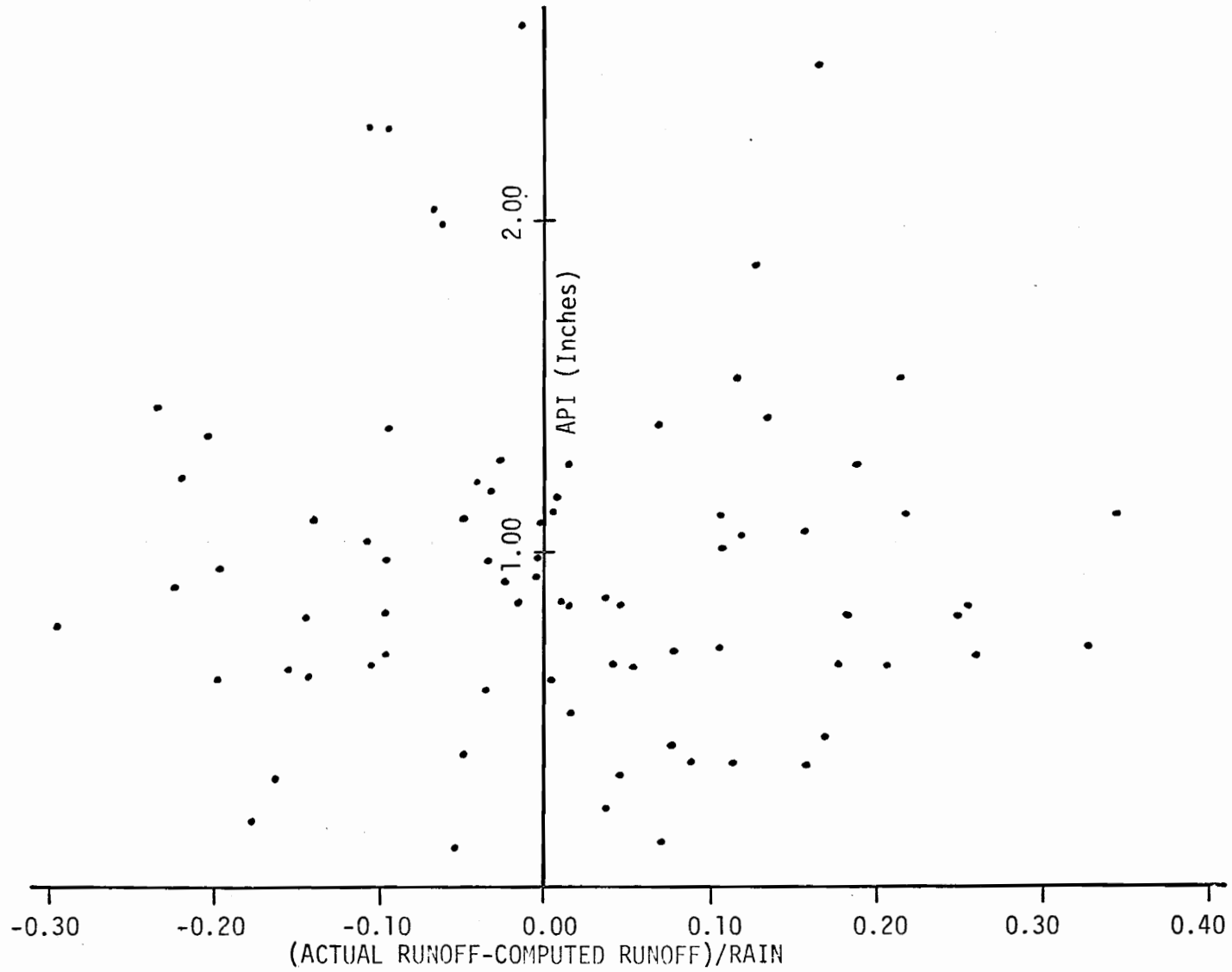


Figure 24 API Versus Percentage Error for Solution Set 3

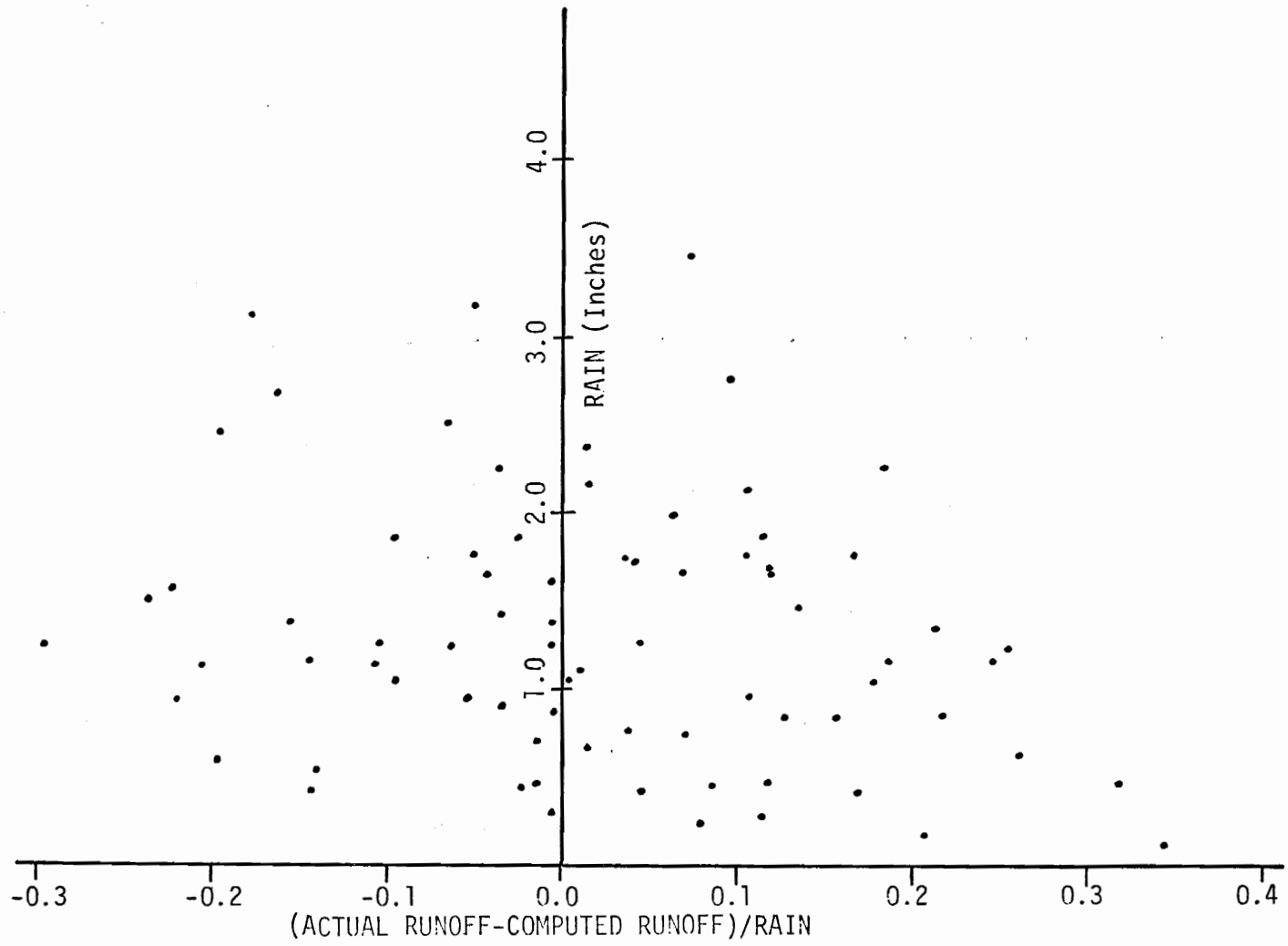


Figure 25 Rain Versus Percentage Error for Solution Set 3

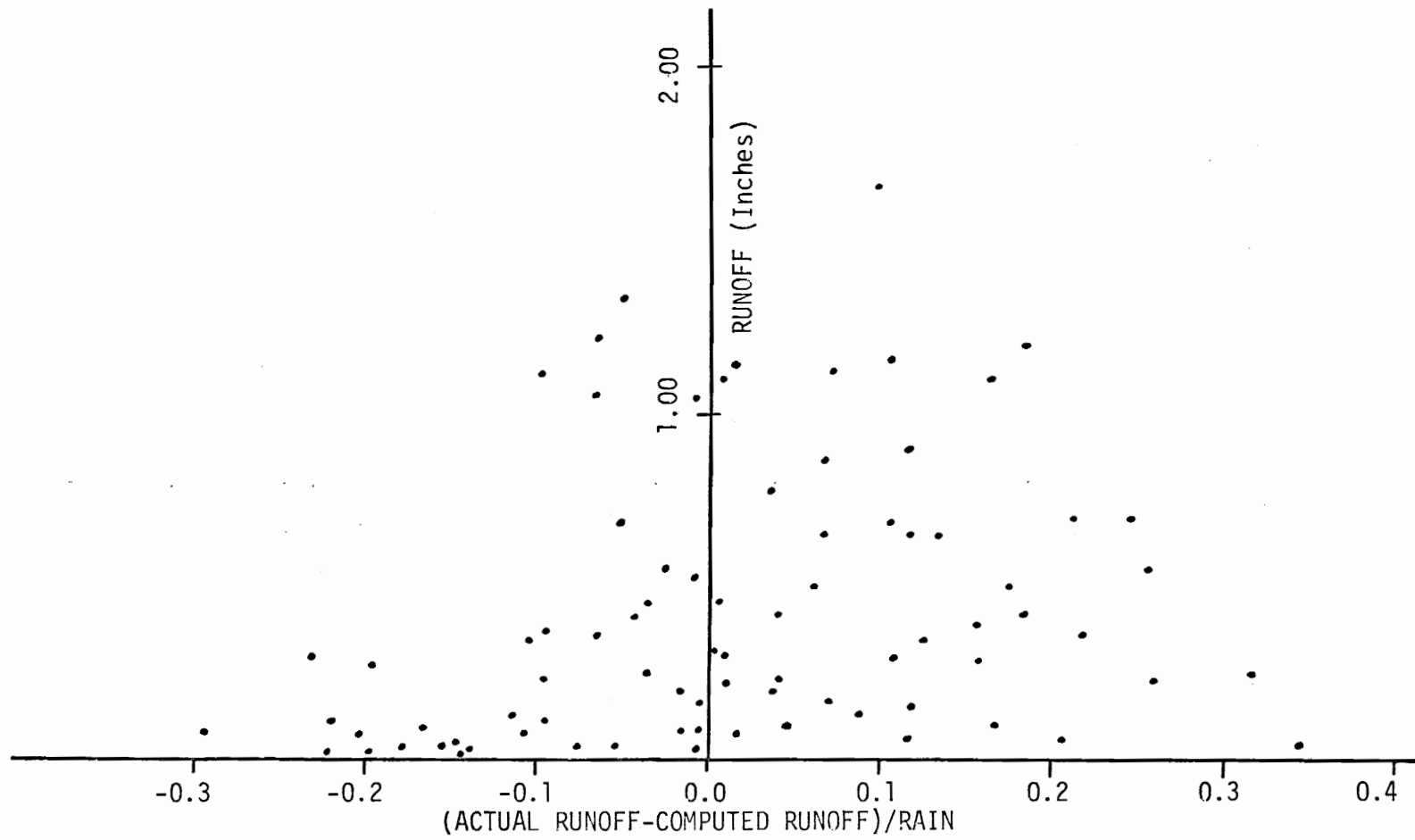


Figure 26 Runoff Versus Percentage Error for Solution Set 3

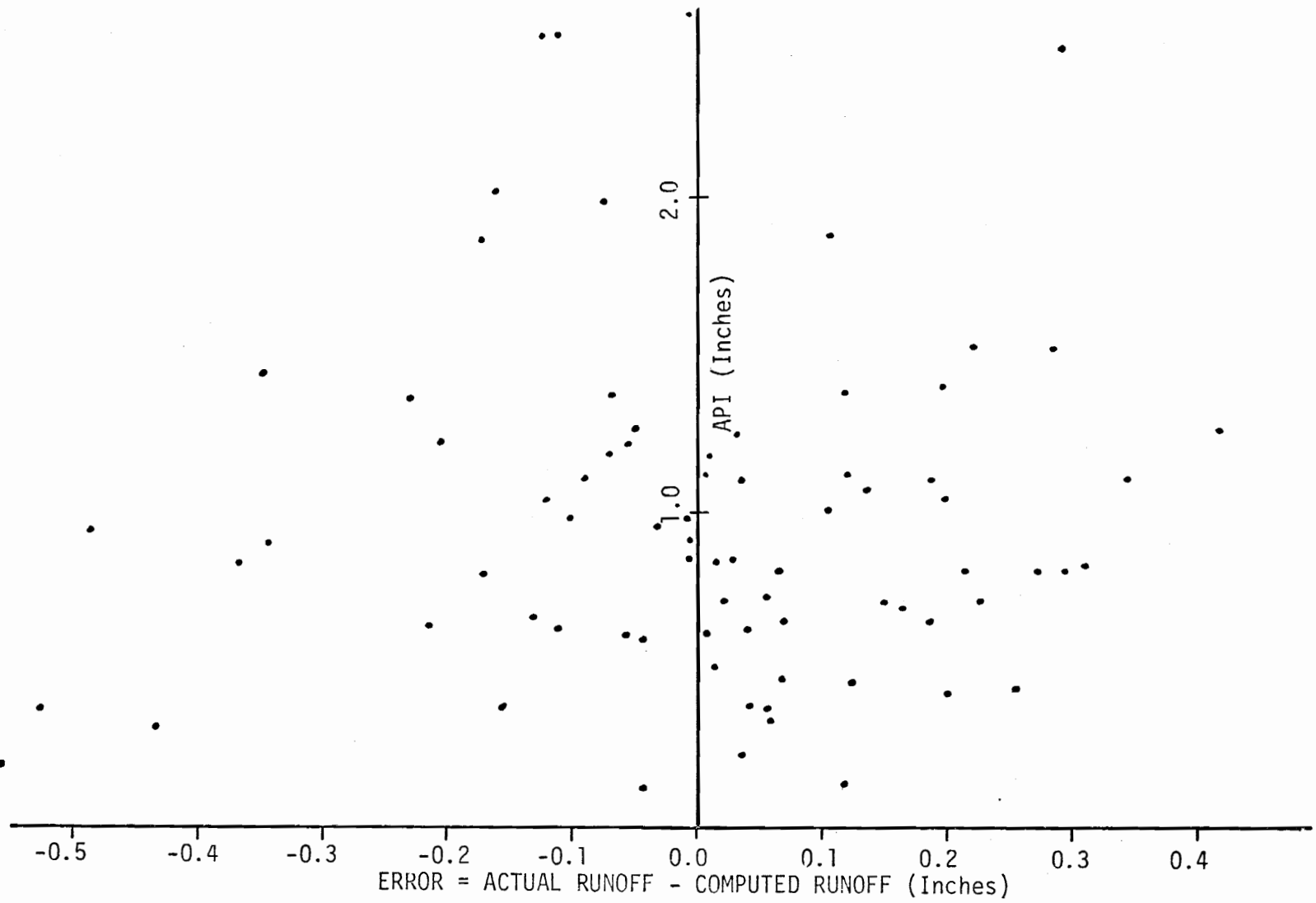


Figure 27 API Versus Error for Solution Set 3

of the Maury basin. The hourly rainfall totals were also taken from a magnetic tape which was provided by the National Climatic Center.

Six hour precipitation totals were determined for the basin. First, six hour totals were calculated for the recording station by:

$$\text{RAIN6}(J) = \sum_{I=t}^{t+6} \text{HRAIN}(I) \quad (38)$$

where  $\text{RAIN6}(J)$  = the six hour precipitation total for the period  $J$  beginning at time  $t$ ; and

$\text{HRAIN}(I)$  = the hourly precipitation value for time  $I$ .

Next nonrecording stations' daily totals were adjusted to reflect the precipitation falling during the same time interval. This was done because the nonrecording stations did not all read the rain gage at the same hour. Adjustment was made by proportioning daily totals.

The proportionment was written:

$$P_t' = \frac{P_t \cdot \text{TREAD} + P_{t+1} (2400 - \text{TREAD})}{2400} \quad (39)$$

where  $P_t'$  = the adjusted daily precipitation for day  $t$ , midnight to midnight;

$P_t$  = the unadjusted daily precipitation for day  $t$ , for the 24 hour period ending at  $\text{TREAD}$ ; and

$\text{TREAD}$  = the hour the 24 hour precipitation total is collected.

Using the adjusted values of daily precipitation, the basin average daily precipitation was then computed as:

$$PB_t = \sum_{i=1}^{NOS} P'_{t,i} \cdot TC_i \quad (40)$$

where  $PB_t$  = the basin average daily precipitation in inches for day  $t$ ; and

$TC_i$  = the Thiessen coefficient for precipitation station  $i$ .

Next the basin average daily precipitation was proportioned into four periods of six hours each. The proportionment was expressed as:

$$HPB_J = PB_t \cdot RAIN6(J) \cdot \left( \sum_{I=1}^4 RAIN6(I) \right)^{-1} + RAIN6(J) \cdot TC_i \quad (41)$$

when  $\sum_{I=1}^4 RAIN6(I) \neq 0$ ; and

where  $HPB_J$  = the 6 hour basin average precipitation for the 6 hour interval  $J$ ;

$PB_t$  = the basin average daily precipitation for day  $t$ ;

$TC_i$  = the Thiessen coefficient for the recording precipitation station; and

$I$  = the 6 hour intervals for day  $t$ .

If  $\sum_{I=1}^4 RAIN6(I) = 0$ , the  $HPB_J$  became zero unless  $PB_t$  was nonzero,

in which case:

$$HPB_J = \frac{PB_t}{4} (1 + TC_i) \quad (42)$$

Thus the six hourly basin average precipitation was calculated to be a Thiessen weighted value that was proportioned in time according to the recording precipitation station.

API was calculated by Equation (3) from the daily average basin precipitation. Week numbers for storm events were taken from the time axis of the mean daily discharge hydrograph. A six hour unit hydrograph was provided by the former Virginia Division of Water Resources.

#### Model Application to Single Storm Events

Although the results for the Maury River solution sets were not as accurate as those obtained by TVA (28), the Maury solution sets were deemed accurate enough to use for single storm simulation. Solution set 3 was selected on the basis of the error analysis. The storm of August 19-20, 1969, or Hurricane Camille was selected for simulation on the basis of data availability. A tri-hourly hydrograph was available for the Maury River near Buena Vista for the storm period (48). Hourly and daily precipitation data were readily available from the National Weather Service. Information about the August 1969 storm is presented in Appendix E. A storm in December 1967 was also selected but lack of hourly precipitation data resulted in unreasonable results.

The storm simulation program was written in PL/1 for use on the Virginia Commonwealth University's and the VPI&SU's computers.

Approximately 40,000 bytes of storage and 15 seconds of compile time were required. A flow chart of the storm simulation program is presented in Figure 28, and a listing of the program is contained in Appendix E.

The storm simulation program generated precipitation excess from precipitation data. Information concerning precipitation stations was provided as input. Hourly and daily precipitation data, initial API, week number, and the unit hydrograph were also input data. Six hour incremental precipitation was calculated as previously described and incremental API was determined by:

$$API_t = API_{t-1} K^{0.25} + HPB_t \quad (43)$$

where  $t$  = the six hour interval.

Using Equations (28) and (31) and Figure 17, the precipitation excess for each six hour increment was calculated for the six hour basin average precipitation.

API was limited to a maximum value above which precipitation excess was set equal to precipitation. The use of a limiting value of API was to provide the simulation program the means to reflect a watershed with all precipitation losses satisfied. Several trial runs were made to determine the best limiting value of API; and a value of 3.00 inches was selected.

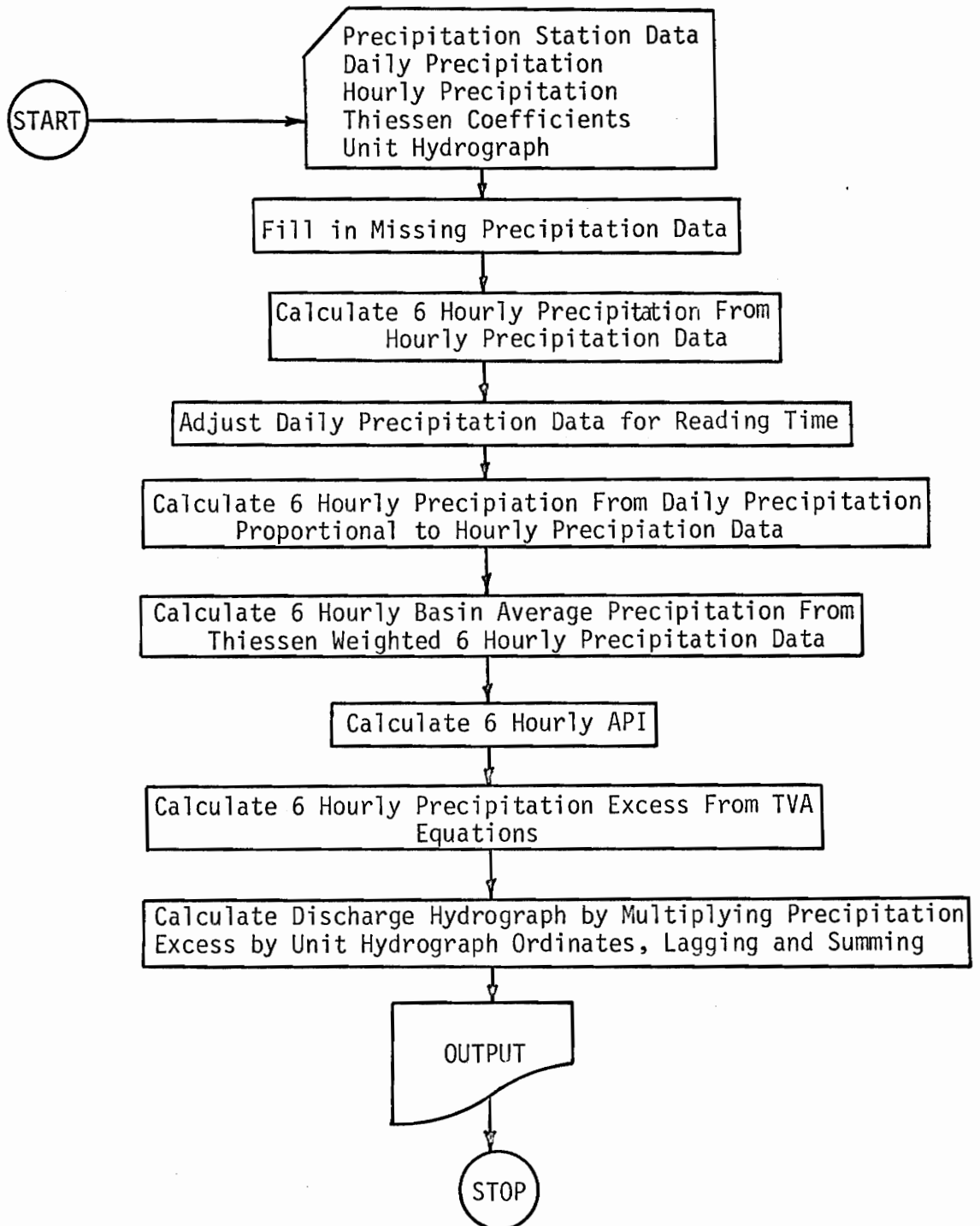


Figure 28 General Flowchart Of Storm Simulation Program

The hydrograph of streamflow was then synthesized from the unit hydrograph of six hour duration and the calculated precipitation excess. Each six hour incremental precipitation excess was multiplied by the ordinates of a six hour hydrograph to yield the streamflow hydrograph resulting from each incremental precipitation excess. Each incremental hydrograph was lagged by six hours from the preceding incremental hydrograph.

The total streamflow hydrograph was calculated by summing the various incremental hydrographs for each time interval. Figure 29 depicts this process. A selected base flow was then added to each ordinate.

#### Storm Simulation Model Results

The storm simulation program was run for the Camille storm of August 1969, and Figure 30 shows the computed hydrograph plotted with the observed hydrograph. Several aspects of the hydrographs were considered.

Those characteristics of the hydrographs which were compared were total volume of runoff, magnitude of peak flow, timing, rising limb, recession limb, and base flow. The computed and the observed hydrographs had similar shapes, but the computed curve contained a greater area. As shown in Figure 30 the computed hydrograph represented 7.9494 inches of total runoff, while the observed hydrograph yielded 4.591 inches of total runoff. Computed total runoff was 173 percent of observed total runoff. The magnitudes

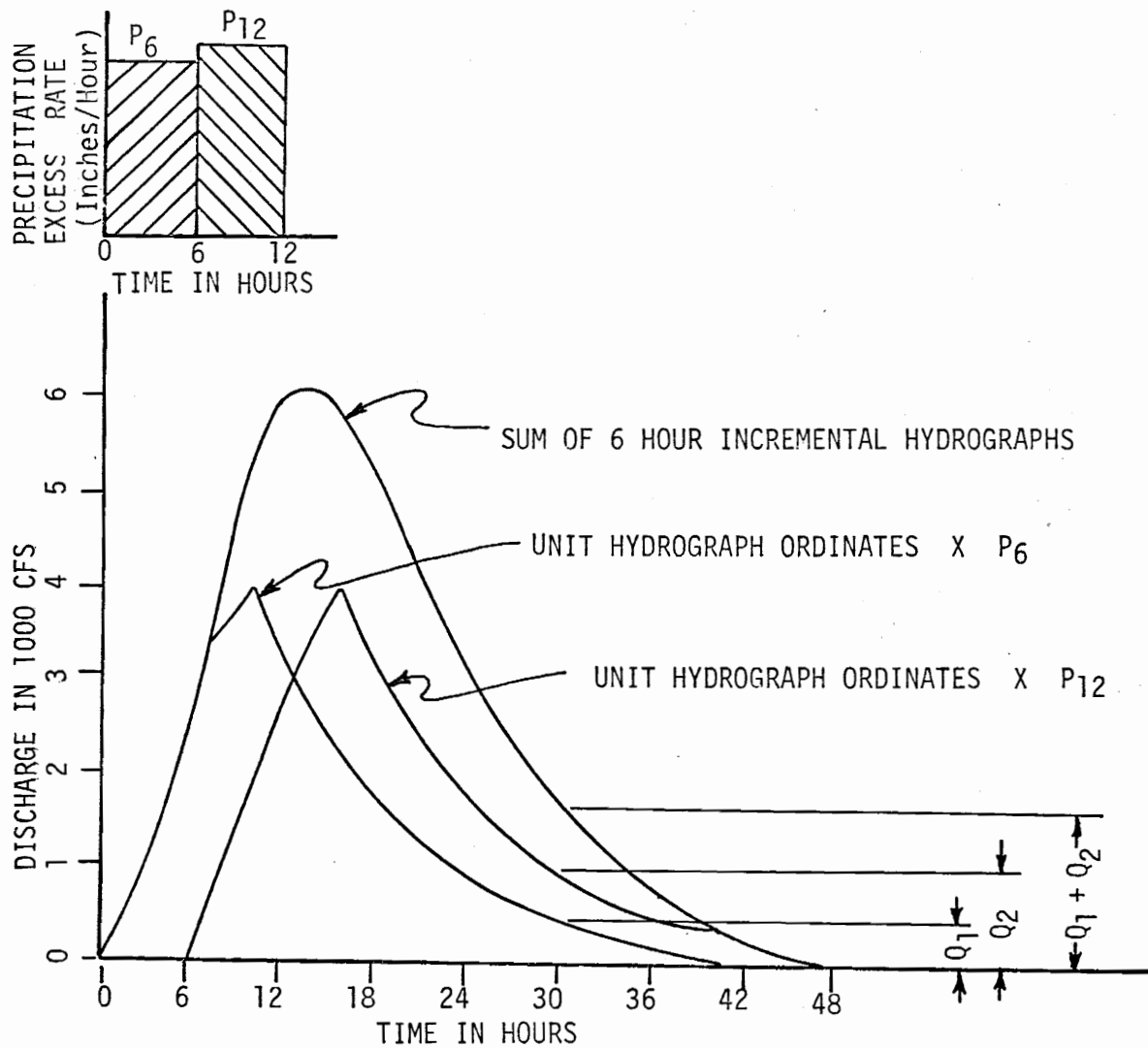


Figure 29 Synthesis of Streamflow Hydrograph from Unit Hydrographs and Precipitation Excesses

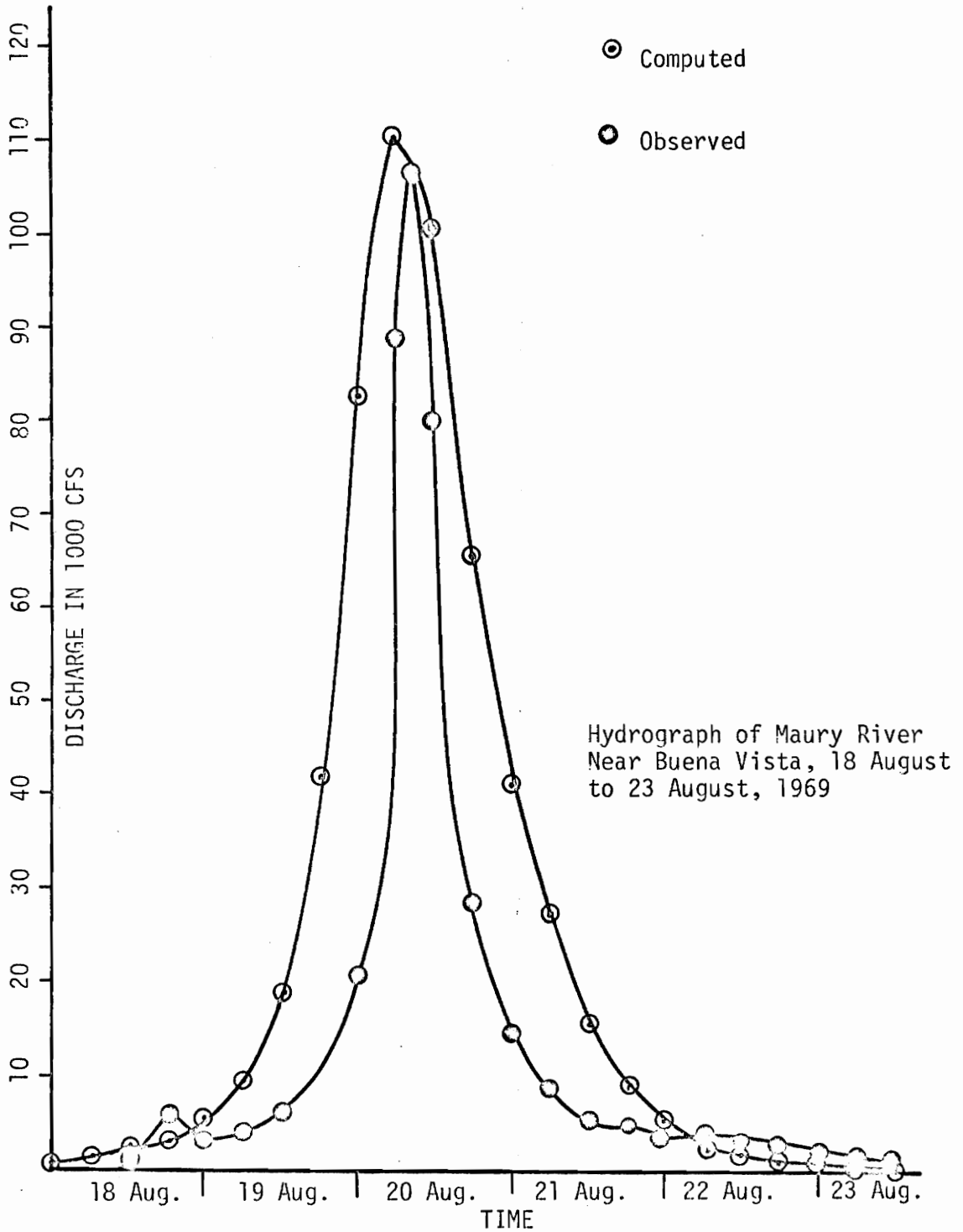


Figure 30 Results of Storm Simulation Program

of the peak flows showed less difference. A peak discharge of 108,765 cfs was calculated. This calculated peak was 104% of the observed peak discharge which was 105,000 cfs. The rising limbs of the computed and observed hydrographs began approximately at the same time but the computed curve led the observed curve slightly. At the points where the hydrographs reached the U.S.G.S. peak base discharge of 6,200 cfs, the computed plot led the observed plot by 11 hours. The computed peak occurred 3 hours before the observed peak. Again reflecting the greater computed volume of runoff, the observed hydrograph approached base flow before the computed hydrograph and at the U.S.G.S. peak base discharge the observed led the computed by 9 hours. On the rising limbs of the hydrographs, the slopes of the curves were similar. On the falling limbs, the computed hydrograph took more time to recede, and the computed slope remained steeper longer. The shape of the recession curves were similar in the lower ranges but the computed curve dropped to the preselected base flow once runoff was terminated.

#### Discussion of Simulation Results

Unlike the calibration results in which calculated total runoff generally was less than observed total runoff, the simulation results showed calculated runoff and runoff rates to be

greater than observed runoff rates. The differences between calculated and observed runoff could have possibly been attributed to erroneous model coefficients, erroneous incremental rainfall or API related errors.

The model coefficients used were those determined in solution set 3 of the calibration process. When the coefficients were calculated they were optimized on the basis of total storm runoff and beginning API. Since the simulation program calculated incremental runoff from incremental rainfall and API, some error could have been expected from the use of calibration-oriented coefficients.

Accumulated error was not limited to coefficient related errors. Errors in incremental rainfall could also have resulted in accumulated error which is reflected in Figure 30. Six hourly incremental precipitation was calculated from seven nonrecording and one recording precipitation stations. The timing of the precipitation was controlled by the recording station at Montebello Fish Nursery, which is located out of the basin; and to some extent by the time of reading correction applied to nonrecording stations. The magnitude of precipitation errors could have affected the results also. In the eight precipitation station

network used, the daily precipitation for August 20, 1969, ranged from 6.87 inches to 1.80 inches, and in the report of the August 1969 flood, Camp and Miller (48) reported greater 24 hour precipitation in the Maury River basin than was found in the Weather Service's data. Thus it was reasonable to expect some error from the use of the adjusted Thiessen weighted incremental rainfall.

Errors in precipitation also affected API. Errors in API resulted in erroneous values of RI in Equation (31) and in SRO in Equation (28). The most significant API related errors may have resulted from setting incremental precipitation excess equal to incremental rainfall when the API exceeded a preselected value. The limiting value of API was reached early on the rising limb of the hydrograph at 0600 hours on August 19, 1969.

Because the incremental hydrographs were combined by superposition, each error in incremental precipitation excess could have been reflected for a time equal to the time base of the unit hydrograph. Therefore if incremental errors in precipitation excess were all the same sign, overall error would increase with time.

It was believed that erroneous model coefficients were the most significant sources of error. Because the model coefficients were calibrated for total storm runoff, and because the August 1969 storm was of such great magnitude, it was believed that errors resulting from erroneous model coefficients were more significant than precipitation or API related errors. Errors in precipitation increments were felt to be less significant than coefficient related errors, but comparably as significant as the errors resulting from the limiting value of API. Because the separation in time of the observed and computed peak flows was small the timing of calculated incremental precipitation was believed to be reasonable. The values of storm precipitation for each precipitation station ranged from 1.8 to over 9 inches, and it was felt as a result some error was introduced. The error resulting from the limiting value of API was believed to be comparable to precipitation related errors. However, it was felt that the limiting value of API was reasonable because from Figure E2 that the slopes of the accumulated rainfall and accumulated runoff curves were equal near the time API reached the limiting value, that is, the rainfall rate equaled the runoff rate.

## V. CONCLUSIONS AND RECOMMENDATIONS

The rainfall-runoff model developed by TVA was calibrated for the Maury River basin using total storm runoff. The calibrated model was then used to simulate the August 1969 storm.

The following conclusions are made based on results of this study:

1. The optimization procedure used in calibrating the model did not determine the global optimum solution set of coefficients.
2. The calibration results showed that the best coefficient solution set yielded greater sums of squares errors for the Maury River basin than the TVA solution sets for the TVA basins. However, the results were comparable.
3. Errors of calibration results showed that percentage errors for individual storm runoff were not correlated with API, week number, precipitation, or runoff.
4. The computed hydrograph for the August 1969 flood was very sensitive to the selection of a limiting value of API, and the small difference between computed and observed peak discharge was somewhat forced by the selection of the limiting value of API.
5. The timing of the computed August 1969 flood hydrograph compared well with the observed hydrograph because of the use of a limiting value of API above which runoff equaled rainfall.

6. Total runoff computed for the August 1969 flood was 173 percent of the observed total runoff, but was less than total storm rainfall.
7. The model was not refined sufficiently to apply to the implicit flood routing scheme.

The following recommendations are made based on the results of the study:

1. Calibration of the model should be made for incremental runoff simulation and total runoff simulation.
2. The calibrated model should be verified against a less extreme event.
3. A better method of determining when incremental runoff equals incremental rainfall should be determined.
4. Additional model refinement should be done in order to incorporate the model in an implicit flood routing program.

## VI. BIBLIOGRAPHY

1. Amein, Michael and Fang, C. S., "Implicit Flood Routing in Natural Channels", Journal of the Hydraulics Division, ASCE Vol. 96, No. HY12, December, 1970.
2. Baltzer, R. A. and Chintu, Lai, "Computer Simulation of Unsteady Flows in Waterways", Journal of the Hydraulics Division, ASCE, Vol. 94, No. HY7, July, 1968.
3. Strelkoff, Theodor, "Numerical Solution of Saint-Venant Equations", Journal of the Hydraulics Division, ASCE, Vol. 96, No. HY1, January, 1970.
4. Garrison, Jack, Grandu, Jean-Pierre and Price, J., "Unsteady Flow Simulation in Rivers and Reservoirs", Journal of the Hydraulics Division, ASCE, Vol. 95, No. HY9, September, 1969.
5. Contractor, D.N. and Wiggert, J. M., "Numerical Study of Unsteady Flow in the James River", Bulletin 51, Water Resources Research Center, Virginia Polytechnic Institute and State University, Blacksburg, Virginia, May, 1972.
6. Contractor, D.N. and Wiggert, J. M., "Flood Routing in the James River", Transactions of the American Geophysical Union, Paper H25, Vol. 52, No. 4, April, 1971.
7. Contractor, D.N. and Wiggert, J. M., "A Computer Model of Flood Flow in the James River", Symposium on Flow--Its Measurement and Control in Science and Industry, Pittsburgh, Pennsylvania, May, 1971.
8. Khan, M. Zulifakar Ali, "Computer Modeling of Low Flows in the James River Basin", Thesis, Virginia Polytechnic Institute and State University, Blacksburg, Virginia, July, 1972.
9. Viessman, Warren, Harbaugh, T. E., and Knapp, J. W., Introduction to Hydrology, Intext Educational Publishers, New York, 1972.
10. Philip, J. R., "An Infiltration Equation with Physical Significance", Soil Science, Vol. 77, 1954.

11. James River Basin - Comprehensive Water Resources Plan, Vol. I, Division of Water Resources, Virginia Department of Conservation and Economic Development, Planning Bulletin 213, Richmond, Virginia, March, 1969.
12. Klute, A., "Numerical Method for Solving the Flow Equation for Water in Porous Materials", Soil Science, Vol. 73, 105-116, 1952.
13. Klute, A., "Some Theoretical Aspects of the Flow of Water in Unsaturated Soils", Soil Science, Vol. 16, 144-149, 1952.
14. Tisdall, A. L. "Antecedent Soil Moisture and Its Relation to Infiltration", Australian Journal of Agricultural Research, Vol. 2, 342-348, 1951.
15. "A Compilation of U. S. Weather Bureau Unit Hydrographs Part 2", United States Water Resources Council, Washington, D. C., 96-99, 1960.
16. Eagleson, Peter S., Dynamic Hydrology, McGraw-Hill Book Company, New York, 325-369, 1970.
17. Morisawa, Marie, Streams Their Dynamics and Morphology, McGraw-Hill Book Company, New York, 153-165, 1968.
18. Sittner, W. T., Schauss, C. E., and Monro, J. C., "Continuous Hydrograph Synthesis with an API-Type Hydrologic Model", Water Resources Research, Vol. 5, No. 5, 1007-1022, 1969.
19. Linsley, R. K., Kohler, M. A., and Paulus, J. H., Applied Hydrology, McGraw-Hill Book Company, New York, 405-427, 1949.
20. Wisler, C. O. and Brater, E. E., Hydrology, John Wiley and Sons, Incorporated, London, 255-265, 1959.
21. Kohler, M. A. and Linsley, R. K., "Predicting the Runoff from Storm Rainfall", U. S. Weather Bureau Research Paper 34, Washington, D. C., 1951.
22. Linsley, R. K. and Franzini, J. B., Elements of Hydraulic Engineering, McGraw-Hill Book Company, New York, 35-37, 1955.
23. Horton, R. E., "Determination of Infiltration Capacity for Large Drainage Basins", Transactions of the American Geophysical Union, Vol. 18, 371-385, 1937.

24. Horton, R. E., "Analyses of Runoff Plot Experiments with Varying Infiltration Capacity", Transactions of the American Geophysical Union, Vol. 20, 693-711, 1939.
25. Horner, W. W., "Role of the Land During Flood Periods", Transactions ASCE, Vol. 109, 1269-1320, 1944.
26. Cook, H. L., "The Infiltration Approach to the Calculation of Surface Runoff", Transactions of the American Geophysical Union, Vol. 27, 726-747, 1946.
27. Tennessee Valley Authority, "Upper Bear Creek Experimental Project - A Continuous Daily Streamflow Model", Water Research Paper No. 8, Knoxville, Tennessee, February, 1972.
28. Betson, R. P., Tucker, R. L., and Haller, F. M., "Using Analytic Methods to Develop a Surface - Runoff Model", Water Resources Research, Vol. 5, No. 1, 102-111, February, 1969.
29. Chow, V. T., Editor, Handbook of Applied Hydrology, McGraw-Hill Book Company, New York, 14-1 - 14-35, 1964.
30. Singh, Krishan P., "Role of Baseflow in Rainfall-Runoff Relations", Water Resources Bulletin, Vol. 8, No. 18, August, 1972.
31. Cooper, Byron N., "Geologic Control of Rainfall-Runoff Relations in the Peak Creek Watershed, Pulaski and Wythe Counties, Virginia", Bulletin 25, Water Resources Research Center, Virginia Polytechnic Institute and State University, Blacksburg, Virginia, May, 1969.
32. Shanholtz, V. O., Burford, J. B., and Lillard, J. H., "Evaluation of a Deterministic Model for Predicting Water Yields from Small Agricultural Watersheds in Virginia", Research Division Bulletin 73, Department of Agricultural Engineering Research Division, Virginia Polytechnic Institute and State University, Blacksburg, Virginia, August, 1972.
33. Narayana, V. V. D. and Bagley, Jay M., "Mathematical Simulation of Small Watershed Hydrologic Phenomena", Utah Water Research Laboratory, College of Engineering, Utah State University, Logan, Utah, December, 1967.

34. Reich, Brian M., "Runoff Estimates for Small Rural Watersheds", Report prepared for Federal Highway Administration Environment Design and Control Division, Washington, D. C., July, 1971.
35. Crawford, N. H. and Linsley, R. K., "Digital Simulation in Hydrology: Stanford Watershed Model IV", Technical Report No. 39, Department of Civil Engineering, Stanford University, 1966.
36. Davis, Darryl W., "Computer Models for Rainfall-Runoff and River Hydraulic Analysis", Technical Paper No. 35, The Hydrologic Engineering Center, United States Army Corps of Engineers, Davis, California, March, 1973.
37. Hydrologic Engineering Methods for Water Resources Development, Vol. 4, Hydrograph Analysis, The Hydrologic Engineering Center, United States Army Corps of Engineers, Davis, California, October, 1973.
38. Burnash, Robert, Ferral, Larry, and McGuire, R. A., "A Generalized Streamflow Simulation System Conceptual Modeling for Digital Computers", United States Department of Commerce, National Weather Service, and California Department of Water Resources, March, 1973.
39. Linsley, R. K., Kohler, Max A., and Paulus, J. L., Hydrology for Engineers, McGraw-Hill Book Company, New York, 162-215, 1958.
40. HEC-1 Flood Hydrograph Package - Users Manual, The Hydrologic Engineering Center, United States Army Corps of Engineers, Davis, California, January, 1970.
41. James River Basin - Comprehensive Water Resources Plan, Vol. III - Hydrologic Analysis, Division of Water Resources, Virginia Department of Conservation and Economic Development, Planning Bulletin 215, Richmond, Virginia, 1970.
42. Water Resources Data for Virginia, 1960-1974, United States Department of the Interior, Geologic Survey, Richmond, Virginia.
43. James River Basin Report - Virginia and West Virginia, United States Department of Agriculture, Richmond, Virginia, June, 1974.
44. Draft James River Basin Report, Norfolk District, United States Army, Corps of Engineers, Norfolk, Virginia, February, 1974.

45. SCS National Engineering Handbook, Section 4, Hydrology, Soil Conservation Service, United States Department of Agriculture, Washington, D. C., January, 1971.
46. Monro, John C. and Anderson, E. A., "National Weather Service River Forecasting System", Journal of the Hydraulics Division, ASCE, Vol. 100, HY5, May 1974.
47. Sittner, Walter T., "Modernization of National Weather Service River Forecasting Techniques", Water Resources Bulletin, Vol. 9, No. 4, 655-659, August, 1973.
48. Camp, J. D. and Miller, E. M., Flood of August 1969 in Virginia, United States Department of the Interior, Geological Survey, Water Resources Division, Richmond, Virginia, 1970.

APPENDIX A  
TEXT NOTATION

The following notations are used in the text of this thesis and are applicable to the equations stated:

a	= model coefficient;
$API_0$	= antecedent precipitation index for day 0, inches;
$API_t$	= antecedent precipitation index for day t, inches;
$ARO(J)$	= observed surface runoff for storm J, inches;
b	= model coefficient;
C	= coefficient controlling the rate of decrease of the precipitation loss rate coefficient;
c	= model coefficient;
CB	= a percolation coefficient;
CN	= SCS curve number;
D	= deficiency parameter;
d	= model coefficient;
da,db,dc	= model coefficients defining D;
$DD(I)$	= percentage change in model coefficient;
$D_i$	= surface detention of time i, inches;
DRC	= interflow detention storage daily recession constant;
$DX(I)$	= change in coefficient;
E	= precipitation loss rate exponent;
ET	= evapotranspiration, inches;
F	= actual retention of precipitation, inches;

HPB <sub>J</sub>	= six hour basin average precipitation for the six hour interval J, inches;
HRAIN(I)	= hourly precipitation value for hour I, inches;
Ia	= initial abstraction of precipitation, inches;
IDS	= interflow detention storage, inches;
K	= API recession coefficient;
K'	= modified precipitation loss rate coefficient;
K <sub>0</sub>	= initial precipitation loss rate coefficient;
K <sub>1</sub>	= precipitation loss rate coefficient decreasing with ground wetness;
L	= precipitation loss rate, $\frac{\text{inches}}{\text{hour}}$ ;
L <sub>1</sub>	= accumulated precipitation loss during a storm;
LZS	= current water in lower zone storage, inches;
LZSN	= nominal lower zone storage, inches;
ML <sub>g</sub>	= minor water gains, inches;
ML <sub>1</sub>	= minor water losses, inches;
N	= degree of curvature parameter;
n	= modified degree of curvature parameter;
na,nb,nc	= model coefficients defining N;
NOS	= number of storms;
P	= potential maximum runoff, inches;
P <sub>1</sub>	= precipitation rate, $\frac{\text{inches}}{\text{hour}}$ ;
PB <sub>t</sub>	= basin average daily precipitation for day t, inches;

PC	= deep percolation, inches;
PRECIP <sub>t</sub>	= precipitation falling during day t, inches;
P <sub>t</sub>	= all natural or applied water at time t, inches;
P' <sub>t</sub>	= adjusted daily precipitation for day t, inches;
Q	= actual storm runoff, inches;
$\bar{q}$	= overland flow rate, $\frac{\text{inches}}{\text{hour}}$ ;
RAIN6(J)	= six hour precipitation total for period J, inches;
RF	= storm rainfall, inches;
RI	= runoff index;
RI <sub>s</sub>	= summer runoff index;
RI <sub>w</sub>	= winter runoff index;
S	= total possible precipitation retention when I <sub>a</sub> > 0, inches;
S'	= potential maximum retention of precipitation neglecting I <sub>a</sub> , inches;
sa, sb, sc	= summer model coefficients;
SI	= season index;
SM <sub>t</sub>	= soil water status at time t, inches;
SRO	= surface runoff, inches;
SSEX	= sum of squares error for initial model coefficient set, inches <sup>2</sup> ;
SSEY(I)	= sum of squares errors for each Y(I), inches <sup>2</sup> ;

- $t$  = time, days;
- $TC_i$  = Thiessen coefficient for nonrecording precipitation station  $i$ ;
- $TC_r$  = Thiessen coefficient for the recording precipitation station;
- TREAD = hour the 24 hour precipitation total is read;
- UZS = current water in upper zone storage, inches;
- UZSN = nominal upper zone storage, inches;
- $w_a, w_b, w_c$  = winter model coefficients;
- $\bar{x}$  = mean moisture supply, inches;
- $x$  = moisture supply, inches;
- $XCRO(I,J)$  = computed surface runoff for storm  $J$ , initial model coefficient  $I$ , inches;
- $X(I)$  = initial coefficient value;
- $YCRO(I,J)$  = computed surface runoff for storm  $J$ , trial model coefficient  $I$ , inches; and
- $Y(I)$  = trial coefficient value.

APPENDIX B

THE MAURY RIVER BASIN

TABLE BI STREAM GAZETTEER OF THE MAURY RIVER BASIN (11)

<u>Stream Name</u>	<u>Drainage Area (Sq.Mi.)</u>	<u>Length Miles</u>	<u>Elevation at Source</u>	<u>Elevation at Mouth</u>	<u>Latitude</u>	<u>Longitude</u>	<u>Mouth In County</u>	<u>Miles Above Mouth</u>
MAURY RIVER	839.30	80.3	3,802	701	37°37'25"	79°26'41"	Rockbridge	280.8
Calfpasture River	236.87	39.7	3,802	1,325	37°56'57"	79°27'36"	Rockbridge	40.6
Ramseys Draft	21.44	12.6	3,860	1,792	38°14'20"	79°20'14"	Augusta	30.3
Hamilton Br.	19.47	9.5	3,320	1,625	38°10'29"	79°24'18"	Augusta	23.6
Mill Creek	46.03	20.5	2,720	1,390	37°31'05"	79°29'41"	Rockbridge	4.9
Bratton Ck.	28.86	10.8	2,472	1,368	37°58'09"	79°30'15"	Rockbridge	3.4
Guys Run	7.32	5.5	3,250	1,346	37°57'35"	79°28'34"	Rockbridge	1.8
Little Calfpasture River	83.06	23.0	3,800	1,325	37°56'57"	79°27'36"	Rockbridge	40.6
Smith Creek	13.16	6.9	2,940	1,447	38°03'04"	79°23'36"	Augusta	10.9
Cove Run	9.74	5.9	2,520	1,392	38°01'13"	79°25'58"	Rockbridge	7.0
Hays Creek	80.51	18.8	1,938	1,090	37°53'53"	79°24'25"	Rockbridge	34.7
Moffatts Ck.	13.59	9.5	1,925	1,370	37°55'31"	79°17'35"	Rockbridge	10.8
Walker Ck.	27.87	10.4	2,081	1,137	37°55'32"	79°23'15"	Rockbridge	3.3

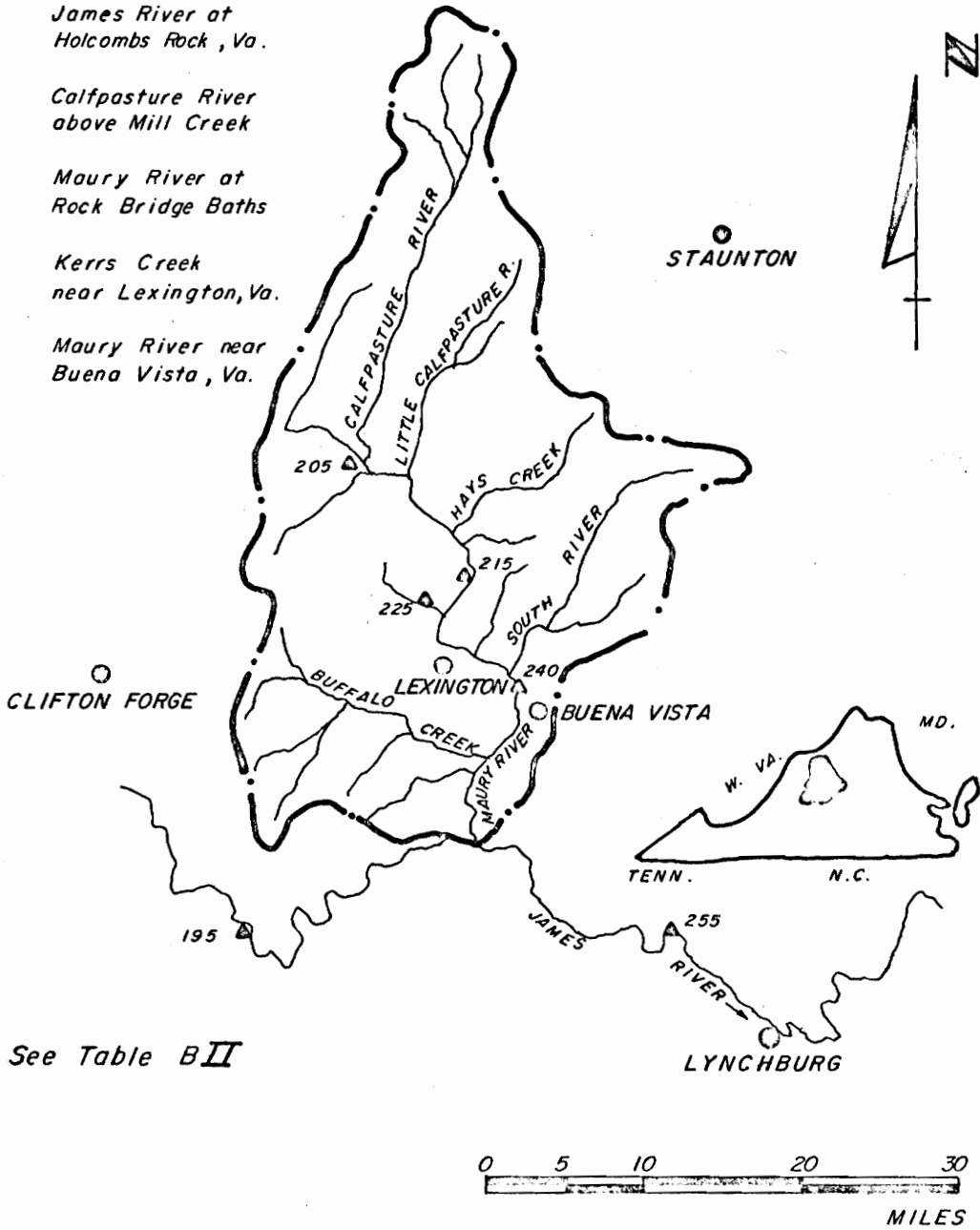
CONTINUED

TABLE BI STREAM GAZETTEER OF THE MAURY RIVER BASIN (11) - CONTINUATION

<u>Stream Name</u>	<u>Drainage Area (Sq.Mi.)</u>	<u>Length Miles</u>	<u>Elevation at Source</u>	<u>Elevation at Mouth</u>	<u>Latitude</u>	<u>Longitude</u>	<u>Mouth In County</u>	<u>Miles Above Mouth</u>
Kerrs Creek	35.50	11.6	2,460	912	37°48'49"	79°26'31"	Rockbridge	22.4
Mill Creek	10.95	8.5	1,710	885	37°47'23"	79°24'58"	Rockbridge	18.9
South River	91.97	17.9	1,600	859	37°46'04"	79°23'04"	Rockbridge	15.2
Saint Marys River	15.87	7.1	3,230	1,600	37°55'48"	79°09'43"	Augusta	17.9
Irish Creek	26.41	13.5	2,880	1,008	37°48'44"	79°19'03"	Rockbridge	5.3
Buffalo Creek	123.66	15.5	1,136	740	37°40'35"	79°25'35"	Rockbridge	4.5
So. Buffalo Creek	21.26	9.8	1,920	1,136	37°44'24"	79°34'19"	Rockbridge	15.5
No. Buffalo Creek	20.62	7.5	2,156	1,136	37°44'24"	79°34'19"	Rockbridge	15.5
Colliers Ck.	36.75	9.1	3,285	1,060	37°45'23"	79°32'36"	Rockbridge	12.7
Broad Creek	12.80	7.4	1,445	880	37°42'59"	79°29'11"	Rockbridge	5.8

GAGE NO.    GAGE NAME

- 195    *James River at Buchanan, Va.*
- 255    *James River at Holcombs Rock, Va.*
- 205    *Calfpasture River above Mill Creek*
- 215    *Maury River at Rock Bridge Baths*
- 225    *Kerrs Creek near Lexington, Va.*
- 240    *Maury River near Buena Vista, Va.*



See Table BII

Figure B1

*Streamflow Gaging Stations In The Vicinity Of The Maury River Basin*

TABLE BII DESCRIPTION OF STREAM GAGING STATIONS (42)

<u>Gage</u>	<u>Location</u>	<u>Drainage Area (mi.<sup>2</sup>)</u>	<u>DISCHARGE - (cfs)</u>		
			<u>Average</u>	<u>Instantaneous Peak</u>	<u>Min. Daily</u>
# 0195 James River at Buchanan, Virginia (Feb.1898 - Sept.1974)	Lat. 37°31'50" Long.79°40'45" Botetourt Co. Mile 301.2	2084	2431 (15.84 $\frac{IN}{YR}$ )	105,000 March, 1913	202 Sept. 1966
# 0255 James River at Holcombs Rock, Va. (Jan.1900 - Sept.1974)	Lat. 37°30'04" Long.79°15'46" Bedford County Mile 268.6	3259	3551 (14.80 $\frac{IN}{YR}$ )	150,000 Aug. 1969	223 July 1930
# 0205 Calfpasture River above Mill Creek at Goshen, Va. (Oct.1938 - Sept.1974)	Lat. 37°59'16" Long.79°29'38" Rockbridge Co.	144	158 (14.90 $\frac{IN}{YR}$ )	20,900 Oct. 1972	0 Sept. 1959
# 0215 Maury River at Rockbridge Baths, Va. (Oct.1928 - Sept.1974)	Lat. 37°54'16" Long.79°25'20" Rockbridge Co.	329	362 (14.94 $\frac{IN}{YR}$ )	33,000 March 1936	5.8 Sept. 1966
# 0225 Kerrs Creek near Lexington, Virginia (Oct.1926 - Sept.1974)	Lat. 37°49'32" Long.79°26'36" Rockbridge Co.	35	35.6 (13.70 $\frac{IN}{YR}$ )	23,000 Sept. 1950	4.0 Aug. 1932
# 0240 Maury River near Buena Vista, Va. (Oct.1938 - Sept.1974)	Lat. 37°45'45" Long.79°23'30" Rockbridge Co.	646	646 (13.58 $\frac{IN}{YR}$ )	105,000 Aug. 1969	37 Sept. 1966

GAGE NO.   GAGE NAME

- 1     McDowell
- 2     Craigsville
- 3     Goshen
- 4     Kerrs Creek
- 5     Lexington
- 6     Montebello Fish Nursery
- 7     Buena Vista
- 8     Deerfield

▲ = Non-Recording Gage  
 □ = Recording Gage

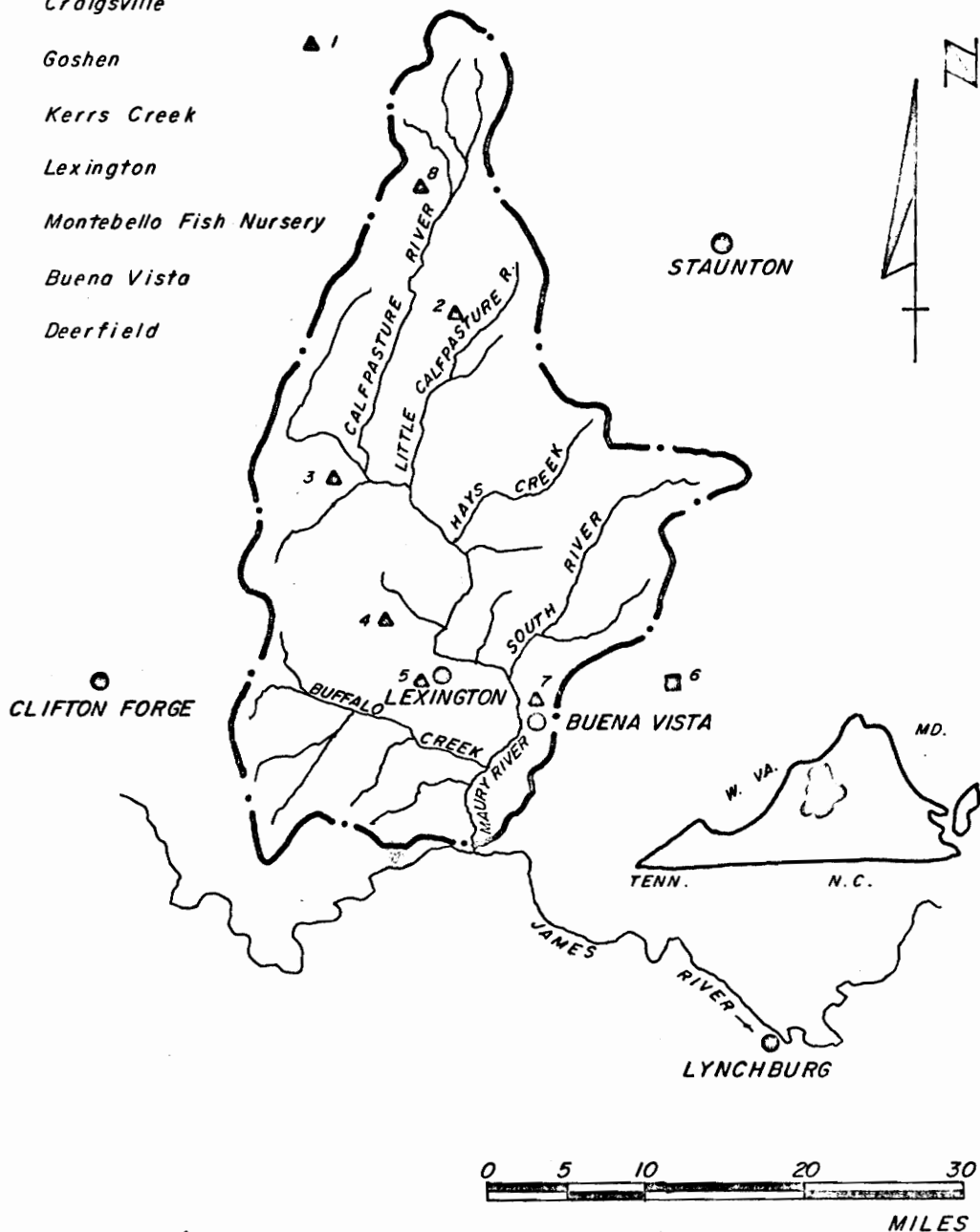


Figure B2

Precipitation Gages In The  
 Maury River Basin

TABLE BIII DESCRIPTION OF PRECIPITATION GAGING STATIONS  
IN THE VICINITY OF THE MAURY RIVER BASIN

<u>Precipitation Station</u>	<u>Latitude Longitude</u>	<u>Type of Gage</u>	<u>Period of Record</u>	<u>Observation Time</u>	<u>Thiessen Coefficient</u>
McDowell # 5414	38 <sup>0</sup> 20' 79 <sup>0</sup> 30'	Non- Recording	Jan. 1963- Present	0700	0.09
Craigsville # 2064	38 <sup>0</sup> 05' 79 <sup>0</sup> 23'	Non- Recording	Jan. 1963- Present	0700	0.23
Goshen # 3470	37 <sup>0</sup> 59' 79 <sup>0</sup> 30'	Non- Recording	Jan. 1948- Present	0700	0.19
Kerrs Creek # 4565	37 <sup>0</sup> 51' 79 <sup>0</sup> 32'	Non- Recording	July 1948- Present	0700	0.12
Lexington # 4876	37 <sup>0</sup> 47' 79 <sup>0</sup> 26'	Non- Recording	July 1948- Present	1800	0.07
Montebello Fish Nursery, #5609	37 <sup>0</sup> 51' 79 <sup>0</sup> 06'	Recording	July 1942- Present	On the Hour	0.09
Buena Vista # 1159	37 <sup>0</sup> 43' 79 <sup>0</sup> 22;	Non- Recording	July 1948- Present	0700	0.06
Deerfield # 2315	38 <sup>0</sup> 10' 79 <sup>0</sup> 22'	Non- Recording	Aug. 1948- Present	0800	0.15

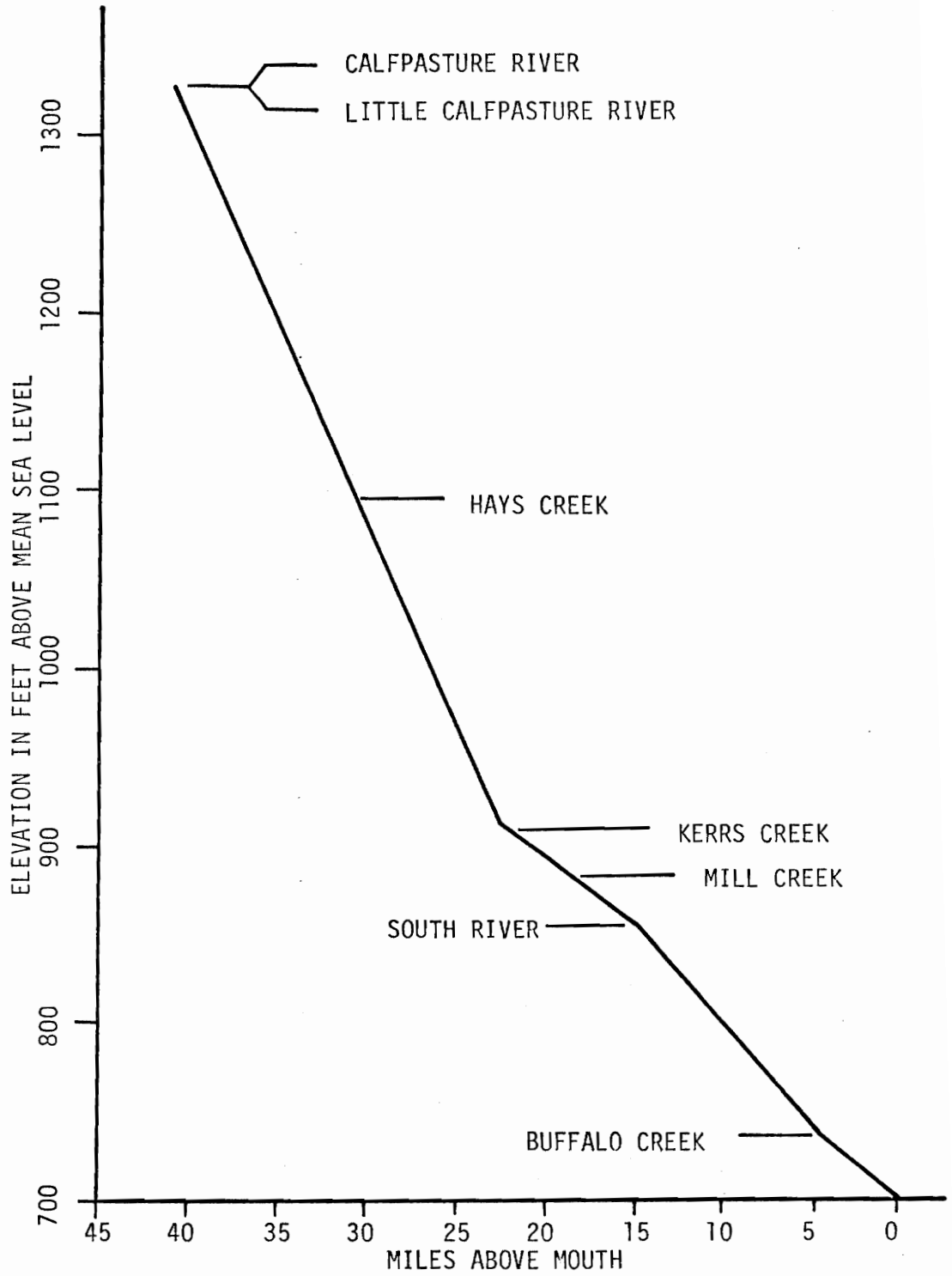


Figure B3 Profile of the Maury River (11)

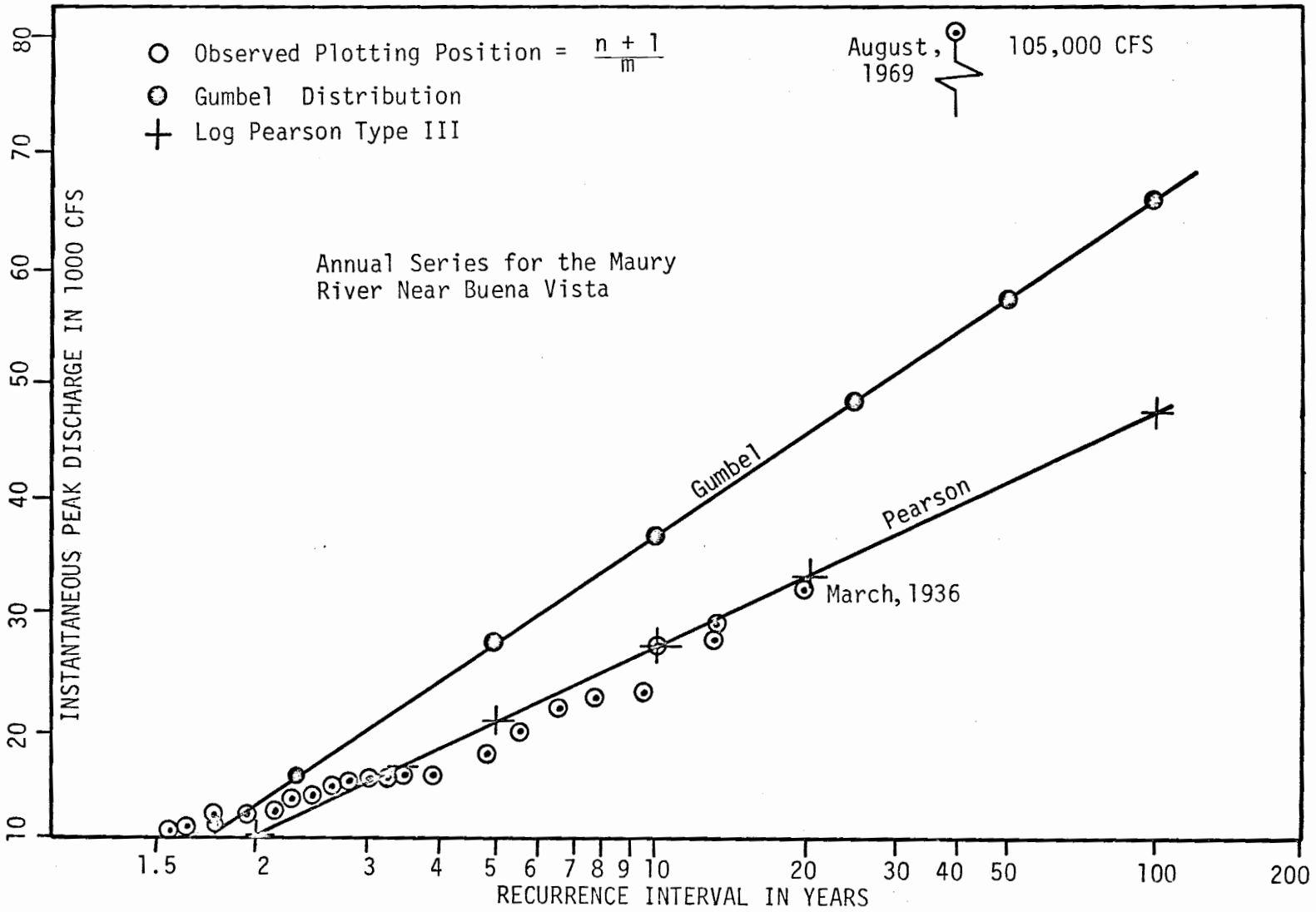


Figure B4 Flood Frequency Curves

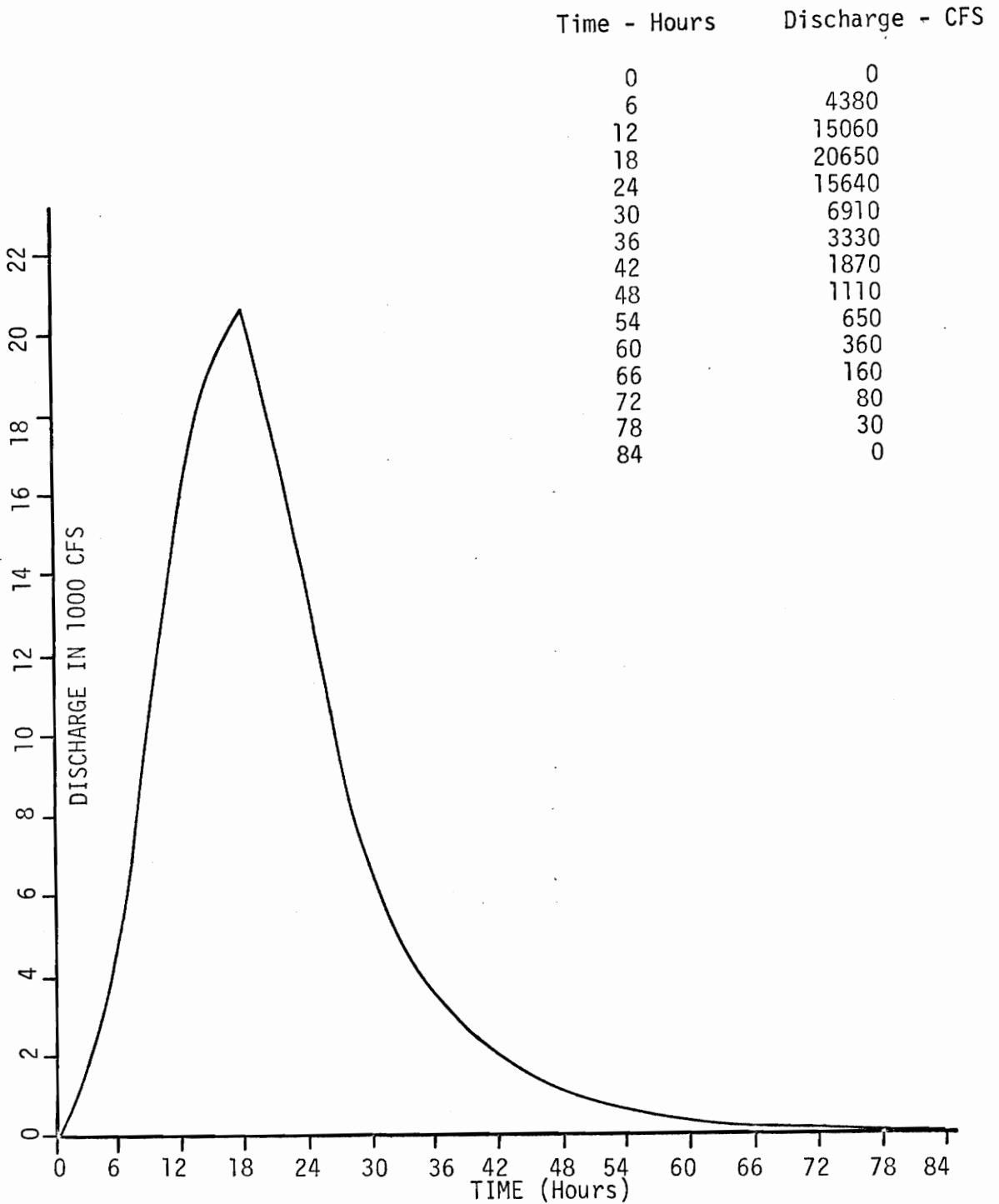





Figure B5 Six Hour Unit Hydrograph for the Maury River Near Buena Vista, Virginia (Virginia Division of Water Resources)

- 
Mississippian, Silurian, Devonian  
Sandstone, Quartzite, Shale, Limestone
- 
Ordovician  
Shale, Limestone, Dolomite
- 
Cambrian  
Limestone, Dolomite

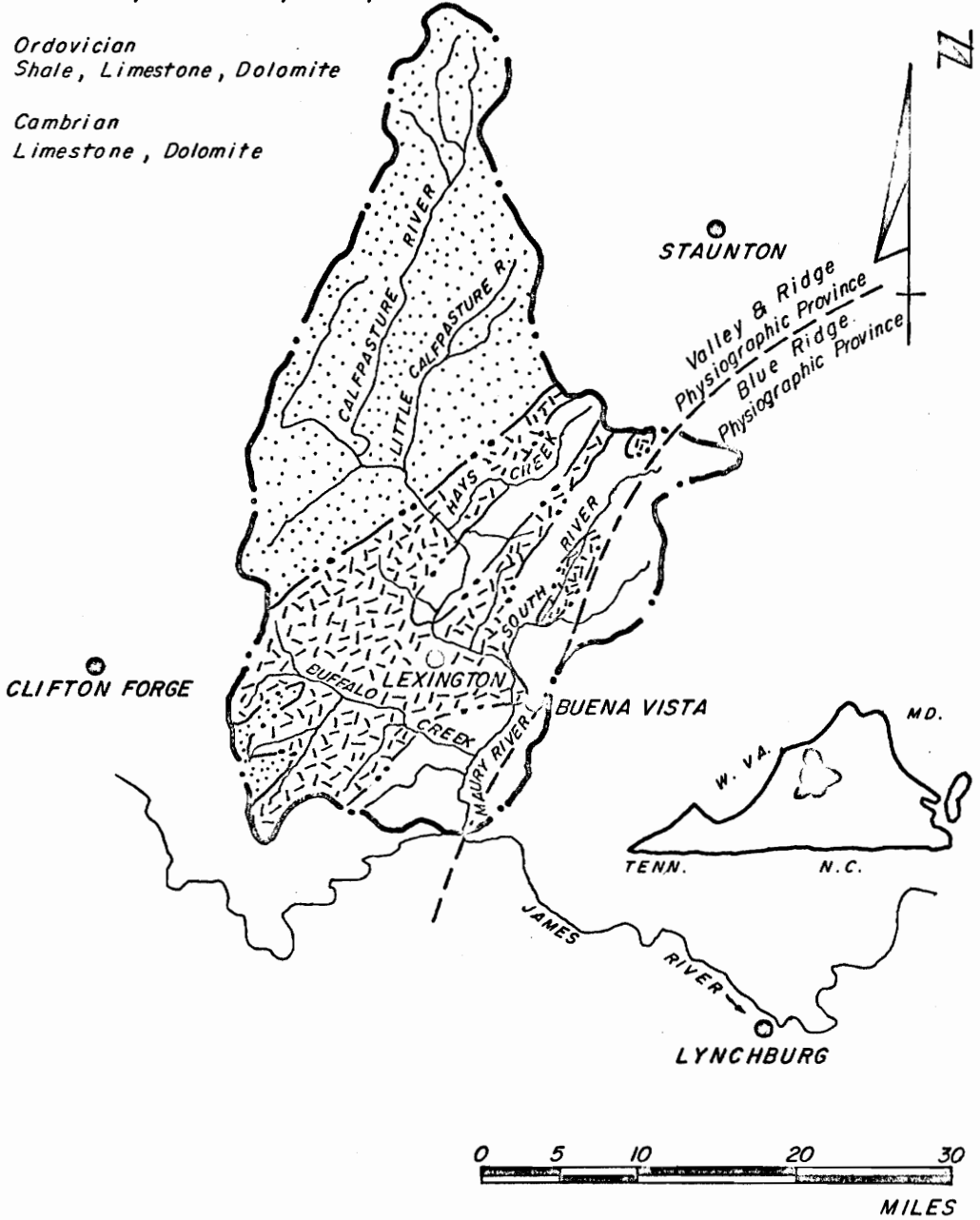


Figure B6

Geological Map Of The  
Maury River Basin(II)

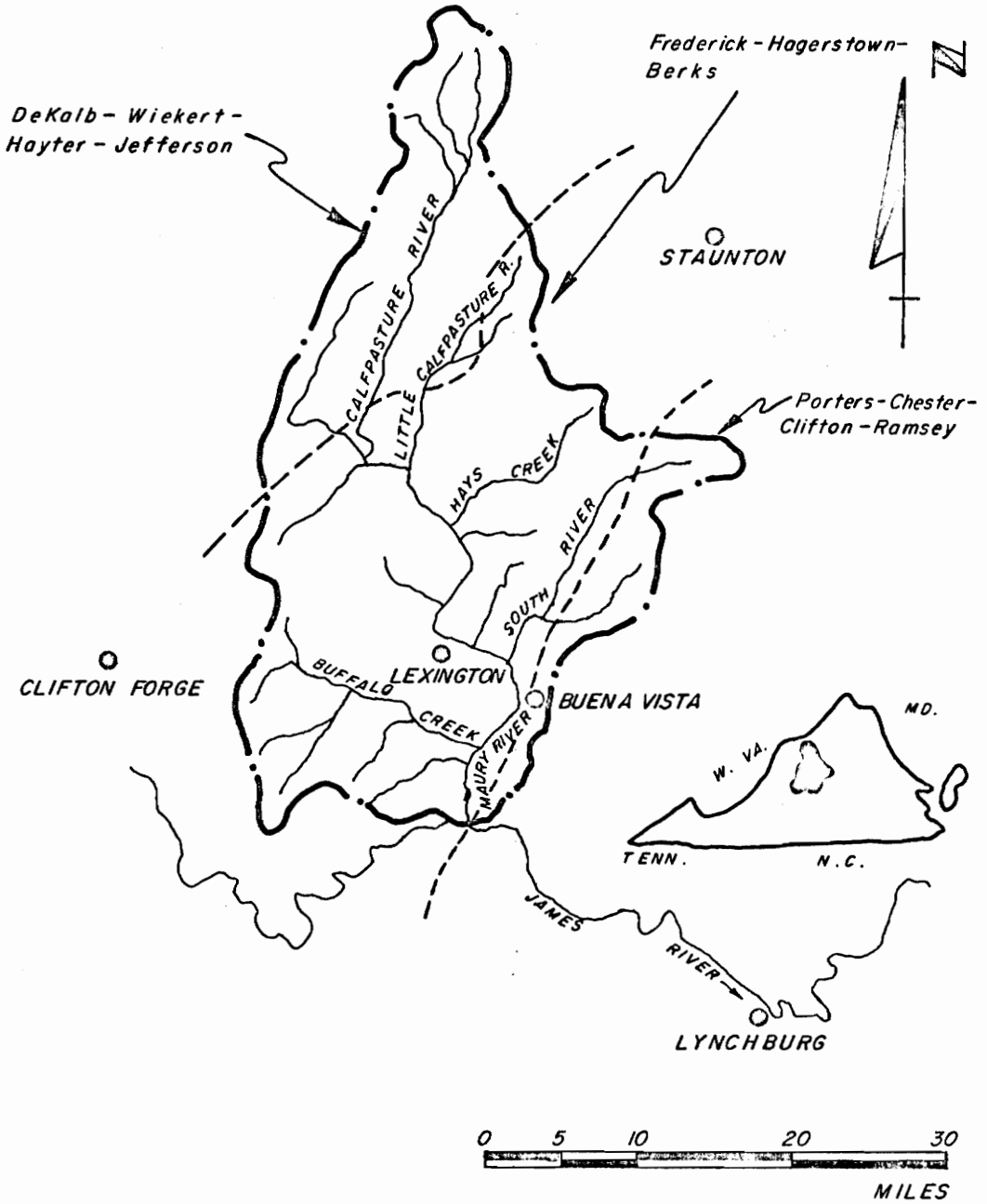


Figure B7

Soil Associations In The  
Maury River Basin(43)

## TABLE BIV DESCRIPTION OF SOIL ASSOCIATIONS (43)

Delkalb, Weikert, Hayter, Jefferson. This association is characterized by shallow to deep soils formed in the weathered products of sandstone and shale. The drainage patterns are well defined. The Delkalb soils have brown to yellowish brown fine sandy loam and stony fine sandy loam surface layers and brownish yellow fine sandy loam subsoils. The Weikert soils have grayish brown loam surface soils where they are present. Hayter soils have brown loam surface soils and strong brown fine sandy clay loam to clay loam subsoils. The Jefferson soils have brown fine sandy loam surface soils and yellowish brown fine sandy clay loam subsoils. Inclusion of soils similar to Jefferson with gragipan 30 inches or more below the surface are common. Other inclusions are limestone soils that range from deep to shallow with silt loam surfaces and clay subsoils and colluvial and alluvial soils that range from well to poorly drained.

Frederick, Hagerstown, Berks. This association is characterized by deep to moderately deep soils formed in the weathered products of limestone and shales with monor inclusions of sandstone. The drainage patterns are not well defined due to sinks in the drainage ways. The Frederick soils have brownish yellow silt loam surface layers and yellowish red to red clay subsoils. The Hagerstown soils have reddish brown silt loam surface layers and reddish brown to red silty clay loam to clay subsoils. The Berks soils have yellowish brown silt loam surface layers and brownish yellow silt loam to silty clay loam B horizons. There are minor inclusions of colluvial and alluvial soils that are well to poorly drained.

Porters-Chester-Clifton-Famsey Association. This association is characterized by moderately deep to very shallow, well drained to excessively well drained soils on the Blue Ridge Mountains. The topography is mostly steep to very steep, with some sloping and moderately steep relief on the mountaintops and in the hollows. Parent material includes granite, granodiorite, greenstone, and quartzite. The drainage patterns are well defined. Most of the surface soils are brown stony loams to stony silt loams. Subsoils, where present, are brown to reddish brown light clay loams. Most of these soils are stony types. There are many areas of stony land and rocky land. There are minor areas of Tusquitee soils and stony colluvium in the hollows.

APPENDIX C

SOIL CONSERVATION SERVICE

CURVE NUMBER METHOD

TABLE CI CURVE NUMBERS FOR HYDROLOGIC SOIL-COVER COMPLEXES (45)

(Antecedent moisture condition II, and  $I_a = 0.2 S$ )

Land Use	Cover Treatment or practice	Hydrologic condition	Hydrologic soil group			
			A	B	C	D
Fallow	Straight Row	----	77	86	91	94
Row Crops	Straight Row	Poor	72	81	88	91
	"	Good	67	78	85	89
	Contoured	Poor	70	79	84	88
	"	Good	65	75	82	86
	" and terraced	Poor	66	74	80	82
	" " "	Good	62	71	78	81
Small Grain	Straight Row	Poor	65	76	84	88
	"	Good	63	75	83	87
	Contoured	Poor	63	74	82	85
	"	Good	61	73	81	84
	" and terraced	Poor	61	72	79	82
	" " "	Good	59	70	78	81
Close-seeded legumes* or rotation meadow	Straight Row	Poor	66	77	85	89
	"	Good	58	72	81	85
	Contoured	Poor	64	75	83	85
	"	Good	55	69	78	83
	" and terraced	Poor	63	73	80	83
	" " "	Good	51	67	76	80
Pasture or range		Poor	68	79	86	89
		Fair	49	69	79	84
		Good	39	61	74	80
	Contoured	Poor	47	67	81	88
	"	Fair	25	59	75	83
	"	Good	6	35	70	79
Meadow		Good	30	58	71	78
Woods		Poor	45	66	77	83
		Fair	36	60	73	79
		Good	25	55	70	77
Farmsteads		----	59	74	82	86
Roads (dirt)+ (hard surface)+		----	72	82	87	89
		----	74	84	90	92

\* Close-drilled or broadcast.

† Including right-of-way.

TABLE CII CURVE NUMBER CONVERSION TABLE FOR ANTECEDENT  
MOISTURE CONDITIONS (45)

1 CN for Condition II	2 CN for Conditions I	3 CN for Conditions III	4 S Values* (inches)	5 Curve Starts* Where P = (inches)
100	100	100	0.00	0.00
95	87	98	.53	.11
90	78	96	1.11	.22
85	70	94	1.76	.35
80	63	91	2.50	.50
75	57	88	3.33	.67
70	51	85	4.28	.86
65	45	82	5.38	1.08
60	40	78	6.67	1.33
55	35	74	8.18	1.64
50	31	70	10.00	2.00
45	26	65	12.20	2.44
40	22	60	15.00	3.00
35	18	55	18.60	3.72
30	15	50	23.30	4.66
25	12	43	30.00	6.00
20	9	37	40.00	8.00
15	6	30	56.70	11.34
10	4	22	90.00	18.00
5	2	13	190.00	38.00
0	0	0	Infinity	Infinity

\* For CN in Column 1.

APPENDIX D

CALIBRATION PROGRAM LISTING



```

ASR(I)=0.
WRITE(6,82)I
32 FORMAT(' RUNOFF GREATER THAN RAIN FOR STORM',I3)
34 CONTINUE
30 FORMAT( 20I4)
31 FORMAT( 10F6.2)
32 FORMAT(16F5.2)
34 FORMAT(16F5.2)
   READ(5,34)(API(I),I=1,NCS)
   WRITE(6,34)(API(I),I=1,NCS)

```

C  
C  
C

COMPUTATION BLOCK            DERIVATION OF COEFFICIENTS

```

7000 CONTINUE
   DO 07 I=1,5
   DDD(I)=DD(I)
   XY(I)=X(I)
07 CONTINUE
   IZMAX=100
   SISET=-1.0
   RISET=0.05
       DO 3000 LLL=1,25
       WRITE(6,53) RISET,SISET
53 FORMAT('1',' DATA AND RESULTS FOR RISET= ',F6.2,' ,AND SISET= ',
&F6.2)
       DO 02 K=1,5
       DD(K)=DDD(K)
       X(K)=XY(K)
       IFF(K)=0
02 CONTINUE
   WRITE(6,40)
   IZ=0

```

```

1000 CONTINUE
    ASRO=0.
    DO 01 I=1,5
    TOTER(I)=0.
01 CONTINUE
C
C    DO LOOP TO COMPUTE OVER ALL STERMS
C
    DO 11 I=1,NCS
    CALL SUBSIN(I)
    ARI=X(3)+(X(1)+X(4)*SI)*EXP(-X(2)*API(I))
    IF(ARI.LE.0.) GO TO 05
    GO TO 06
05 CONTINUE
83 FORMAT('0',' ARI < OR=0  I=',I4,'X(1)= ',F10.3,' X(4)= ',F10.3,' SI
&= ',F5.3,' ARI= ',F10.3,' IWN(I)= ',I4)
    ARI=RISST
06 CONTINUE
    ASRO=ASRO+((((RF(I)**X(5)+ARI**X(5))**(1./X(5))-ARI-ASP(I))
2    **2
    DO 111 J=1,5
    DX(J)=DD(J)*X(J)
    Y(J)= X(J)+DX(J)
111 CONTINUE
    RI(1)=X(3)+(Y(1)+X(4)*SI)*EXP(-X(2)*API(I))
    RI(2)=X(3)+(X(1)+X(4)*SI)*EXP(-X(2)*API(I))
    RI(3)=Y(3)+(X(1)+X(4)*SI)*EXP(-X(2)*API(I))
14 FORMAT('0',5(F15.5,F10.5))
    RI(4)=X(3)+(X(1)+Y(4)*SI)*EXP(-X(2)*API(I))
    RI(5)=X(3)+(X(1)+X(4)*SI)*EXP(-X(2)*API(I))
    RNCS=NCS
    DO 112 K=1,4

```

```

      EN(K)=X(5)
112  CONTINUE
      EN(5)=Y(5)
      DO 113 J=1,5
      IF(RI(J).LE.0.) GO TO 1131
      GO TO 1132
1131 CONTINUE
      34 FORMAT('D', 'RI < OR=0 J= ', I4, ' X(1)= ', F10.3, 'X(4)= ', F10.3, ' SI= ', F5.2,
      & ', F5.2, ' RI(J)=', F10.3, ' INN(J)= ', I4, ' I= ', I5)
      RI(J)= RISET
1132 CONTINUE
      13 FORMAT(' RI(', I4, ')=', F10.5)
      SRG(J)=(RF(1)**EN(J)+RI(J)**EN(J))**(1./EN(J))-RI(J)
      ERROR(J)=((SRG(J)-ASR(I))
      )**2
      TOTER(J)= ERROR(J)/RNCS+TOTER(J)
113  CONTINUE
      11 CONTINUE
      WRITE(6,14) X(1),Y(1),X(2),Y(2),X(3),Y(3), X(4),Y(4),X(5),Y(5)
      ASRC=ASRG/RNCS

```

```

C
C EVALUATION OF INCREMENTED VALUES ( A COMPARISION OF ERRORS( & CHANGES OF INC
C

```

```

      DO 22 J=1,5
      IF(ABS(ASRG).GT.ABS(TOTER(J))) X(J)=Y(J)
      IF(ABS(ASRG).LT.ABS(TOTER(J))) GO TO 221
      GO TO 222
221 CONTINUE
      DD(J)=-DD(J)
      IFF(J)=IFF(J)+1
      IF(IFF(J).GE.2) DD(J)=0.5*DD(J)
      IF(IFF(J).GE.2) IFF(J)=0
222 CONTINUE

```

```

22 CONTINUE
   IZ=IZ+1
39 FORMAT(' #S#2BP? ;+### NO. ITERATIONS EXCEEDED MAXIMUM ALLOWED'
      &,' EXECUTION TERMINATED')
   DO 225 I=1,5
225 WRITE(6,50) IZ,I,X(I),Y(I),TETER(I),DD(I),ASRD
   IF ( IZ .GT. IZMAX) GO TO 3002
   N=0
   DO 33 J=1,5
   IF(ABS(DX(J)/X(J)).LT. 0.01 ) GO TO 331
   GO TO 332
331 CONTINUE
   N=N+1
   DD(J)=0.
332 CONTINUE
   IF(N.GE.5) GO TO 2000
33 CONTINUE
   GO TO 1000
2000 CONTINUE
   WRITE(6,61)(X(J),J=1,5)
61 FORMAT('0',' FINAL VALUES OF  A,B,C,D,N,RESPECTIVELY  ',5F10.3)
C
C   EVALUATION OF FINAL VALUES OF A,B,C,D,N
   WRITE(6,60)
60 FORMAT('1',' STEPM NO.',5X,'WEEK',5X,'API',5X,'RAIN',5X,'COMPUTED
&RUNCFF',5X,'ACTUAL RUNCFF',5X,' ARC-CRG ', ' CA      CC      DRD      DC')
&(ARD-SRD)/RAIN')
70 FORMAT(I5,T17,I2,T20,F5.2,T34,F5.2,T40,F5.2,T68,F5.2,
& T82,F6.3,T89,3F7.3,F10.3)
   SSE=0.
   ABER=0.
   RMST=0.

```

```

    CFF=0.
    DZ=1.0
    IRI=0
    DC I=1,NDS
    CALL SUBSIN(I)
    ARI=X(3)+(X(1)+X(4)*SI)*EXP(-X(2)*API(I))
    IF(ARI.LE.0.) GO TO 1591
    GO TO 1592
1591 CONTINUE
    WRITE(6,099)
    FORMAT(' *****ARI SET TO RISET FOR NEXT ENTRY ')
    ARI=RISET
    IRI=IRI+1
1592 CONTINUE
    SRR=((RF(I)**X(5)+ARI**X(5))**(.1./X(5)))-ARI
    RMS=ASR(I)-SRR
    CA=ASR(I)/RF(I)
    CC=SRR/KF(I)
    SK(I)=SRR
    DPC=RMS/ASR(I)
    DC=(CA-CC)/CA
    ERR(I)=(ASR(I)-SRR)/RF(I)
    SSE=SSE+(ASP(I)-SRR)**2/RNDS
    CFF=CFF+ERR(I)/NDS
    ABER=ABER+ABS(ERR(I))/NDS
    WRITE(6,70) I,IMN(I),API(I),RF(I),SPP,ASR(I),RMS
    8,CA,CC, DC,ERR(I)
    RMST=RMST+ABS(RMS)
159 CONTINUE
    WRITE(6,87)
    WRITE(6,91) CFF
    WRITE(6,86) ABER

```

```

81 FORMAT('  AVERAGE VALUE OF (ARC-CRC)/RAIN = ',F6.3)
   RMSTA=RMST/NOS
   WRITE(6,80) RMSTA
   WRITE(6,93) SSE
93 FORMAT('  SUM OF (ARC-CRC)**2/NOS = ',F10.4)
   WRITE(6,88) IRI
88 FORMAT('  NO. OF TIMES ARI WAS SET TO KISSET= ',I6)
80 FORMAT('  AVERAGE VALUE OF ABS(ARC-CRC) = ',F6.3)
50 FORMAT(I4,I3,14X,F8.3,3X,F8.3,4X,F8.3,5X,F8.3,3X,F8.3 )
40 FORMAT('0',' IZ  'I',17X,'X(I)',7X,'Y(I)',6X,'TOTER(I)',6X,'DD(I)'
   &,9X,'ASRC')
   CALL CORREL
   WRITE(6,91)
   WRITE(6,92)
91 FORMAT('0',' DISTRIBUTION OF ERRORS...ERRCR=(ARC-CRC)/RAIN')
92 FORMAT('  LOWER LIMIT  UPPER LIMIT  NO.  PERCENTAGE  ')
   DD 44 J=1,20
   DZZ=DZ
   DZ=DZ-0.1
   ICCUNT=0
   PER=0.
   DO 441 I=1,NOS
   IF(ERR(I).LT.DZ) GO TO 441
   IF(ERR(I).GE.DZZ) GO TO 441
   ICCUNT=ICCUNT+1
   PER=ICCUNT*100./RNOS
441 CONTINUE
85 FORMAT(F11.2,F13.2, I11,F11.1)
   WRITE(6,85) DZ,DZZ,ICCUNT, PER
86 FORMAT('  AVERAGE VALUE OF ABS((ARC-CRC)/RAIN) = ',F10.3)
44 CONTINUE
07 FORMAT
      ('0',' ERROR ANALYSIS')

```

```

        RISET=RISET+0.1
        IF(IRI.LE.0) GO TO 3001
3000 CONTINUE
        GO TO 3001
3002 CONTINUE
        WRITE(6,89)
3001 CONTINUE
        READ(5,10) NOS,(X(I),I=1,5)
        WRITE(6,7002)(X(I),I=1,5)
7002 FORMAT('1','*** NEW INITIAL VALUES OF A,B,C,D,N = ',5F10.4)
        DO 7003 I=1,5
        DD(I)= DDD(I)
7003 CONTINUE
        GO TO 7000
        STOP
        END

```

C  
C  
C

SUBROUTINE TO CALCULATE SEASONAL INDEX

```

SUBROUTINE SUBSIN(I)
COMMON/BLK1/ SI,IWN(140),SISSET
        IWN=IWN(I)
        IF(IWN(I)-11)10,10,20
10 CONTINUE
        SI=SISSET
        GO TO 11
20 CONTINUE
        IF(IWN(I)-27)30,30,40
30 CONTINUE
        M=(1.-SISSET)/16.
        B=1.-M*27.
        SI=M*IWN+B

```

```

      GO TO 11
40 CONTINUE
      IF(I*IN(I).LE.42) SI=1.
      IF(I*IN(I).GT.42.) GO TO 50
      GO TO 11
50 CONTINUE
      V=(SISET-1.)/10.
      B=1.-V**42.
      SI=4*IN+B
11 CONTINUE
      RETURN
      END
C
C SUBROUTINE TO CALCULATE CORRELATION COEFFICIENT OF CC TO CA
C
SUBROUTINE CORREL
COMMON/BLK2/ SR(150),ASR(150),NCS,COR
YS=0.
XS=0.
XY=0.
SI=0.
S2=0.
S3=0.
S4=0.
S5=0.
EN=NCS
DO 11 I=1,NCS
  X=SR(I)
  Y=ASR(I)
  XY=XY+X*Y
  XS=XS+X**2
  YS=YS+Y**2

```

```

S1=S1+X
S2=S2+Y
S3=S3+X**Y
11 CONTINUE
XM=S1/EN
YM=S2/EN
DO 22 I=1,NCS
S4=S4+(SR(I)-XM)**2
S5=S5+(ASR(I)-YM)**2
22 CONTINUE
SX=SQR(T(S4/(EN-1.)))
SY=SQR(T(S5/(EN-1.)))
COR=(S3-EN*XM*YM)/(SX*SY)
COR=COR/EN
S2XY=SQR(T( (YS-(XY**2/XS))/(EN-2) ) )
WRITE(6,10) COR
WRITE(6,20) S2XY
WRITE(6,30) XM, YM, SX, SY
30 FORMAT(' MEAN CRD = ',F6.3,' MEAN ARC = ',F6.3,
2 ' STD DEV CRD = ',F6.3,' STD DEV ARC = ',F6.3)
10 FORMAT(' CORRELATION COEFFICIENT RELATING ARC TO CRD = ',F10.3)
20 FORMAT(' STANDARD ERROR OF ESTIMATE = ',F10.3)
RETURN
END

```

APPENDIX E  
STORM SIMULATION LISTING  
AND INPUT DATA

```

UNHY: PROCEDURE OPTIONS (MAIN);
/* PROGRAM TO COMPUTE DISCHARGE HYDROGRAPHS */
  DECLARE(K,M,I,J,K1,K2,J1,J2 ,N,ZCOUNT )DECIMAL,FLOAT;
  DECLARE(BASIN) CHARACTER(80);
  DECLARE(NAME(9)) CHARACTER(40);
  DECLARE RAIN(245) INITIAL((245)0);
  DECLARE RAIN6(150) INITIAL ((150)0);
  DECLARE(NDS,LAG,
           ID(9), CT(9), ALL(9),TBASE,TBASE6,UH(30),API(250),TREAD(9),
           TSTORM, WK, HOURS,HSTORM,PRECIP(9,25),HRRAIN(2,480),X(5),
           CC,
           TOTAL,RI,SI,SRC,OPT1,T,QH(85),
           BASEQ,Z
           )FLOAT;
  SUBSIN: PROCEDURE(WKN,SII);
/* SUBROUTINE TO CALCULATE SEASONAL INDEX*/
  DECLARE(WKN,SII,SISET,B,M,CI )FLOAT;
  SISET=-1.0 ;
  IF WKN<=11.0 THEN SII=SISET;
  ELSE IF WKN<=27.0 THEN GO TO S1;
  ELSE IF WKN<=42.0 THEN SII=1.0;
  ELSE GO TO S2;
  GO TO S4;
S1: M=(1.-SISET)/16.0;
  B=1.-M*27.;
  GO TO S3;
S2: M=(SISET-1.)/10. ;
  B=1.-M*42.;
S3: SII=M*WKN+B;
S4: RETURN;
END SUBSIN;
/* */
(SUBSCRIPTRANGE):
HGRAPH: PROCEDURE(I1,EXCESS);

```

```

/* SUBROUTINE TO MULTIPLY UNIT HYDROGRAPH ORDINATES BY 6HR INCREMENTAL
PRECIPITATION TO OBTAIN DISCHARGE HYDROGRAPH*/
/* */
DECLARE(EXCESS,I1 )FLOAT;
DECLARE( I2,II,IJ )FIXED BINARY;
II=I1;
I2=I1-1.+TBASE6;
H2: DO IJ=1 TO TBASE6;
ON SUBSCRIPTRANGE PUT DATA ( II,I2,IJ ) ;
QH(II)=QH(II)+UH(IJ)*EXCESS;
IF II>=80. THEN GO TO S2;
II=II+1;
END H2;
/* IF TRAFEL TIME FROM GAGE TO MOUTH >3HR LAG BY 6 HOURS */
IF I1<=1. THEN GO TO S1;
GO TO S2;
S1: IF LAG<3.0 THEN GO TO S2;
L3: DO II=I2 BY -1 TO I1;
QH(II+1)=QH(II);
END L3;
S2: RETURN;
END HGRAPH;
/* */
A1: PUT PAGE;
T=0.;
OPT1=1;
OPT1=0 ;
ZCOUNT=0;
N=0;
RISET=0.8 ;
/* INPUT */
/* BASIN PARAMETERS */

```

```

GET EDIT(BASIN)(A(30));
PUT EDIT(BASIN)(A(30));
GET LIST(NOS,LAG,APIMAX );
PUT SKIP;
PUT EDIT(NOS,LAG,APIMAX )(F(3),F(5,1),F(5,2) );
GET LIST((X(I) DO I=1 TO 5));
PUT SKIP;
PUT EDIT((X(I) DO I=1 TO 5))(5F(6,2));
GET LIST(TBASE);
PUT SKIP;
PUT EDIT(TBASE)(F(5));
TBASE6=TBASE/6. ;
GET EDIT((UH(I) DO I=1 TO TBASE6))
(COLUMN(1),20 F(8,0));
PUT SKIP;
PUT EDIT((UH(I) DO I=1 TO TBASE6))(10F(8,0));
/* */
/* METEOROLOGIC CONDITIONS */
GET LIST(API(1),TSTORM,Z,WK);
PUT SKIP;
PUT EDIT(API(1),TSTORM,Z,WK)(F(5,2),F(4),F(5,2),F(3));
GET LIST(BASEQ);
PUT SKIP;
PUT EDIT(BASEQ)(F(7));
HOURS=TSTORM*24.;
HSTORM=HOURS/6.;
L2: DO I=1 TO NOS;
GET EDIT(NAME(I),ID(I),CT(I),ALL(I),TREAD(I))
(COLUMN(1),A(40),F(6),2 F(5,2),F(5)) ;
PUT EDIT(NAME(I),ID(I),CT(I),ALL(I),TREAD(I))
(COLUMN(1),A(40),F(6),2 F(5,2),F(5)) ;
IF ID(I)<0. THEN GO TO L21;

```

```

GO TO L22;
/* L21 IS FOR DAILY PRECIP STATIONS*/
L21: GET EDIT((PRECIP(I,J) DO J=1 TO TSTORM))
      (COLUMN(1), 12 F(6,2)) ;
PUT SKIP;
      PUT EDIT((PRECIP(I,J) DO J=1 TO TSTORM))
      (COLUMN(1), 12 F(6,2)) ;
GO TO L23;
/*      HOURLY PRECIP STATIONS*/
L22: N=N+1 ;
      GET EDIT((HRAIN(N,J) DO J=1 TO HOURS))
      (COLUMN(1), 12 F(6,2)) ;
/*      */
PUT SKIP;
      PUT EDIT((HRAIN(N,J) DO J=1 TO HOURS))
      (COLUMN(1), 12 F(6,2)) ;
L23: END L2;
/*      CALCULATION OF AVE 6 HOURLY BASIN PRECIP*/
QH=BASEQ;
L3: DO J=1 TO TSTORM;
CC=0.      ;
      K1=J*4-3;
      K2=J*4;
      J1=J*24-22-1;
      J2=J*24;
L31: DO I= 1 TO NOS;
      N=I-7;
      IF ID(I)>0. THEN GO TO L41;
      ELSE IF PRECIP(I,J)=99.99 THEN CC=CC+CT(I);
ELSE GO TO L310;
GO TO L5;
/* TIME DISTRIBUTION ADJUSTMENT FOR STATIONS NOT READING AT

```

```

2400 HOURS      */
L310: IF J = TSTORM THEN GO TO L311;
PRECIP(I,J)=(PRECIP(I,J+1)*(2400.-TREAD(I))+PRECIP(I,J)*TREAD(I))/
2400.;
GO TO L312;
L311: PRECIP(I,J)=PRECIP(I,J)*TREAD(I)/2400.;
L312: RAIN(J)=RAIN(J)+CT(I)*PRECIP(I,J);
GO TO L5;
/* ROUTINE TO CALCULATE 6HR. INCREMENTAL RAINFALL FROM HOURLY RAIN DATA
*/
L41: DO K=J1 TO J2;
IF HRAIN(N,K)=99.99 THEN HRAIN(N,K)=ALL(I)/(24.);
END L41;
L42: DO K=K1 TO K2;
M=K*6.-5. ;
RAIN6(K)=RAIN6(K)+(HRAIN(N,M)+HRAIN(N,M+1)+HRAIN(N,M+2)+HRAIN(N,
M+3)+HRAIN(N,M+4)+HRAIN(N,M+5))*CT(I);
END L42;
L5: END L31;
RAIN(J)=RAIN(J)*(1.+CC);
TOTAL=RAIN6(K1)+RAIN6(K1+1)+RAIN6(K1+2)+RAIN6(K2);
L6: DO K=K1 TO K2;
IF TOTAL<=0. THEN GO TO L61;
RAIN6(K)=RAIN6(K)*(1.+1./TOTAL*RAIN(J));
L61: IF(RAIN(J) >0.)&(RAIN6(K)=0.) THEN RAIN6(K)=RAIN(J)/4.;
END L3;
/* TO BE REMOVED */
/* OUTPUT OF RAIN6 */
PUT SKIP;
PUT LIST(' 6 HOUR INCREMENTAL PRECIPITATION ');
PUT SKIP;
PUT LIST(' TIME IN HOURS X 6 RAIN (IN)');

```

```

ZZ1: DO K=1 TO K2;
PUT EDIT (K,RAIN6(K)) ( COL(1),F(7,0),X(17),F(10,4));
END ZZ1;
/* TO BE REMOVED */
PUT PAGE;
PUT LIST(' OUT PUT OF RESULTS AND ASSORTED GOODIES');
PUT SKIP;
PUT LIST(' TIME(6HR)          6HR RAIN(IN)          API(IN)
RI          SRD(IN)');
/* COMPUTE RUNOFF
*/
COUNT=0.;
CALL SUBSIN(WK,SI);
L7: DO J=1 TO K2;
COUNT=COUNT+1;
API(J+1)=API(J)*Z**0.25+RAIN6(J);
IF COUNT <28 THEN GO TO L70;
COUNT=0.;
WK=WK+1;
IF WK>52 THEN WK=1;
CALL SUBSIN(WK,SI);
L70: RI=X(3)+(X(1)+X(4)*SI)*EXP(-X(2)*API(J));
IF RI<=0. THEN GO TO L72;
ELSE GO TO L73;
L72: PUT EDIT(' RI<=0 FOR J = ',J)(A,F(5))(' SI= ',SI)(A,F(5,2))
(' RI = ',RI)( A,F(10,2));
RI = RISET;
L73: SRD=(RAIN6(J)**X(5)+RI**X(5))**(1./X(5))-RI;
IF API(J) >= APIMAX THEN SRD = RAIN6(J);
IF SRD<0. THEN SRD=0.;
PUT SKIP;
PUT EDIT(J,RAIN6(J),API(J),RI,SRD)(F(8),2F(20,2),2F(15,2));

```

```

CALL HGRAPH(J,SRO);
IF OPT1=+1 THEN GO TO L71;
GC TO L8;
L71: PUT SKIP;
      PUT EDIT(' INCREMENTAL HYDROGRAPH, TIME = ',J,' *6 HOURS')
      (A,F(4), A);
PUT SKIP;
PUT LIST (' TIME (6HR) Q(CFS)');
PUT EDIT((I,QH(I) DC I=1 TO HSTORM))
(COL(1), F(5),E(20,4));
L8: END L7;
/* OUT PUT */
PUT SKIP(5);
PUT EDIT(' FINAL HYDROGRAPH FOR ',BASIN)(A,A(80));
PUT SKIP;
PUT LIST(' TIME (HOURS) DISCHARGE (CFS)');
T=0.;
L9: DO I=1 TO HSTORM ;
PUT EDIT(T,QH(I)) (COL(1),F(10),F(20));
T=T+6.;
END L9;
GO TO A1;
END UNHY;

```

TABLE EI DAILY PRECIPITATION FOR AUGUST 1969 STORM (inches)

Station	Date in August 1969											
	13	14	15	16	17	18	19	20	21	22	23	24
Buena Vista	0.00	0.01	0.00	0.36	1.36	0.00	1.48	4.00	0.00	0.00	0.00	0.00
Craigsville	0.00	0.00	0.06	0.50	0.62	0.06	0.67	3.02	0.00	0.00	0.00	0.00
Deerfield	0.00	0.01	0.03	0.58	0.68	0.06	0.40	2.00	0.00	0.00	0.00	0.00
Goshen	0.00	0.00	0.01	0.10	0.48	0.18	0.73	6.14	0.00	0.00	0.00	0.00
Kerrs Creek	0.00	0.00	0.00	0.33	0.57	0.00	0.92	6.87	0.00	0.00	0.00	0.00
Lexington	0.00	0.01	0.17	1.13	0.00	0.70	0.02	4.95	0.00	0.00	0.00	0.00
McDowell	0.00	0.00	0.00	0.08	0.61	0.18	0.02	1.80	0.00	0.00	0.00	0.00

TABLE EII HOURLY PRECIPITATION FOR MONTEBELLO FISH NURSERY FOR AUGUST 1969 STORM

Date August 1969	Time											
	1	2	3	4	5	6	7	8	9	10	11	12
13 a.m.	0.00	0.00	0.00	0.00	0.00	0.00	0.00	0.00	0.00	0.00	0.00	0.00
p.m.	0.00	0.00	0.00	0.00	0.00	0.00	0.00	0.00	0.00	0.00	0.00	0.00
14 a.m.	0.00	0.00	0.00	0.00	0.00	0.00	0.00	0.02	0.02	0.00	0.01	0.00
p.m.	0.03	0.02	0.00	0.00	0.00	0.00	0.00	0.00	0.00	0.00	0.00	0.00
15 a.m.	0.00	0.00	0.00	0.00	0.00	0.00	0.00	0.00	0.00	0.00	0.00	0.00
p.m.	0.00	0.00	0.00	0.00	0.00	0.00	0.00	0.00	0.00	0.00	0.00	0.00
16 a.m.	0.46	0.05	0.00	0.00	0.00	0.00	0.00	0.00	0.00	0.02	0.08	0.49
p.m.	0.11	0.00	0.00	0.00	0.00	0.00	0.00	0.00	0.00	0.00	0.00	0.00
17 a.m.	0.00	0.00	0.00	0.00	0.00	0.00	0.00	0.00	0.00	0.00	0.00	0.00
p.m.	0.00	0.00	0.00	0.00	0.00	0.00	0.00	0.00	0.00	0.00	0.00	0.00
18 a.m.	0.00	0.00	0.00	0.00	0.00	0.00	0.00	0.00	0.00	0.00	0.00	0.00
p.m.	0.00	0.00	0.95	0.41	0.03	0.01	0.00	0.00	0.00	0.00	0.00	0.00
19 a.m.	0.00	0.00	0.00	0.00	0.00	0.00	0.00	0.00	0.00	0.00	0.00	0.00
p.m.	0.00	0.00	0.00	0.00	0.00	0.00	0.95	0.98	1.01	1.03	1.06	1.02
20 a.m.	1.02	1.06	0.95	0.56	0.59	0.70	0.00	0.00	0.00	0.00	0.00	0.00
p.m.	0.00	0.00	0.00	0.00	0.00	0.00	0.00	0.00	0.00	0.00	0.00	0.00
21 a.m.	0.00	0.00	0.00	0.00	0.00	0.00	0.00	0.00	0.00	0.00	0.00	0.00
p.m.	0.00	0.00	0.00	0.00	0.00	0.00	0.00	0.00	0.00	0.00	0.00	0.00

CONTINUED

TABLE EII HOURLY PRECIPITATION FOR MONTEBELLO FISH NURSERY FOR AUGUST 1969 STORM - CONTINUED

Date August 1969	Time											
	1	2	3	4	5	6	7	8	9	10	11	12
22 a.m.	0.00	0.00	0.00	0.00	0.00	0.00	0.00	0.00	0.00	0.00	0.00	0.00
p.m.	0.00	0.00	0.00	0.00	0.00	0.00	0.00	0.00	0.00	0.00	0.00	0.00
23 a.m.	0.00	0.00	0.00	0.00	0.00	0.00	0.00	0.00	0.00	0.00	0.00	0.00
p.m.	0.00	0.00	0.00	0.00	0.00	0.00	0.00	0.00	0.00	0.00	0.00	0.00
24 a.m.	0.00	0.00	0.00	0.00	0.00	0.00	0.00	0.00	0.00	0.00	0.00	0.00
p.m.	0.00	0.00	0.00	0.00	0.00	0.00	0.00	0.00	0.00	0.00	0.00	0.00

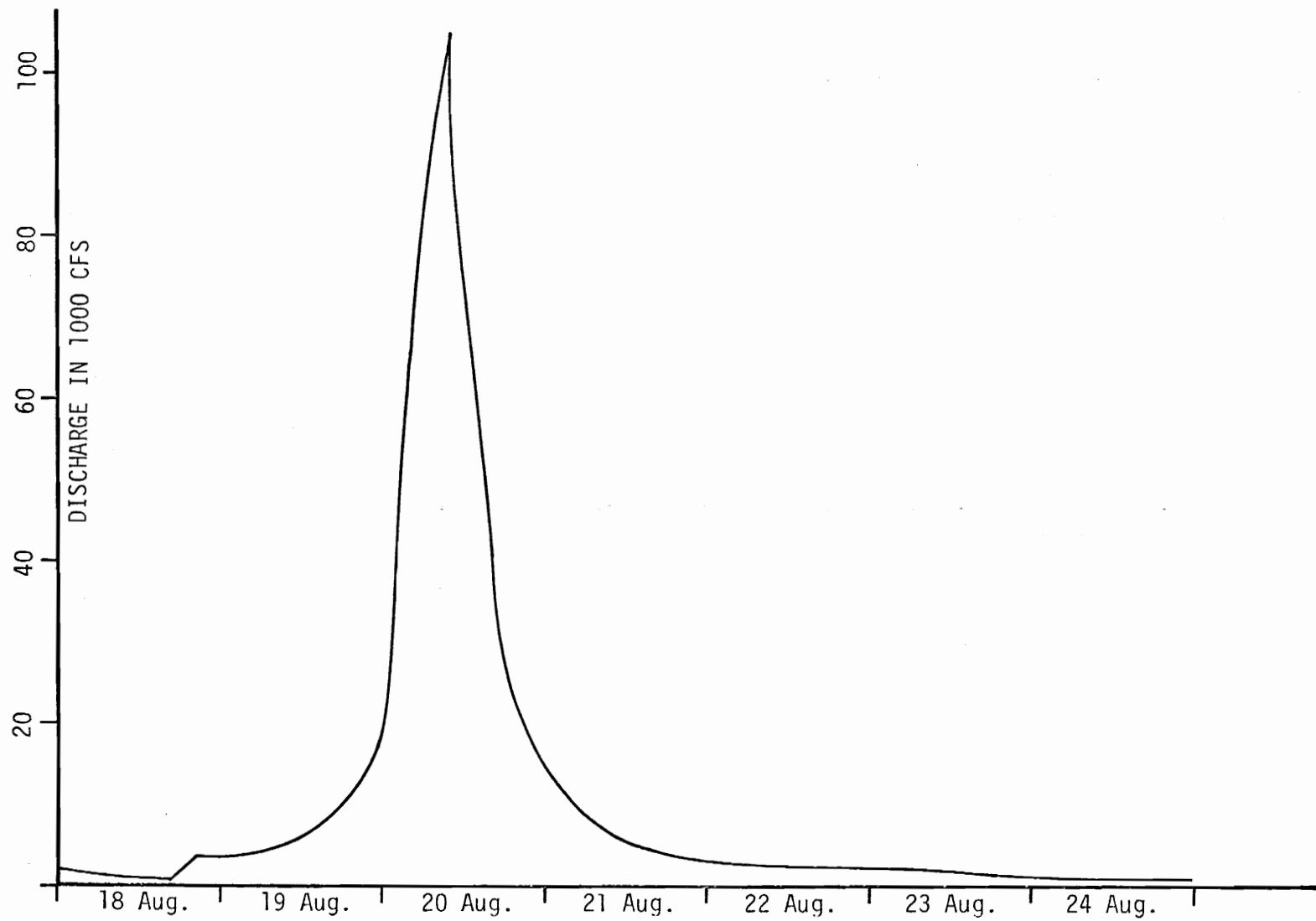


Figure E1 Maury River Near Buena Vista, August 1969 Flood

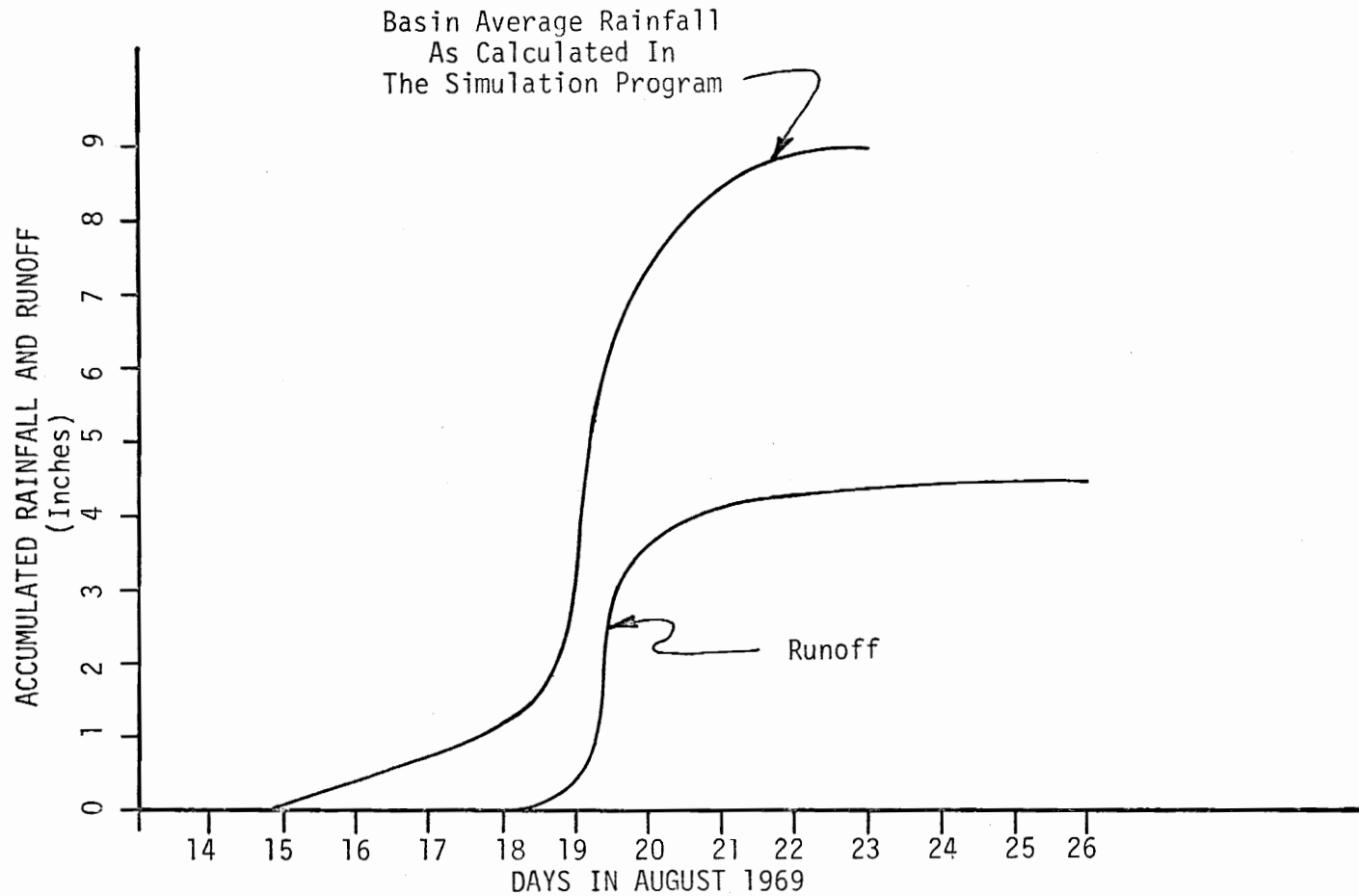


Figure E2 Double Mass Curve for Storm of August 1969 at the Maury River near Buena Vista

TABLE EIII DISCHARGE FOR MAURY RIVER NEAR BUENA VISTA  
FOR AUGUST 1969 STORM (48)

Time	Discharge	Time	Discharge	Time	Discharge
<u>Aug. 18</u>		<u>Aug. 20</u>		<u>Aug. 22</u>	
0300	1,170	0300	55,000	1200	2,420
0600	1,080	0600	87,000	2400	1,660
0900	935	0900	105,000	Mean	2,510
1200	877	1200	79,000		
1500	846	1500	59,000	<u>Aug. 23</u>	
1600	922	1800	28,000	1200	1,360
1630	1,230	2100	20,400	2400	1,070
1700	1,840	2400	14,200	Mean	1,360
1730	3,370	Mean	56,000		
1800	5,640			<u>Aug. 24</u>	
1830	5,790	<u>Aug. 21</u>		1200	1,000
1900	4,960	0300	10,500	2400	968
2000	3,570	0600	8,300	Mean	1,010
2200	2,850	0900	6,790		
2400	2,730	1200	5,710	<u>Aug. 25</u>	
Mean	1,720	1500	5,010	1200	935
<u>Aug. 19</u>		1800	4,620	2400	810
0300	3,310	2100	4,000	Mean	912
0600	3,880	2400	3,530		
0900	4,880	Mean	6,060	<u>Aug. 26</u>	
1200	6,010			1200	782
1500	7,950			2400	754
1800	10,100			Mean	782
2100	13,400				
2400	20,400				
Mean	8,740				

## VII. VITA

Thomas Mayfield Slaydon was born on January 20, 1950, in Martinsville, Virginia. He received his elementary and high school education in the City of Martinsville school system, and was graduated from Martinsville High School in June, 1968. In September, 1968, he entered Virginia Polytechnic Institute and received a Bachelor of Science degree in Civil Engineering in June, 1972.

In September, 1972, he returned to Virginia Polytechnic Institute and State University to begin studies toward a Master of Science degree in Civil Engineering.

In September, 1973, he was employed as a water resources planning hydrologist with the Virginia State Water Control Board in Richmond, Virginia. In September, 1974, he was promoted to the position of water resources planning engineer and transferred to the West Central Regional Office in Roanoke, Virginia.

Mr. Slaydon is registered in Virginia as a Professional Engineer.

*Thomas Mayfield Slaydon*

APPLICATION OF A RAINFALL-RUNOFF MODEL  
TO THE MAURY RIVER BASIN IN VIRGINIA

by

Thomas Mayfield Slaydon

(ABSTRACT)

Several rainfall-runoff models were investigated in order to select a precipitation excess generator for an implicit flood routing scheme for the James River. The Maury River basin was chosen for testing the model. Because of ease of application and data requirements, an antecedent precipitation index type of model was selected.

The model utilizes two equations to predict total storm runoff from storm and lumped basin parameters. Five coefficients describe the basin's hydrologic behavior and the storm parameters include precipitation, API, and week number.

Calibration was performed by optimizing the basin coefficients by the method of steepest descent. After minor modification the model was utilized to predict six hourly incremental runoff. By applying unit hydrograph theory, a streamflow hydrograph was computed.

The model was tested for the August 1969 flood. Agreement between computed and observed hydrographs was good with regard to the magnitude of the peak flows and the overall timing, but the computed runoff volume was considerably greater than the observed volume.